5-2018

Droplet Spreading on a Substrate

Chao-Ying Chen
Purdue University

DROPLET SPREADING ON A SUBSTRATE

A Thesis

Submitted to the Faculty

of

Purdue University

by

Chao-Ying Chen

In Partial Fulfillment of the

Requirements for the Degree

of

Master of Science

May 2018

Purdue University

West Lafayette, Indiana

THE PURDUE UNIVERSITY GRADUATE SCHOOL
STATEMENT OF DISSERTATION APPROVAL

Dr. Arezoo Motavalizadeh Ardekani, Co-Chair

School of Mehcanical Engineering

Dr. Sadegh Dabiri, Co-Chair

Department of Agricultural and Biological Engineering and School of Mechanical Engineering

Dr. Jun Chen

School of Mehcanical Engineering

Approved by:

Dr. Jay P. Gore

Head of the School Graduate Program

ACKNOWLEDGMENTS

I express my heartfelt gratitude and appreciation to my advisors, Professor Arezoo Motavalizadeh Ardekani and Professor Sadegh Dabiri for their constant guidance and invaluable advice throughout the course of this study. I thank them for their unfailing support and phenomenal patience in helping me through difficult times and for their wisdom in challenging and encouraging me to discover new frontiers, at the most appropriate times. I will forever be indebted to them.

I would like to express my endless gratitude to my parents who financially support me to study aboard and help me realize my dream. Besides, I always have their full support for my decisions. I can even say that I can not be here without them.

I am very grateful to Vaseem Shaik, an outstanding PhD candidate, for his instructional suggestions about my analytical derivation that helped me derive the equations from the basic principles.

I would also like to express my gratitude to my friend, Ziyang Huang, for his solid background of computational fluid dynamics and valuable discussions that helped me better understand numerical methods.

I also wish to express my appreciation to all my teachers and mentors at Purdue University, who have made my stay here a memorable and rich learning experience.

I thank all my friends at Purdue University for making life here a lot of fun and worth all the challenge.

TABLE OF CONTENTS

LIST OF TABLES

LIST OF FIGURES

Figure Page

SYMBOLS

r	radial variable in cylindrical coordinate system
z	vertical variable in cylindrical coordinate system
t	time
h	profile of droplet
h_p	profile of wetting front
u	tangential velocity inside the droplet
w	vertical velocity inside the droplet
u_p	tangential velocity inside the porous medium
w_p	vertical velocity inside the droplet
u_c	characteristic velocity in radial direction
w_c	characteristic velocity in vertical direction
p_c	characteristic pressure
L	characteristic length in radial direction
H	characteristic length in vertical direction
ϵ	the ratio of L to H
R	radius of droplet
ϕ	porosity of the porous substrate
κ	permeability of the porous substrate
μ	viscosity of liquid
ρ	density of liquid
σ	surface tension coefficient of air/liquid system
g	gravity constant
$\vec{e}_r$	unit vector in radial direction
$\vec{e}_z$	unit vector in vertical direction

ABSTRACT

Chen, Chao-Ying M.S.M.E., Purdue University, May 2018. Droplet Spreading on a Substrate. Major Professors: Arezoo Ardekani and Sadegh Dabiri, School of Mechanical Engineering.

The present work focuses on spreading dynamics of thin viscous droplets on a planar and smooth substrate in a small Reynolds number regime. The droplets are affected by gravity, surface tension and viscous forces. For triple-phase zone, the moving contact-line models are provided to remove the singularity at the edge of the droplet. Our aim of this study is to predict the experimental results and extend the analysis to spreading on a porous substrate. Besides, we quantify the role of rheological parameters, for example, exponent for power-law liquids, on the spreading dynamics.

The mathematical models for a Newtonian droplet and power-law droplet spreading over different substrates are derived using the lubrication theory. The flow inside the saturated porous media is described by the Darcy's law for Newtonian liquids or modified Darcy's law for power-law fluids, assuming a discontinuous wetting front separating the saturated from the unsaturated domain. In the cases for spreading over porous media, we use the Beavers and Joseph boundary condition for tangential velocity on the surface of the substrate. In the end of the theoretical derivation, we have a fourth order nonlinear diffusion partial differential equation for the profile of droplet and a second order nonlinear diffusion partial differential equation for the wetting front for the case of porous substrate.

The governing equations are solved numerically using a finite difference formulation, augmented by the use of Newton-Raphson iteration scheme to treat the nonlinearity. We choose a backward-Euler method for the time advancement algorithm. Finally, numerical results are presented to demonstrate the dependence of spreading

exponent on rheological properties of fluids and the results are validated by the Tanner's law when the liquid is Newtonian. The dependence well matches the analytical relation (Starov *et al.* [1]) despite different choices of contact-line conditions. For the case of shear-thinning droplet spreading on a solid substrate, the numerical results are compared with the experimental data for xanthane droplet (Rafaï, Bonn, & Boudaoud [2]). Our analysis for spreading over an impermeable substrate can capture the behavior of the Tanner's law when the permeability number is zero. For cases of spreading over a porous substrate, the evolution of the contact radius and central height of the droplet follows the Tanner's law during the initial spreading period. The dependence of the evolution of radius and central height on the permeability number is reported in this study. Finally, we compare the evolution of contact radius of a PDMS droplet against the experimental results reported in Denesuk *et al.* [3] and the numerical results from Alleborn & Raszillier [4].

1. INTRODUCTION

The spreading of a droplet on a smooth solid surface is not only an interesting phenomenon but also a difficult moving-boundary problem in fluid mechanics. Besides its difficulty associated with the moving interface, the motion of a fluid in the neighborhood of the contact line presents an additional complexity. The no-slip condition, which is normally used at the boundary between a solid and a liquid, introduces a force singularity at the contact line (Huh & Scriven [5]; Dussan & Davis [6]; and Gennes [7]). This condition is replaced with the Navier slip boundary condition to relax the singularity at the contact line (Dussan & Davis [6]; Huh & Mason [8]; Hocking [9]; Davis [10]; and Haley & Miksis [11]). Many experiments found that the behavior of the contact angle is a complicated function of contact-line speed. The relation between contact angle and contact-line speed has been experimentally determined (e.g. Hoffman [12]; Johnson, Dettre & Brandeth [13]; Dussan [14]; Chen [15]). Tanner's law is observed in these experiments. The competition between capillary and viscous forces determines the speed of the contact line, leading to Tanner's law, $R \sim t^{1/10}$ (Tanner [16]). In this study, we use the experimental fitting relation from Chen *et al.* [15] and the molecular kinematic theory from Blake *et al.* [17] to represent the contact-line dynamics for cases of the spreading on a smooth, solid substrate.

There are many studies investigating the spreading of a small droplet on a surface. For instance, Greenspan [18] and Lopez, Miller, & Ruckenstein [19] constructed a model for the movement of a small viscous droplet on a surface that is based on the lubrication equations and uses the dynamic contact angle to describe the forces acting on the fluid at the contact line. Haley & Miksis [11] investigated how different relations between the contact angle and contact-line speed affect the spreading of a droplet. They found that the spreading rates strongly depend on the form of these relationships but the qualitative features of the droplet motion are similar in all

cases. More comparisons against the experiments should be carried out to study the accuracies of different contact-line descriptions.

The spreading of non-Newtonian liquids is more complicated than the spreading of Newtonian liquids. The main difficulty of studying the spreading dynamics of non-Newtonian fluids is that many constitutive models are nonlinear. It is difficult to analytically include the complex constitutive models and to form the lubrication equations. However, it is still possible to numerically solve the Navier-Stoke's equation coupled with the constitutive equation (Izbassarov & Muradoglu [20]; Tome *et al.* [21]). Many theoretical studies and experiments use power-law fluids to focus on the shear-thinning behavior (King [22]; Starov *et al.* [1]; Rafaï, Bonn, & Boudaoud [2]). In the present study, we consider a power-law fluid in our mathematical formulation. The detailed derivation is shown in Section 2.3.

Capillary and gravitational spreading of particulate thin films or droplets coupled with absorption into substrate is an important industrial process for applications like coating-flow and ink-jet printing. For cases of a Newtonian droplet spreading on a porous substrate, there are two ways to study the dynamics of the spreading and the absorption of a droplet. We can numerically solve the Navier-Stoke's equations coupled with the movement of the free surface (Reis, Griffiths, & Santos [23]). This method requires an interface capturing technique, for example, volume of fluid or level-set method, to capture the movement of the free surface (Nichols, Hirt, & Hotchkiss [24]; Zheng & Zhang [25]; Reis, Griffiths, & Santos [23]). During the numerical implementation, special attention should be given to the effects of surface tension and capillary forces, the movement of the wetting front inside the porous substrate, and the link between the flow outside and inside the porous medium. The advantage of this method is that the governing equations don't require the droplet to be thin and are not limited to a low Reynolds number regime. Therefore, we can study the impact, spreading, impingement of a spherical droplet on the substrate. However, this method requires more efforts on numerical programing and implementation. Besides, it demands more computational resources than solving the one-dimensional

lubrication equation to achieve the same level of the accuracy. Another approach is to construct two coupled lubrication-type equations (Eq. 2.176 and Eq. 2.187 in chapter 2) based on the thin film approximation (Alleborn & Raszillier [4]; Zadražil, Stepanek, & Matar [26]; Espín & Kumar [27]). Small ratio of the characteristic height to the characteristic radius and low Reynolds number are required. Despite these limitations, this method requires less effort on the numerical implementation. Several authors conducted the experiments to quantify the competition of the spreading and absorption (Daniel & Berg [28]; Denesuk *et al.* [3]). Two simple models under two limiting cases are proposed to model the kinetic behavior of the droplet: constant-drawing-area model and decreasing-drawing-area model. In decreasing-drawing-area model, the contact angle of the droplet remains constant as the liquid penetrates into the porous substrate. The radius of the droplet decreases as the penetration proceeds. In constant-drawing-area model, the position of the contact line remains constant through the absorption process, with an associated contact-line hysteresis. A schematic representation (Fig. 1.1) is provided below to demonstrate the ideas mentioned above. Although these two limiting cases can not represent the entire experiments, they can indicate the upper and lower limits on the liquid depletion time (Denesuk *et al.* [3]). The competition between the viscous spreading of liquid on a substrate and the absorption by the substrate is analytically studied by Davis & Hocking [29], [30] for a pure Newtonian droplet spreading on a porous substrate for some limiting cases, for instance, cases of small porosities and case of zero porosity (i.e., spreading over an impermeable medium).

The required information for the mathematical formulation is given in section 1.1, 1.2 and 1.3.

1.1 Lubrication Theory (Thin Film Approximation)

The lubrication theory, or thin film approximation, describes the flow of fluids in a geometry in which one dimension is significantly smaller than the others. Mathemat-

ically, thin film approximation can be seen as exploiting the large difference between two main spatial scales. In the free film lubrication theory, the position of the surface is unknown. The lubrication theory can be used to find the equation describing the position of the free surface. Surface tension plays an essential role. For an extremely thin film, Van der waals forces or disjoining pressure may play a crucial role when the film thickness is small. However, in this work, we don't include the disjoining pressure.

In the present study, the vertical length scale H is the original height of the droplet and the horizontal length L is the initial radius of the droplet. The key requirement is that the ratio $\epsilon \equiv H/L \ll 1$ or $\epsilon \to 0$. A second requirement is that the Reynolds number must be small. In this work, the Reynolds number of the flow inside the droplet is around 1×10^{-5} to 0.1. The inertial terms are negligible in the lubrication limit compared to pressure gradient, body forces, and viscous terms. Moreover, the transverse pressure gradient is negligible while longitudinal pressure gradient is important. In sections 2.3 and 2.4, the details of simplification of the governing equations are described.

1.2 The Slip Boundary Condition

The no-slip boundary condition between a fluid and a solid can cause a non-physical issue in systems with a moving contact line. Several authors (Huh & Scriven [5]; and Dussan & Davis [6]) have shown that the issue of stress singularity occurring at the contact-line is resulted from the application of no slip boundary condition at solid boundaries. The normal way to alleviate the singularity is to allow the liquid near contact line slip on the solid surface (Dussan & Davis [6]; Huh & Mason [8]; Hocking [9]; Davis [10]; and Haley & Miksis [11]). Therefore, in the present study, the slip effect is only implemented near the contact line using the Navier's slip given as follows:

$$u|_{z=0} = \lambda(h)\vec{n} \cdot \underline{\underline{E}} \cdot \vec{t} \neq 0 \ . \tag{1.1}$$

Here, $\vec{n}$ and $\vec{t}$ are the unit normal and tangential vectors at the fluid solid interface. $\underline{\underline{E}}$ is the rate-of-deformation tensor. The slip model, $\lambda(h)$, is a function of droplet height defined as follows (Haley & Miksis [11]):

$$\lambda_0(h) = \beta_0,\ \lambda_1(h) = \frac{\beta_1}{h},\ \lambda_2(h) = \frac{\beta_2}{h^2}\ , \tag{1.2}$$

where β_0, β_1, and β_2 are the slip coefficients corresponding to different slip models, λ_0, $\lambda_1(h)$, and $\lambda_2(h)$, respectively.

1.3 Beavers and Joseph Boundary Condition

The continuity of normal velocity and pressure holds for the droplet on a porous substrate. However, the no slip condition for the tangential velocity is not accurate. The condition for the flow over a porous medium has been investigated by Beavers & Joseph [31]. They proposed that the tangential velocity rapidly changes from Darcian velocity to the fluid velocity at the surface of the medium as shown in Fig. 1.2 :

$$\frac{du}{dz}|_{z=o} = \frac{\beta}{\sqrt{\kappa}}(u|_{z=0} - u_p)\ , \tag{1.3}$$

where β is the slip coefficient, κ is the permeability of the porous medium, and u_p is the volume-average velocity inside the porous substrate. The boundary condition is experimentally validated by Beavers & Joseph [31].

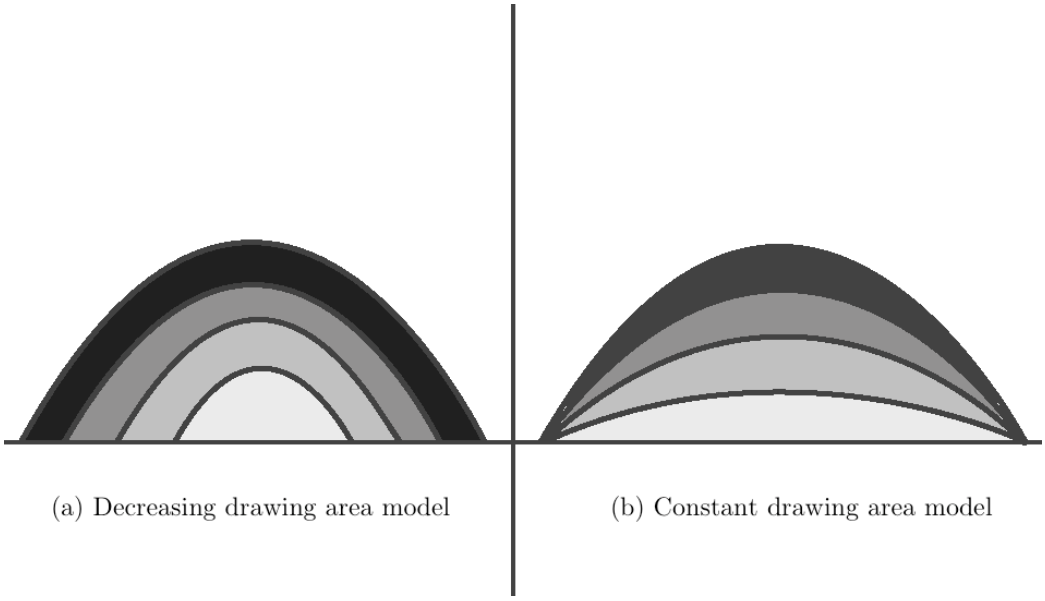

(a) Decreasing drawing area model (b) Constant drawing area model

Figure 1.1. Schematic representation of (a) the decreasing drawing area and (b) constant drawing area models.

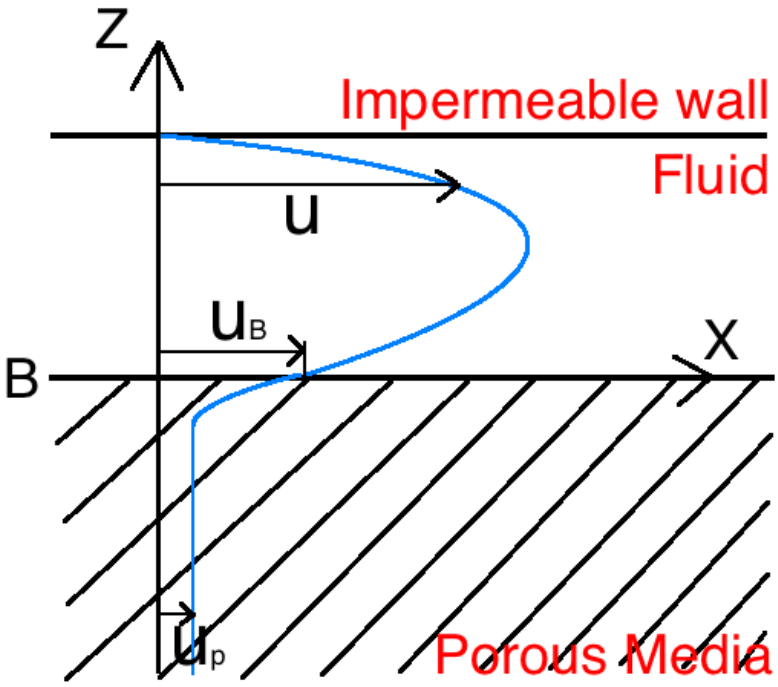

Figure 1.2. Schematic of Beavers and Joseph boundary condition.

2. MATHEMATICAL FORMULATION

2.1 Problem Description and Physical Model

Consider an axisymmetric thin droplet of incompressible viscous liquid placed on a smooth, solid substrate as shown in Fig. 2.1. The droplet spreads under the effect of gravity and the unbalanced surface forces. The spreading is affected by the properties of the fluid and the interaction in three phase zone. The nature of spreading dynamics is characterized by the movement of the contact point, flow near the edge, and surface properties of the solid. The spreading rate strongly depends on the contact line motion. The effect of Navier's slip condition will only be included in the case of Newtonian fluid spreading over a solid surface to resolve the issue of stress singularity at the contact point. For the case of power-law droplet spreading over a solid, Navier's slip condition won't be implemented in the formulation and discussion will be made regarding the decision.

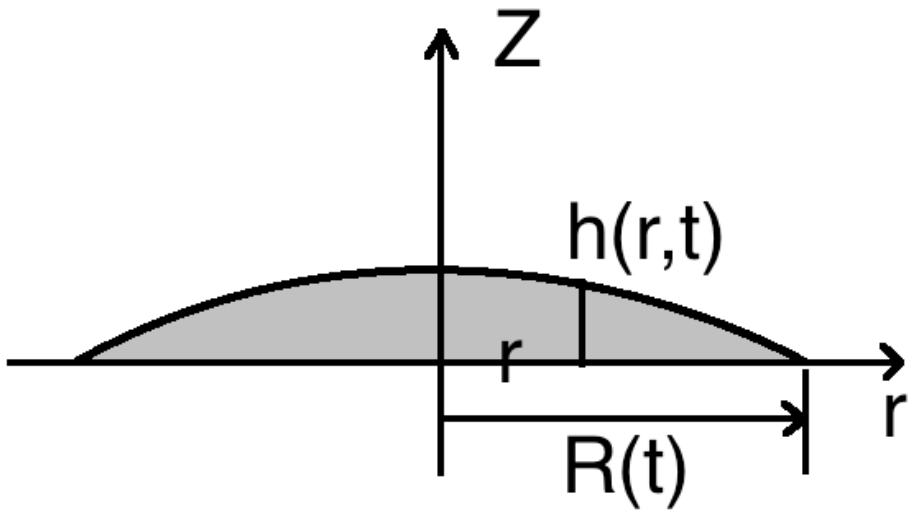

Figure 2.1. Schematic of droplet spreading over a solid surface.

Let r be the horizontal spatial variable and z be the vertical spatial variable. Due to the axisymmetry of the problem, we choose cylindrical coordinate to present the independent variables. Besides, the velocity in θ-direction and the partial derivative with respect to θ are zero. The fluids flow inside the drop can be modeled by the mass conservation equation and Navier-Stoke's equation in dimensional form:

$$\frac{1}{r}\frac{\partial}{\partial r}(ru) + \frac{\partial w}{\partial z} = 0 \tag{2.1}$$

$$\rho(\frac{\partial u}{\partial t} + u\frac{\partial u}{\partial r} + w\frac{\partial u}{\partial z}) = -\frac{\partial p}{\partial r} + \mu\Delta u \tag{2.2}$$

$$\rho(\frac{\partial w}{\partial t} + u\frac{\partial w}{\partial r} + w\frac{\partial w}{\partial z}) = -\frac{\partial p}{\partial z} + \mu\Delta w - \rho g \tag{2.3}$$

Here, $u(r, z, t)$ and $w(r, z, t)$ denote the tangential and vertical velocity, respectively, inside the droplet. **No slip boundary condition** at the surface of substrate is written as

$$u|_{z=0} = w|_{z=0} = 0 \ , \tag{2.4}$$

where $F \equiv z - h(r, t)$ and $\vec{n} = \nabla F/|\nabla F|$. The **kinematic boundary condition** at the liquid-gas interface is written as

$$\vec{u} \cdot \vec{n} = -\frac{1}{|\nabla F|}\frac{\partial F}{\partial t} \ . \tag{2.5}$$

After applying the gradient operator to F, we can write

$$\nabla F = 1 \cdot \vec{e}_z - \nabla h. \tag{2.6}$$

The normal vector $\vec{n}$ to a three-dimensional surface $G(x, y, z) \equiv 0$ has the form

$$\vec{n} = \frac{\nabla G}{\sqrt{(G_x)^2 + (G_y)^2 + (G_z)^2}} \ , \tag{2.7}$$

where subscripts x, y and z, indicates the partial derivatives with respective to x, y, and z. In our case, the normal vector can be expressed as follows

$$\vec{n} = \frac{\vec{e}_z - \nabla h}{\sqrt{1 + |\nabla h|^2}} \ , \tag{2.8}$$

where

$$\nabla h = \frac{\partial h}{\partial r}\vec{e}_r + \frac{\partial h}{\partial z}\vec{e}_z \ . \tag{2.9}$$

Substituting Eq. (2.6) and Eq. (2.8) into Eq. (2.5), we can find the free surface boundary condition in the vector form:

$$\vec{u}\cdot\vec{n} = (u\vec{e}_r + w\vec{e}_z)\cdot(\frac{1}{\sqrt{1+|\nabla h|^2}}\vec{e}_z - \frac{\nabla h}{\sqrt{1+|\nabla h|^2}}) \tag{2.10}$$

$$= \frac{w}{\sqrt{1+|\nabla h|^2}} - \frac{u\frac{\partial h}{\partial r}}{\sqrt{1+|\nabla h|^2}} \tag{2.11}$$

$$= -\frac{1}{\sqrt{1+|\nabla h|^2}}\frac{\partial F}{\partial t} \ . \tag{2.12}$$

Equating Eq. (2.11) and Eq. (2.12), the final form of kinematic boundary condition at $z = h$ becomes

$$\frac{\partial h}{\partial t} + u\frac{\partial h}{\partial r} - w = 0 \ . \tag{2.13}$$

Normal stress balance condition at $z = h$ can be written as

$$P - P_a - 2\mu(\underline{\underline{E}}\cdot\vec{n}\cdot\vec{n}) = \sigma(\nabla\cdot\vec{n}) \ , \tag{2.14}$$

where the rate-of-strain tensor is

$$\underline{\underline{E}} = \frac{1}{2}(\nabla\vec{u} + \nabla\vec{u}^T) \tag{2.15}$$

$$= \begin{pmatrix} \frac{\partial u}{\partial r} & 0 & \frac{1}{2}(\frac{\partial u}{\partial z} + \frac{\partial w}{\partial r}) \\ 0 & \frac{u}{r} & 0 \\ \frac{1}{2}(\frac{\partial w}{\partial r} + \frac{\partial u}{\partial z}) & 0 & \frac{\partial w}{\partial z} \end{pmatrix} \tag{2.16}$$

and the normal vector

$$\vec{n} = \frac{-\frac{\partial h}{\partial r}}{\sqrt{1+(\frac{\partial h}{\partial r})^2}}\vec{e}_r + \frac{1}{\sqrt{1+(\frac{\partial h}{\partial r})^2}}\vec{e}_z \ . \tag{2.17}$$

We, thus, have

$$\underline{\underline{E}}\cdot\vec{n} = \frac{1}{\sqrt{1+(\frac{\partial h}{\partial r})^2}} \begin{pmatrix} -\frac{\partial u}{\partial r}\frac{\partial h}{\partial r} + \frac{1}{2}(\frac{\partial u}{\partial z} + \frac{\partial w}{\partial r}) \\ 0 \\ -\frac{1}{2}(\frac{\partial u}{\partial z} + \frac{\partial w}{\partial r})\frac{\partial h}{\partial r} + \frac{\partial w}{\partial z} \end{pmatrix} \ , \tag{2.18}$$

$$\underline{\underline{E}} \cdot \vec{n} \cdot \vec{n} = \frac{1}{1+(\frac{\partial h}{\partial r})^2}\left[\frac{\partial u}{\partial r}(\frac{\partial h}{\partial r})^2 - \frac{\partial h}{\partial r}(\frac{\partial u}{\partial z}+\frac{\partial w}{\partial r}) + \frac{\partial w}{\partial z}\right] , \tag{2.19}$$

$$\nabla \cdot \vec{n} = \nabla \cdot \left[-\frac{\frac{\partial h}{\partial r}}{\sqrt{1+(\frac{\partial h}{\partial r})^2}}\vec{e}_r + 0 \cdot \vec{e}_\theta + \frac{1}{\sqrt{1+(\frac{\partial h}{\partial r})^2}}\vec{e}_z \right] \tag{2.20}$$

$$= -\frac{1}{r}\frac{\partial}{\partial r}\left[\frac{r\frac{\partial h}{\partial r}}{\sqrt{1+(\frac{\partial h}{\partial r})^2}}\right] + \frac{\partial}{\partial z}\left[\frac{1}{\sqrt{1+(\frac{\partial h}{\partial r})^2}}\right] . \tag{2.21}$$

Substituting Eq. (2.19) and Eq. (2.21) into Eq. (2.14), we can have the final form of normal stress balance condition as

$$P - P_a = \frac{2\mu}{1+(\frac{\partial h}{\partial r})^2}\left[\frac{\partial u}{\partial r}(\frac{\partial h}{\partial r})^2 - \frac{\partial h}{\partial r}(\frac{\partial u}{\partial z}+\frac{\partial w}{\partial r}) + \frac{\partial w}{\partial z}\right] + \sigma\left\{ -\frac{1}{r}\frac{\partial}{\partial r}\left[\frac{r\frac{\partial h}{\partial r}}{\sqrt{1+(\frac{\partial h}{\partial r})^2}}\right] + \frac{\partial}{\partial z}\left[\frac{1}{\sqrt{1+(\frac{\partial h}{\partial r})^2}}\right]\right\} . \tag{2.22}$$

The shear stress balance condition at $z = h$ can be written as

$$2\mu(\underline{\underline{E}} \cdot \vec{n} \cdot \vec{t_i}) - (\nabla_s \sigma) \cdot \vec{t_i} = \tau_{ext} , \tag{2.23}$$

where τ_{ext} stands for the externally applied shear stress and the surface gradient is defined as

$$\nabla_s \equiv \nabla - \vec{n}(\vec{n} \cdot \nabla) . \tag{2.24}$$

In the present work, there is no externally applied shear stress. We treat surface tension coefficient as a constant, neglecting Marangoni effects in the problem. Therefore, Eq. (2.23) becomes

$$2\mu\underline{\underline{E}} \cdot \vec{n} \cdot \vec{t_i} = 0 . \tag{2.25}$$

Let tangential vector have the form

$$\vec{t_i} = \frac{1}{\sqrt{1+(\frac{\partial h}{\partial r})^2}}\vec{e}_r + \frac{\frac{\partial h}{\partial r}}{\sqrt{1+(\frac{\partial h}{\partial r})^2}}\vec{e}_z . \tag{2.26}$$

Substituting Eq. (2.17) and Eq. (2.26) into Eq. (2.25), we can find that

$$\underline{\underline{E}}\cdot\vec{n}\cdot\vec{t_i} = \frac{1}{\sqrt{1+(\frac{\partial h}{\partial r})^2}}\left[-\frac{\partial u}{\partial r}\frac{\partial h}{\partial r}+\frac{1}{2}\left(\frac{\partial u}{\partial z}+\frac{\partial w}{\partial r}\right)-\frac{1}{2}\left(\frac{\partial u}{\partial z}+\frac{\partial w}{\partial r}\right)\left(\frac{\partial h}{\partial r}\right)^2+\frac{\partial w}{\partial z}\frac{\partial h}{\partial r}\right] = 0\ . \tag{2.27}$$

Eq. (2.1), Eq. (2.2), and Eq. (2.3) together with boundary conditions Eq. (2.4), Eq. (2.13), Eq. (2.22), and Eq. (2.27) present the case for a Newtonian droplet spreading over a solid surface.

2.2 Mathematical Formulation (Newtonian Droplet)

A Newtonian droplet spreading either over a solid or porous substrate have already been widely studied. However, there still exist some issues regarding the physical representation of contact line motion over a solid or porous substrate. For cases of spreading over a smooth and solid substrate, the Navier slip model is applied in our analytical derivation and numerical computation to alleviate the stress singularity at the contact line. Because the radius of the droplet is time dependent, we need the contact-line boundary condition to govern the behavior of spreading. In the present study, we apply two different contact line models in our simulation and provide a comprehensive comparison of numerical results against experiments.

Moreover, the case of spreading over a porous substrate is investigated using Beavers and Joseph conditions instead of no slip boundary conditions at the interface of fluid-porous medium. The contact-line boundary condition on porous medium is not completely known yet. Thus, we circumvent the inclusion of contact-line boundary condition in numerical computation by using the idea of fixed-domain computation. The details of numerical implementation for stretched-grid method and fixed-domain computation are described in chapter 3. The results and comparisons are reported in chapter 3 as well.

2.2.1 Spreading Over a Solid Substrate

To analyze the system described in the previous section, Navier-Stokes equations as well as the boundary condition from Section 2.1 are made dimensionless by the following relations:

$$u = u_c \cdot u', h = H \cdot h', r = L \cdot r', p = p_c \cdot p'$$

$$w = w_c \cdot w', z = H \cdot z', t = \left(\frac{L}{u_c}\right) t'$$

Note that the variables with primes denotes the dimensionless ones. Substituting above relations, we can rewrite Eq. (2.1) as

$$\frac{1}{L\cdot r'}\frac{\partial(L\cdot r'\cdot u_c\cdot u')}{L\partial r'}+\frac{\partial(w_c\cdot w')}{H\partial z'}=0\ , \tag{2.28}$$

$$\frac{u_c}{L}\frac{1}{r'}\frac{\partial(r'u')}{\partial r'}+\frac{w_c}{H}\frac{\partial w'}{\partial z'}=0\ . \tag{2.29}$$

From the continuity condition, we have

$$\frac{u_c}{L}=\frac{w_c}{H}\ , \tag{2.30}$$

$$\epsilon\equiv\frac{H}{L}=\frac{w_c}{u_c}\ll 1\ . \tag{2.31}$$

For r-direction momentum equation, Eq. (2.2) becomes

$$\rho\left(\frac{\partial u}{\partial t}+u\frac{\partial u}{\partial r}+w\frac{\partial u}{\partial z}\right)=-\frac{\partial p}{\partial r}+\mu\Delta u\ , \tag{2.32}$$

$$\rho\left(\frac{u_c}{L/u_c}\frac{\partial u'}{\partial t'}+u_cu'\frac{u_c}{L}\frac{\partial u'}{\partial r'}+\epsilon u_cw'\frac{u_c}{H}\frac{\partial u'}{\partial z'}\right)= -\frac{p_c}{L}\frac{\partial p'}{\partial r'}+\mu\left\{\frac{u_c}{L^2}\frac{\partial}{\partial r'}\left[\frac{1}{r}\frac{\partial}{\partial r'}(r'u')\right]+\frac{u_c}{H^2}\frac{\partial^2u'}{\partial z'^2}\right\}\ , \tag{2.33}$$

$$\rho\left(\frac{u_c^2}{L}\frac{\partial u'}{\partial t'}+\frac{u_c^2}{L}u'\frac{\partial u'}{\partial r'}+\frac{u_c^2}{L}w'\frac{\partial u'}{\partial z'}\right)=-\frac{p_c}{L}\frac{\partial p'}{\partial r'}+\mu\left\{\frac{u_c}{L^2}\frac{\partial}{\partial r'}\left[\frac{1}{r'}\frac{\partial}{\partial r'}(r'u')\right]+\frac{u_c}{H^2}\frac{\partial^2u'}{\partial z'^2}\right\}\ , \tag{2.34}$$

$$\frac{\partial u'}{\partial t'}+u'\frac{\partial u'}{\partial r'}+w'\frac{\partial u'}{\partial z'}=-\frac{p_c}{\rho u_c^2}\frac{\partial p'}{\partial r'}+\frac{\mu L}{\rho u_c^2}\left\{\frac{u_c}{L^2}\frac{\partial}{\partial r'}\left[\frac{1}{r'}\frac{\partial}{\partial r'}(r'u')\right]+\frac{u_c}{H^2}\frac{\partial^2u'}{\partial z'^2}\right\}\ . \tag{2.35}$$

For z-direction momentum equation, Eq. (2.3) becomes

$$\rho(\frac{\partial w}{\partial t}+u\frac{\partial w}{\partial r}+w\frac{\partial w}{\partial z})=-\frac{\partial p}{\partial z}+\mu\Delta w-\rho g\ , \tag{2.36}$$

$$\rho(\frac{\epsilon u_c}{L/u_c}\frac{\partial w'}{\partial t'}+\frac{\epsilon u_c^2}{L}u'\frac{\partial w'}{\partial r'}+\frac{\epsilon^2u_c^2}{H}w'\frac{\partial w'}{\partial z'})= -\frac{p_c}{H}\frac{\partial p'}{\partial z'}+\mu\left[\frac{\epsilon u_c}{L^2}\frac{1}{r'}\frac{\partial}{\partial r'}\left(Lr'\frac{1}{L}\frac{\partial w'}{\partial r'}\right)+\frac{\epsilon u_c}{H^2}\frac{\partial^2w'}{\partial z'^2}\right]-\rho g\ , \tag{2.37}$$

$$\rho(\frac{\epsilon u_c^2}{L}\frac{\partial w'}{\partial t'} + \frac{\epsilon u_c^2}{L}u'\frac{\partial w'}{\partial r'} + \frac{\epsilon u_c^2}{L}w'\frac{\partial w'}{\partial z'}) = \\ -\frac{p_c}{H}\frac{\partial p'}{\partial z'} + \mu\left[\frac{\epsilon u_c}{L^2}\frac{1}{r'}\frac{\partial}{\partial r'}\left(r'\frac{\partial w'}{\partial r'}\right) + \frac{\epsilon u_c}{H^2}\frac{\partial^2 w'}{\partial z'^2}\right] - \rho g \ , \quad (2.38)$$

$$\rho\left(\frac{\partial w'}{\partial t'} + u'\frac{\partial w'}{\partial r'} + w'\frac{\partial w'}{\partial z'}\right) = \\ -\frac{Lp_c}{\epsilon\rho u_c^2 H}\frac{\partial p'}{\partial z'} + \frac{\mu L}{\epsilon\rho u_c^2}\left[\frac{\epsilon u_c}{L^2}\frac{1}{r'}\frac{\partial}{\partial r'}\left(r'\frac{\partial w'}{\partial r'}\right) + \frac{\epsilon u_c}{H^2}\frac{\partial^2 w'}{\partial z'^2}\right] - g\cdot\frac{L}{\epsilon u_c^2} \ . \quad (2.39)$$

We, thus, have

$$\frac{1}{r'}\frac{\partial(r'u')}{\partial r'} + \frac{\partial w'}{\partial z'} = 0 \ , \quad (2.40)$$

$$\frac{\partial u'}{\partial t'} + u'\frac{\partial u'}{\partial r'} + w'\frac{\partial u'}{\partial z'} = -\frac{p_c}{\rho u_c^2}\frac{\partial p'}{\partial r'} + \frac{\mu L}{\rho u_c^2}\left\{\frac{u_c}{L^2}\frac{\partial}{\partial r'}\left[\frac{1}{r'}\frac{\partial}{\partial r'}(r'u')\right] + \frac{u_c}{H^2}\frac{\partial^2 u'}{\partial z'^2}\right\} \ , \quad (2.41)$$

$$\frac{\partial w'}{\partial t'} + u'\frac{\partial w'}{\partial r'} + w'\frac{\partial w'}{\partial z'} = \\ -\frac{Lp_c}{\epsilon\rho u_c^2 H}\frac{\partial p'}{\partial z'} + \frac{\mu L}{\epsilon\rho u_c^2}\left[\frac{\epsilon u_c}{L^2}\frac{1}{r'}\frac{\partial}{\partial r'}\left(r'\frac{\partial w'}{\partial r'}\right) + \frac{\epsilon u_c}{H^2}\frac{\partial^2 w'}{\partial z'^2}\right] - g\cdot\frac{L}{\epsilon u_c^2} \ . \quad (2.42)$$

Then, we choose $p_c = \frac{\mu u_c}{L}\frac{1}{\epsilon^2}$ and substitute it into Eq. (2.41) and Eq. (2.42)

For r-direction momentum equation:

$$\epsilon^2\cdot Re\left(\frac{\partial u'}{\partial t'} + u'\frac{\partial u'}{\partial r'} + w'\frac{\partial u'}{\partial z'}\right) = -\frac{\partial p'}{\partial r'} + \epsilon^2\frac{\partial}{\partial r'}\left[\frac{1}{r'}\frac{\partial}{\partial r'}(r'u')\right] + \frac{\partial^2 u'}{\partial z'^2} \ . \quad (2.43)$$

For z-direction momentum equation:

$$\epsilon^4\cdot Re\left(\frac{\partial w'}{\partial t'} + u'\frac{\partial w'}{\partial r'} + w'\frac{\partial w'}{\partial z'}\right) = -\frac{\partial p'}{\partial z'} + \left[\epsilon^4\frac{1}{r'}\frac{\partial}{\partial r'}\left(r'\frac{\partial w'}{\partial r'}\right) + \epsilon^2\frac{\partial^2 w'}{\partial z'^2}\right] - \frac{\rho g L^2\epsilon^3}{\mu u_c} \ . \quad (2.44)$$

where the Reynolds number, ratio of inertia forces to viscous forces, is defined as

$$Re \equiv \frac{\rho u_c L}{\mu} \ ,$$

which is in the range of $10^{-1} \sim 10^{-4}$ for the spreading of a thin and small droplet

$$Re \approx \frac{10^3 \times 10^{-3} \times 10^{-4}}{1 \sim 1 \times 10^{-3}} \approx 10^{-1} \sim 10^{-4} \ .$$

Therefore, Eq. (2.43) and Eq. (2.44), up to leading order approximation, can be written in much simpler form (after dropping primes):

$$-\frac{\partial p}{\partial r} + \frac{\partial^2 u}{\partial z^2} + \cancelto{0}{\mathcal{O}(\epsilon^2, Re \cdot \epsilon^2)} = 0 \ , \tag{2.45}$$

$$\frac{\partial p}{\partial z} + \frac{\rho g L^2 \epsilon^3}{\mu u_c} + \cancelto{0}{\mathcal{O}(\epsilon^2, \epsilon^4, Re \cdot \epsilon^4)} = 0 \ , \tag{2.46}$$

$$\frac{1}{r}\frac{\partial (ru)}{\partial r} + \frac{\partial w}{\partial z} = 0 \ . \tag{2.47}$$

The boundary conditions (Eq. (2.4), Eq. (2.13), Eq. (2.22), and Eq. (2.27)) in the dimensionless form are written as follows. **The no slip boundary condition** at $z = 0$ can be written as

$$u_c u'\Big|_{z'=0} = w_c w'\Big|_{z'=0} = 0 \ , \tag{2.48}$$

or (after dropping primes)

$$u = w = 0 \ . \tag{2.49}$$

The kinematic boundary condition at the free surface ($z = h$) can be written as

$$\frac{\partial h}{\partial t} + u\frac{\partial h}{\partial r} - w = 0 \ , \tag{2.50}$$

$$\frac{\cancel{H}}{\cancel{L}/u_c}\frac{\partial h'}{\partial t'} + \frac{u_c \cancel{H}}{\cancel{L}} u' \frac{\partial h'}{\partial r'} - \cancel{\epsilon u_c} w' = 0 \ , \tag{2.51}$$

or (after dropping primes)

$$\frac{\partial h}{\partial t} + u\frac{\partial h}{\partial r} - w = 0 \ . \tag{2.52}$$

The normal stress balance condition at free surface ($z = h$) can be written as

$$\begin{aligned} p - P_a = \frac{2\mu}{1 + (\frac{\partial h}{\partial r})^2}\left[\frac{\partial u}{\partial r}\left(\frac{\partial h}{\partial r}\right)^2 - \frac{\partial h}{\partial r}\left(\frac{\partial u}{\partial z} + \frac{\partial w}{\partial r}\right) + \frac{\partial w}{\partial z}\right] \\ + \sigma\left\{ -\frac{1}{r}\frac{\partial}{\partial r}\left[\frac{r\frac{\partial h}{\partial r}}{\sqrt{1 + (\frac{\partial h}{\partial r})^2}}\right] + \frac{\partial}{\partial z}\left[\frac{1}{\sqrt{1 + (\frac{\partial h}{\partial r})^2}}\right]\right\} \ , \end{aligned} \tag{2.53}$$

$$p_c \cdot p' - p_c \cdot P'_a$$
$$= \frac{2\mu}{1+\frac{H^2}{L^2}(\frac{\partial h'}{\partial r'})^2}\left[\frac{u_c \cdot H^2}{L^3}\frac{\partial u'}{\partial r'}\left(\frac{\partial h'}{\partial r'}\right)^2 - \frac{H}{L}\frac{\partial h'}{\partial r'}\left(\frac{u_c \cdot \partial u'}{H \cdot \partial z'} + \frac{\epsilon u_c}{L}\frac{\partial w'}{\partial r'}\right) + \frac{\epsilon u_c \cdot \partial w'}{H \cdot \partial z'}\right]$$
$$- \sigma\left\{\frac{1}{L \cdot r'}\frac{\partial}{L \cdot \partial r'}\left[\frac{H \cdot r'\frac{\partial h'}{\partial r'}}{\sqrt{1+\frac{H^2}{L^2}(\frac{\partial h'}{\partial r'})^2}}\right]\right\}, \quad (2.54)$$

$$p_c \cdot p' - p_c \cdot P'_a$$
$$= \frac{2\mu}{1+\epsilon^2(\frac{\partial h'}{\partial r'})^2}\left[\epsilon^2\frac{u_c}{L}\frac{\partial u'}{\partial r'}\left(\frac{\partial h'}{\partial r'}\right)^2 - \frac{\partial h'}{\partial r'}\left(\frac{u_c}{L}\frac{\partial u'}{\partial z'} + \epsilon^2\frac{u_c}{L}\frac{\partial w'}{\partial r'}\right) + \frac{u_c}{L}\frac{\partial w'}{\partial z'}\right]$$
$$- \sigma\left\{\frac{\epsilon}{L}\frac{1}{r'}\frac{\partial}{\partial r'}\left[\frac{r'\frac{\partial h'}{\partial r'}}{\sqrt{1+\epsilon^2(\frac{\partial h'}{\partial r'})^2}}\right]\right\}. \quad (2.55)$$

After neglecting the term $\epsilon^2(\frac{\partial h'}{\partial r'})^2$, Eq. (2.55) can be written as

$$p_c \cdot p' - p_c \cdot P'_a$$
$$= 2\mu\left[\epsilon^2\frac{u_c}{L}\frac{\partial u'}{\partial r'}\left(\frac{\partial h'}{\partial r'}\right)^2 - \frac{\partial h'}{\partial r'}\left(\frac{u_c}{L}\frac{\partial u'}{\partial z'} + \epsilon^2\frac{u_c}{L}\frac{\partial w'}{\partial r'}\right) + \frac{u_c}{L}\frac{\partial w'}{\partial z'}\right]$$
$$- \sigma\left[\frac{\epsilon}{L}\frac{1}{r'}\frac{\partial}{\partial r'}\left(r'\frac{\partial h'}{\partial r'}\right)\right]. \quad (2.56)$$

We divide both sides by p_c and replaced p_c with $\frac{\mu u_c}{L}\frac{1}{\epsilon^2}$,

$$p' - P'_a = \frac{2L \cdot \epsilon^2}{u_c}\left[\epsilon^2\frac{u_c}{L}\frac{\partial u'}{\partial r'}\left(\frac{\partial h'}{\partial r'}\right)^2 - \frac{\partial h'}{\partial r'}\left(\frac{u_c}{L}\frac{\partial u'}{\partial z'} + \epsilon^2\frac{u_c}{L}\frac{\partial w'}{\partial r'}\right) + \frac{u_c}{L}\frac{\partial w'}{\partial z'}\right]$$
$$- \frac{\sigma\epsilon^3}{\mu u_c}\left[\frac{1}{r'}\frac{\partial}{\partial r'}\left(r'\frac{\partial h'}{\partial r'}\right)\right], \quad (2.57)$$

or

$$p' - P'_a = 2\left[\epsilon^4\frac{\partial u'}{\partial r'}\left(\frac{\partial h'}{\partial r'}\right)^2 - \frac{\partial h'}{\partial r'}\left(\epsilon^2\frac{\partial u'}{\partial z'} + \epsilon^4\frac{\partial w'}{\partial r'}\right) + \epsilon^2\frac{\partial w'}{\partial z'}\right]$$
$$- \frac{\sigma\epsilon^3}{\mu u_c}\left[\frac{1}{r'}\frac{\partial}{\partial r'}\left(r'\frac{\partial h'}{\partial r'}\right)\right]. \quad (2.58)$$

The dimensionless normal stress balance condition to the leading order approximation can be rewritten as:

$$p' - P'_a = -\frac{\sigma\epsilon^3}{\mu u_c}\left[\frac{1}{r'}\frac{\partial}{\partial r'}\left(r'\frac{\partial h'}{\partial r'}\right)\right]. \quad (2.59)$$

Let capillary number $Ca = \mu u_c/(\sigma\epsilon^3)$, Eq. (2.59) becomes (after dropping primes)

$$p - P_a = -\frac{1}{Ca}\left[\frac{1}{r}\frac{\partial}{\partial r}\left(r\frac{\partial h}{\partial r}\right)\right] . \tag{2.60}$$

The shear stress balance boundary condition at the free surface ($z = h$) is

$$\frac{1}{\sqrt{1+(\frac{\partial h}{\partial r})^2}}\left[-\frac{\partial u}{\partial r}\frac{\partial h}{\partial r}+\frac{1}{2}\left(\frac{\partial u}{\partial z}+\frac{\partial w}{\partial r}\right)-\frac{1}{2}\left(\frac{\partial u}{\partial z}+\frac{\partial w}{\partial r}\right)\left(\frac{\partial h}{\partial r}\right)^2+\frac{\partial w}{\partial z}\frac{\partial h}{\partial r}\right] = 0 . \tag{2.61}$$

After replacing all dimensional variables with dimensionless variables and characteristic scales, we can rewrite Eq. (2.61) as

$$\begin{aligned} -\epsilon\frac{u_c}{L}\frac{\partial u'}{\partial r'}\frac{\partial h'}{\partial r'}+\frac{1}{2}\left(\frac{u_c}{H}\frac{\partial u'}{\partial z'}+\frac{\epsilon u_c}{L}\frac{\partial w'}{\partial r'}\right) \\ -\frac{1}{2}\left(\frac{u_c}{H}\frac{\partial u'}{\partial z'}+\frac{\epsilon u_c}{L}\frac{\partial w'}{\partial r'}\right)\left(\epsilon\frac{\partial h'}{\partial r'}\right)^2+\frac{\epsilon^2 u_c}{H}\frac{\partial w'}{\partial z'}\frac{\partial h'}{\partial r'} = 0 , \end{aligned} \tag{2.62}$$

$$-\epsilon^2\frac{\partial u'}{\partial r'}\frac{\partial h'}{\partial r'}+\frac{1}{2}\left(\frac{\partial u'}{\partial z'}+\epsilon^2\frac{\partial w'}{\partial r'}\right)-\frac{1}{2}\left(\frac{\partial u'}{\partial z'}+\epsilon^2\frac{\partial w'}{\partial r'}\right)\left(\epsilon\frac{\partial h'}{\partial r'}\right)^2+\epsilon^2\frac{\partial w'}{\partial z'}\frac{\partial h'}{\partial r'} = 0 , \tag{2.63}$$

or

$$\frac{1}{2}\frac{\partial u'}{\partial z'}+\cancelto{0}{\mathcal{O}(\epsilon,\epsilon^2,\epsilon^4)} = 0 . \tag{2.64}$$

Eq. (2.64) to the leading order approximation becomes (after dropping primes)

$$\left.\frac{\partial u}{\partial z}\right|_{z=h} = 0 . \tag{2.65}$$

We summarize the dimensionless governing equations:

$$\frac{1}{r}\frac{\partial(ru)}{\partial r}+\frac{\partial w}{\partial z} = 0 , \tag{2.66}$$

$$-\frac{\partial p}{\partial r}+\frac{\partial^2 u}{\partial z^2} = 0 , \tag{2.67}$$

$$\frac{\partial p}{\partial z}+\frac{\rho g L^2\epsilon^3}{\mu u_c} = 0 , \tag{2.68}$$

with boundary conditions

$$u|_{z=0} = w|_{z=0} = 0 , \tag{2.69}$$

$$\frac{\partial h}{\partial t} + u|_{z=h}\frac{\partial h}{\partial r} - w|_{z=h} = 0 \ , \tag{2.70}$$

$$P|_{z=h} - P_a = -\frac{1}{Ca}\frac{1}{r}\frac{\partial}{\partial r}\left(r\frac{\partial h}{\partial r}\right) \ , \tag{2.71}$$

$$\left.\frac{\partial u}{\partial z}\right|_{z=h} = 0 \ , \tag{2.72}$$

In the next step, we need to solve Eq. (2.68) with boundary condition Eq. (2.69) to find the pressure p. Once we have the expression for pressure, we can find the tangential velocity using Eq. (2.67). By integrating Eq (2.68) over z, we can find the pressure with one unknown coefficient $C_1(r,t)$

$$p = -\frac{\epsilon^3 L^2 \rho g}{\mu u_c} z + C_1(r,t) \ . \tag{2.73}$$

We apply Eq. 2.75 to Eq. 2.77 to find $C_1(r,t)$

$$-\frac{\epsilon^3 L^2 \rho g}{\mu u_c} \cdot h + C_1(r,t) = P_a - \frac{1}{Ca}\left[\frac{1}{r}\frac{\partial}{\partial r}\left(r\frac{\partial h}{\partial r}\right)\right] \ , \tag{2.74}$$

$$C_1(r,t) = P_a + \frac{\epsilon^3 L^2 \rho g}{\mu u_c} \cdot h - \frac{1}{Ca}\left[\frac{1}{r}\frac{\partial}{\partial r}\left(r\frac{\partial h}{\partial r}\right)\right] \ . \tag{2.75}$$

Therefore,

$$p(r,t) = P_a + \frac{\epsilon^3 L^2 \rho g}{\mu u_c} \cdot (h - z) - \frac{1}{Ca}\left[\frac{1}{r}\frac{\partial}{\partial r}\left(r\frac{\partial h}{\partial r}\right)\right] \ . \tag{2.76}$$

The pressure gradient in the r-direction is

$$\frac{\partial p}{\partial r} = \frac{\epsilon^3 L^2 \rho g}{\mu u_c} \cdot \frac{\partial h}{\partial r} - \frac{1}{Ca}\frac{\partial}{\partial r}\left[\frac{1}{r}\frac{\partial}{\partial r}\left(r\frac{\partial h}{\partial r}\right)\right] \ . \tag{2.77}$$

We integrate Eq. (2.68) twice over z,

$$u = \frac{1}{2}\frac{\partial p}{\partial r} z^2 + C_2(r,t) \cdot z + C_3(r,t) \ . \tag{2.78}$$

Due to the no slip condition (Eq. (2.69)), we can immediately recognize that

$$C_3(r,t) = 0 \ . \tag{2.79}$$

From shear stress balance condition, we have one condition for $C_2(r,t)$

$$\left.\frac{\partial u}{\partial z}\right|_{z=h} = \frac{\partial p}{\partial r} \cdot h + C_2(r,t) = 0 \ , \tag{2.80}$$

$$C_2(r,t) = -\frac{\partial p}{\partial r} \cdot h \ . \tag{2.81}$$

The tangential velocity can be expressed as

$$u = \frac{1}{2}\frac{\partial p}{\partial r} z^2 - \frac{\partial p}{\partial r} \cdot h \cdot z \ . \tag{2.82}$$

After substituting Eq. (2.77) into Eq. (2.82), we have the final expression for the tangential velocity

$$u(r,z,t) = \left\{ \frac{\epsilon^3 L^2 \rho g}{\mu u_c} \frac{\partial h}{\partial r} - \frac{1}{Ca} \frac{\partial}{\partial r} \left[\frac{1}{r} \frac{\partial}{\partial r} \left(r \frac{\partial h}{\partial r} \right) \right] \right\} \cdot \left(\frac{1}{2} z^2 - hz \right) \ . \tag{2.83}$$

We integrate the continuity equation (Eq. (2.67)) with respect to z,

$$\int_0^h \left[\frac{1}{r} \frac{\partial}{\partial r} (ru) \right] dz + w \Big|_{z=0}^{z=h} = 0 \ . \tag{2.84}$$

Due to no penetration condition at the interface ($z = 0$), we can recognize that $w\ _{z=0} = 0$ and Eq. (2.84) becomes

$$\int_0^h \left[\frac{1}{r} \frac{\partial}{\partial r} (ru) \right] dz + w\ _{z=h} = 0 \ . \tag{2.85}$$

Then, we substitute Eq. (2.85) into kinematic boundary condition (Eq. (2.70)),

$$\frac{\partial h}{\partial t} + u|_{z=h} \frac{\partial h}{\partial r} + \int_0^h \left[\frac{1}{r} \frac{\partial}{\partial r} (ru) \right] dz = 0 \ . \tag{2.86}$$

According to the Leibniz's integral rule, we have

$$\frac{1}{r} \frac{\partial}{\partial r} \left(\int_0^{h(r,t)} ru \cdot dz \right) = r \cdot u\ _{z=h} \cdot \frac{1}{r} \frac{\partial h}{\partial r} + \int_0^h \left[\frac{1}{r} \frac{\partial}{\partial r} (ru) \right] dz \tag{2.87}$$

$$= u\ _{z=h} \cdot \frac{\partial h}{\partial r} + \int_0^h \left[\frac{1}{r} \frac{\partial}{\partial r} (ru) \right] dz \ . \tag{2.88}$$

Therefore, we can replace the second and third terms in Eq. (2.86) with left hand side of the Eq. (2.87):

$$\frac{\partial h}{\partial t} + \frac{1}{r} \frac{\partial}{\partial r} \left(\int_0^{h(r,t)} ru \cdot dz \right) = 0 \ . \tag{2.89}$$

The vertically averaged horizontal velocity is found to be

$$\overline{u} = \frac{1}{h} \int_0^h u dz = \frac{1}{h} \frac{\partial p}{\partial r} \left(-\frac{1}{3} h^3 \right) \ . \tag{2.90}$$

Then, Eq. (2.89) can expressed as

$$\frac{\partial h}{\partial t} - \frac{1}{r}\frac{\partial}{\partial r}\left(\frac{1}{3}rh^3\frac{\partial p}{\partial r}\right) = 0 \ , \tag{2.91}$$

where the pressure is given by

$$p = Pa + \frac{\epsilon^3 L^2 \rho g}{\mu u_c}(h - z) - \frac{1}{Ca}\frac{1}{r}\frac{\partial}{\partial r}\left(r\frac{\partial h}{\partial r}\right) \ . \tag{2.92}$$

and the capillary number is defined as

$$Ca = \frac{\mu u_c}{\sigma \epsilon^3} \ . \tag{2.93}$$

The no slip boundary condition is enforced at points away from the contact line. For points near the contact line, we need to incorporate the Navier slip model into our governing equation to avoid the force-singularity issue. Therefore, Eq. (2.4) can be expressed as

$$u\underset{z=0}{} = \lambda(h)\left[\frac{\partial u}{\partial z} + \frac{\partial w}{\partial r}\right] \ . \tag{2.94}$$

After following the same derivation in this subsection, we can arrive at the similar lubrication equation for the droplet profile with the above mentioned slip models (Haley & Miksis [11]) :

$$\frac{\partial h}{\partial t} - \frac{1}{r}\frac{\partial}{\partial r}\left(r\left[\frac{1}{3}h^3 + \lambda(h)\cdot h^2\right]\frac{\partial p}{\partial r}\right) = 0 \ . \tag{2.95}$$

There are two regimes of spreading in this problem: gravitational spreading and capillary spreading. Gravitational spreading occurs when gravitational effects dominate

$$Bo \equiv \frac{\rho g L^2}{\sigma} \gg 1 \ . \tag{2.96}$$

The spreading is due to the action of gravity, or, more accurately, due to the gradient in hydrostatic pressure which is caused by nonuniform depth of the droplet. Therefore, we can neglect the capillary pressure as well as the Marangoni effect (Marangoni effect has already been ruled out due to constant surface tension coefficient: $\nabla_s \sigma = 0$ in Eq. (2.23)) and replace u_c with $\sigma\epsilon^3/\mu$. The pressure p can be written as (setting ambient pressure to be zero for simplicity)

$$p = Bo \cdot h \ . \tag{2.97}$$

The equation governing shape function of droplet h becomes

$$\frac{\partial h}{\partial t} - Bo \cdot \frac{1}{r}\frac{\partial}{\partial r}\left(\frac{1}{3}rh^3\frac{\partial h}{\partial r}\right) = 0 \ . \tag{2.98}$$

It was originally investigated by Huppert & Simpson [32], and subsequently a relevant analysis has been performed by Leal [33] to answer the question regarding to spreading rate and the shape as a function time. For capillary spreading, the spreading is driven by capillary effect. It is required that

$$Bo \equiv \frac{\rho g L^2}{\sigma} \ll 1 \ . \tag{2.99}$$

The pressure p can then be written as

$$p = -\frac{1}{Ca}\frac{1}{r}\frac{\partial}{\partial r}\left(r\frac{\partial h}{\partial r}\right) \ . \tag{2.100}$$

The equation governing shape function of droplet h becomes

$$\frac{\partial h}{\partial t} + \frac{1}{Ca}\frac{1}{r}\frac{\partial}{\partial r}\left\{\frac{1}{3}rh^3\frac{\partial}{\partial r}\left[\frac{1}{r}\frac{\partial}{\partial r}\left(r\frac{\partial h}{\partial r}\right)\right]\right\} = 0 \ . \tag{2.101}$$

One can think of the internal motion which leads to the deformation of shape as being caused by the internal pressure gradients that are determined by the local gradients of surface curvature along the interface.

The methodology to solve Eq. (2.98) and Eq. (2.101) is discussed in Chapter 3. We can use analytical method or numerical simulations to obtain the solution to gravitational spreading and verify against the experiments while we can only resort to numerics to have the solution of the capillary spreading. However, some scaling argument has been purposed by Warren [34] to accurately predict the rate of spreading which can be verified by the Tanner's spreading law for the Newtonian case.

2.2.2 Spreading Over a Porous Substrate with the Beavers and Joseph Condition

In this section, the case of a Newtonian droplet spreading over a homogeneous porous medium (Fig. 2.2) has been investigated. The surface of the porous substrate is assumed to be ideally smooth which avoids implementation for surface topology. Therefore, the contact-line hysteresis doesn't occur in our theoretical investigation and numerical results. The no slip boundary condition is replaced with the Beavers and Joseph condition to describe the problem more accurately and realistically.

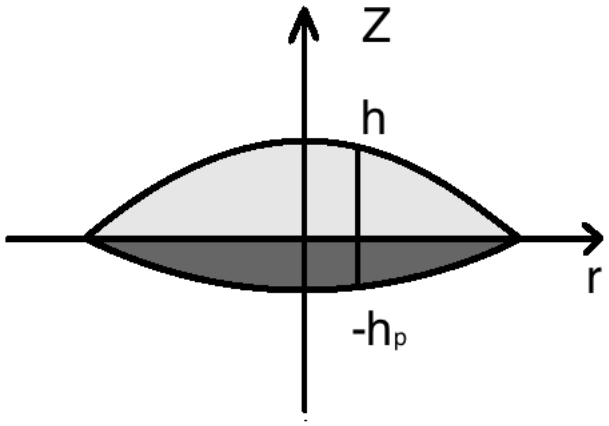

Figure 2.2. Schematic of a droplet spreading over a porous media.

For fluid flow above the surface of substrate, we start from the dimensionless governing equations and the boundary conditions we've derived in the previous section. Note that the variables with subscript "p" denote the variables in porous-media and the variables with primes denotes the dimensionless variables.

$$\frac{1}{r'}\frac{\partial(r'u')}{\partial r'} + \frac{\partial w'}{\partial z'} = 0 \ , \tag{2.102}$$

$$-\frac{\partial p'}{\partial r'} + \frac{\partial^2 u'}{\partial z'^2} = 0 \ , \tag{2.103}$$

$$\frac{\partial p'}{\partial z'} + \frac{\rho g L^2 \epsilon^3}{\mu u_c} = 0 \ , \tag{2.104}$$

with the dimensionless boundary conditions

$$\left.\frac{du'}{dz'}\right|_{z'=0} = \frac{\beta \cdot H}{\sqrt{\kappa}}(u'|_{z=0} - u'_p|_{z=0}) \ , \tag{2.105}$$

$$\frac{\partial h'}{\partial t'} + u'|_{z=h}\frac{\partial h'}{\partial r'} - w'|_{z'=h} = 0 \ , \tag{2.106}$$

$$p'|_{z=h} - P'_a = -\frac{1}{Ca}\left[\frac{1}{r'}\frac{\partial}{\partial r'}\left(r'\frac{\partial h'}{\partial r'}\right)\right] \ , \tag{2.107}$$

$$\left.\frac{\partial u'}{\partial z'}\right|_{z'=h'} = 0 \ . \tag{2.108}$$

We have the continuity of the normal velocity and the pressure at the surface of substrate,

$$w'_{z=0} = w'_{p\,z=0} \ , \tag{2.109}$$

$$p'_{z=0} = p'_{p\,z=0} \ . \tag{2.110}$$

From Eq. (2.103), we know that the horizontal velocity can be written as

$$u' = \frac{1}{2}\frac{\partial p'}{\partial r'}z'^2 + C_1(r',t') \cdot z' + C_2(r',t') \ , \tag{2.111}$$

Given the expression for u' is known, the tangential velocity and the shear rate at the surface of the porous substrate ($z = 0$) can be written in terms of the unknown coefficients, C_1 and C_2

$$u'_{z'=0} = C_2(r',t') \ , \tag{2.112}$$

$$\frac{\partial u'}{\partial z'} = \frac{\partial p'}{\partial r'}z' + C_1(r',t') \ , \tag{2.113}$$

$$\left.\frac{\partial u'}{\partial z'}\right|_{z'=0} = C_1(r',t') \ . \tag{2.114}$$

After applying Eq. (2.108) to the tangential velocity, we can have one more equation for the unknown coefficient

$$\left.\frac{\partial u'}{\partial z'}\right|_{z'=h'} = \frac{\partial p'}{\partial r'}h' + C_1 = 0 \ , \tag{2.115}$$

$$C_1 = -\frac{\partial p'}{\partial r'} \cdot h' \ . \tag{2.116}$$

The unknown coefficients C_2 can be determined by applying the Eq. (2.112) and Eq. (2.116) into Eq. (2.105). The tangential velocity inside the porous medium is needed in Eq. (2.105) and, therefore, should be determined from the governing equations inside the porous medium.

We assume the flow inside the porous substrate is governed by the Darcy's law, and the Darcian velocities u_p and w_p are volume-averaged velocities. The Darcy's law in horizontal and vertical directions can be written as

$$u_p = -\frac{\kappa}{\mu}\frac{\partial p_p}{\partial r} \ , \tag{2.117}$$

$$w_p = -\frac{\kappa}{\mu}\left(\frac{\partial p_p}{\partial z} + \rho g\right) \ . \tag{2.118}$$

In fact, u_p and w_p are not the velocities which the fluid traveling through the pores is experiencing. However, they can still be calculated knowing the porosity of the substrate :

$$\vec{V} = \frac{\vec{v_p}}{\phi} \ . \tag{2.119}$$

Besides, the Darcy velocity still satisfies the continuity equation :

$$\nabla \cdot \left(\frac{\vec{v_p}}{\phi}\right) = 0 \ , \tag{2.120}$$

or

$$\nabla \cdot \vec{v_p} = 0 \ . \tag{2.121}$$

Therefore, the dimensional continuity equation in the cylindrical coordinate system still holds

$$\frac{1}{r}\frac{\partial (r u_p)}{\partial r} + \frac{\partial w_p}{\partial z} = 0 \ . \tag{2.122}$$

The boundary conditions at the wetting front ($z = -h_p$) are

$$p_p|_{z=-h_p} = P_a - P_{ca} \ , \tag{2.123}$$

$$\phi\frac{\partial h_p}{\partial t} + u_p\Big|_{z=-h_p}\frac{\partial h_p}{\partial r} + w_p\Big|_{z=-h_p} = 0 \ , \tag{2.124}$$

where P_{ca} is the capillary pressure representing the pressure jump between saturated and unsaturated domain. The capillary pressure is defined as

$$P_{ca} = p_{non-wetting\ phase} - p_{wetting\ phase}\ , \tag{2.125}$$

and can be calculated by the most commonly used variation of capillary pressure equation

$$P_{ca} = \frac{2\sigma Cos\theta}{r_c}\ , \tag{2.126}$$

where θ is the the wetting angle of the liquid on the surface of the capillary, r_c is the effective pore radius.

Substituting Eq. (2.117) and Eq. (2.118) into Eq. (2.122), we can find that the continuity equation is transformed to a Laplace equation for pressure.

$$\frac{1}{r}\frac{\partial}{\partial r}\left(- r\frac{\kappa}{\mu}\frac{\partial p_p}{\partial r}\right) + \frac{\partial}{\partial z}\left[- \frac{\kappa}{\mu}\left(\frac{\partial p_p}{\partial z} + \rho g\right)\right] = 0 \tag{2.127}$$

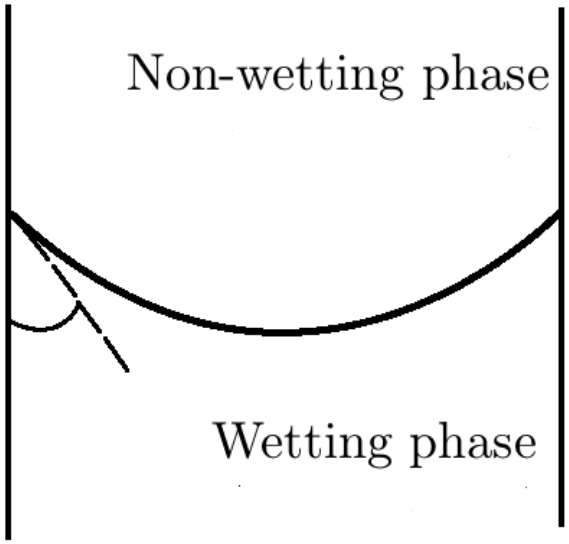

Figure 2.3. Schematic of capillary pressure in a thin tube.

$$\frac{1}{r}\frac{\partial}{\partial r}\left(r\frac{\partial p_p}{\partial r}\right)+\frac{\partial^2 p_p}{\partial z^2}=0 \tag{2.128}$$

By using the following relations, we are able to write Eq. (2.128) in the dimensionless form,

$$u \equiv u_c \cdot u',\ h \equiv H \cdot h',\ r \equiv L \cdot r',\ p \equiv p_c \cdot p',$$
$$w \equiv w_c \cdot w',\ z \equiv H \cdot z',\ \text{and } t \equiv \left(\frac{L}{u_c}\right)t' \ ,$$

Thus, Eq. (2.128) can be written as

$$\epsilon^2\frac{1}{r'}\frac{\partial}{\partial r'}\left(r'\frac{\partial p'_p}{\partial r'}\right)+\frac{\partial^2 p'_p}{\partial z'^2}=0 \ . \tag{2.129}$$

We calculate the flow field and profile of a thin droplet. We can further simplify Eq. (2.129) because the ratio of height to radius of a thin droplet is around or below 0.1. Therefore, Eq. (2.129) to the leading order approximation is given by

$$\frac{\partial^2 p'_p}{\partial z'^2}+\cancelto{0}{\mathcal{O}(\epsilon^2)}=0 \ . \tag{2.130}$$

After integrating Eq. (2.130) twice with respect to z, we can have the expression for pressure field of flow inside the porous medium.

$$p'_p = C_3(r,t)\cdot z + C_4(r,t) \ . \tag{2.131}$$

Eq. (2.110) and Eq. (2.123) are made dimensionless first and rewritten in terms of the unknown coefficients C_3 and C_4 by applying Eq. (2.131) to them,

$$p'_{p\,\big|_{z'=0}} = C_4(r',t') = p'_{\big|_{z'=0}} \ , \tag{2.132}$$

$$C_3(r,t)\cdot(-h'_p)+C_4(r,t)=P'_a-P'_{ca} \ . \tag{2.133}$$

Then, the horizontal velocity inside the medium u'_p can be written as

$$u'_p=-\frac{\kappa}{\mu}\frac{p_{ca}}{u_c L}\left(\frac{\partial C_3}{\partial r}z+\frac{\partial C_4}{\partial r}\right) \ , \tag{2.134}$$

$$u'_{p\,\big|_{z'=0}}=-\frac{\kappa}{\mu}\frac{p_{ca}}{u_c L}\frac{\partial C_4}{\partial r'} \ . \tag{2.135}$$

After substituting Eq. (2.112), Eq. (2.114), and Eq. (2.135) into Eq. (2.105), the Beavers and Joseph condition can be written in terms unknown coefficients,

$$C_1(r',t') = \frac{\beta \cdot H}{\sqrt{\kappa}}\left(C_2(r',t') - \frac{\kappa p_c}{\mu u_c L}\frac{\partial C_4}{\partial r'}\right) . \tag{2.136}$$

The goal here is to find the expression for C_1, C_2, C_3, and C_4. The solution steps can be described as follows : (i) Using Eq. (2.104) and Eq. (2.107) to find pressure p, (ii) determining $C_1(r',t')$, $C_3(r',t')$, and $C_4(r',t')$ from Eq. (2.116), Eq. (2.132), and Eq. (2.133), respectively, (iii) substituting $C_1(r',t')$, $C_3(r',t')$, and $C_4(r',t')$ into Eq. (2.136) to determine $C_2(r',t')$, (iv) then expressing tangential velocity u' and u'_p in terms of C_1, C_2, C_3, and C_4.

We start our derivation from step (i). The pressure can be determine by integrating Eq. (2.104)

$$\frac{\partial p'}{\partial z'} = -\frac{\rho g L^2 \epsilon^3}{\mu u_c} , \tag{2.137}$$

$$p' = -\frac{\rho g L^2 \epsilon^3}{\mu u_c} z + K_1(r,t) . \tag{2.138}$$

After applying Eq. (2.107) to Eq. (2.138), we can determine the integration coefficient, K_1, and obtain the final form of pressure

$$P'_a - \frac{\sigma H^3}{\mu L^3 u_c}\frac{1}{r'}\frac{\partial}{\partial r'}\left(r\frac{\partial h'}{\partial r'}\right) = -\frac{\rho g L^2 \epsilon^3}{\mu u_c} h' + K_1(r,t) , \tag{2.139}$$

$$K_1(r,t) = p'_a + \frac{\rho g L^2 \epsilon^3}{\mu u_c} h' - \frac{\sigma H^3}{\mu L^3 u_c}\frac{1}{r'}\frac{\partial}{\partial r'}\left(r\frac{\partial h'}{\partial r'}\right) , \tag{2.140}$$

$$p' = P'_a + \frac{\rho g L^2 \epsilon^3}{\mu u_c}(h' - z') - \frac{\sigma H^3}{\mu L^3 u_c}\frac{1}{r'}\frac{\partial}{\partial r'}\left(r\frac{\partial h'}{\partial r'}\right) . \tag{2.141}$$

After substituting Eq. (2.141) into Eq. (2.116), we can obtain the expression for the unknown coefficient $C_1(r',t')$

$$\begin{aligned} C_1(r',t') &= -\frac{\partial p'}{\partial r'} \cdot h' \\ &= -\left\{\frac{\rho g \epsilon^3 L^2}{\mu u_c}\frac{\partial h'}{\partial r'} - \frac{\sigma H^3}{\mu L^3 u_c}\frac{\partial}{\partial r'}\left[\frac{1}{r'}\frac{\partial}{\partial r'}\left(r'\frac{\partial h'}{\partial r'}\right)\right]\right\} \cdot h' . \end{aligned} \tag{2.142}$$

After substituting Eq. (2.141) into Eq. (2.132), we can obtain the expression for the unknown coefficient $C_4(r',t')$

$$p'_p{}_{z'=0} = C_4(r',t') = p'_{z'=0} , \tag{2.143}$$

$$C_4(r',t') = P'_a + \frac{\rho g \epsilon^3 L^2}{\mu u_c} h' - \frac{\sigma H^3}{\mu L^3 u_c} \frac{1}{r'} \frac{\partial}{\partial r'} \left(r' \frac{\partial h'}{\partial r'} \right) . \tag{2.144}$$

After substituting Eq. (2.141) and Eq. (2.144) into Eq. (2.133), we can obtain the expression for the unknown coefficient $C_3(r',t')$

$$C_3(r,t) \cdot (-h'_p) + C_4(r,t) = P'_a - P'_{ca} , \tag{2.145}$$

$$- C_3(r,t) \cdot h'_p + P'_a + \frac{\rho g \epsilon^3 L^2}{\mu u_c} h' - \frac{\sigma H^3}{\mu L^3 u_c} \frac{1}{r} \frac{\partial}{\partial r'} \left(r' \frac{\partial h'}{\partial r'} \right) = P'_a - p'_{ca} , \tag{2.146}$$

$$C_3(r',t') \ = \frac{\rho g \epsilon^3 L^2}{\mu u_c} \frac{h'}{h'_p} - \frac{\sigma H^3}{\mu L^3 u_c} \frac{1}{h'_p} \frac{1}{r} \frac{\partial}{\partial r'} \left(r' \frac{\partial h'}{\partial r'} \right) + \frac{P'_{ca}}{h'_p} . \tag{2.147}$$

Plugging Eq. (2.142), Eq. (2.144) into Eq. (2.136), we then have the equation to determine the final unknown coefficient $C_2(r',t')$

$$\begin{aligned} &- \left\{ \frac{\rho g \epsilon^3 L^2}{\mu u_c} \frac{\partial h'}{\partial r'} - \frac{\sigma H^3}{\mu L^3 u_c} \frac{\partial}{\partial r'} \left[\frac{1}{r'} \frac{\partial}{\partial r'} \left(r' \frac{\partial h'}{\partial r'} \right) \right] \right\} \cdot h' \\ &\quad = \frac{\beta H}{\sqrt{\kappa}} \left[C_2 + \frac{\kappa p_c}{\mu u_c L} \left(\frac{\rho g \epsilon^3 L^2}{\mu u_c} \frac{\partial h'}{\partial r'} - \frac{\sigma H^3}{\mu L^3 u_c} \frac{\partial}{\partial r'} \left(\frac{1}{r'} \frac{\partial}{\partial r'} \left(r' \frac{\partial h'}{\partial r'} \right) \right) \right) \right] , \end{aligned} \tag{2.148}$$

or

$$- \frac{\partial p'}{\partial r'} \cdot h' = \frac{\beta H}{\sqrt{\kappa}} \left[C_2 + \frac{\kappa p_c}{\mu u_c L} \frac{\partial p'}{\partial r'} \right] , \tag{2.149}$$

$$- \frac{\partial p'}{\partial r'} \cdot \left(h' + \frac{\sqrt{\kappa} \epsilon \beta p_c}{\mu u_c} \right) = \frac{\beta H}{\sqrt{\kappa}} C_2 , \tag{2.150}$$

$$C_2(r',t') = - \frac{\partial p'}{\partial r'} \cdot \left(\frac{\sqrt{\kappa}}{\beta H} h' + \frac{\kappa p_c}{\mu u_c L} \right) . \tag{2.151}$$

Thus, we have the tangential velocity in terms of r' and h'

$$u' = - \frac{1}{2} \frac{\partial p'}{\partial r'} z^2 + C_1 \cdot z + C_2 \tag{2.152}$$

$$= - \frac{1}{2} \frac{\partial p'}{\partial r'} z^2 + \left(- \frac{\partial p'}{\partial r'} h' \right) \cdot z + - \frac{\partial p'}{\partial r'} \left(\frac{\sqrt{\kappa}}{\beta H} h' + \frac{\kappa p_c}{\mu u_c L} \right) \tag{2.153}$$

$$= \left[\frac{1}{2} z'^2 - h' z' - \left(\frac{\sqrt{\kappa}}{\beta H} h' + \frac{\kappa p_c}{\mu u_c L} \right) \right] \frac{\partial p'}{\partial r'} . \tag{2.154}$$

We integrate the continuity equation (Eq. (2.102)) with respect to z,

$$\int_0^{h'} \left[\frac{1}{r'} \frac{\partial}{\partial r'} (r' u') \right] dz' + w \Big|_{z'=0}^{z'=h} = 0 , \tag{2.155}$$

or

$$-w'_{z'=h'} = \int_0^{h'} \left[\frac{1}{r'}\frac{\partial}{\partial r'}(r'u')\right]dz' - w_{z'=0} . \tag{2.156}$$

We, then, substitute Eq. (2.156) into Eq. (2.106), and rewrite the kinematic boundary condition.

$$\frac{\partial h'}{\partial t'} + u'|_{z'=h'}\frac{\partial h'}{\partial r'} + \int_0^{h'} \left[\frac{1}{r'}\frac{\partial}{\partial r'}(r'u')\right]dz' - w'_{z'=0} = 0 . \tag{2.157}$$

According to the Leibniz integral rule, we have

$$\frac{1}{r'}\frac{\partial}{\partial r'}\left(\int_0^{h'(r',t')} r'u'\cdot dz'\right) = r'\cdot u'_{z'=h'}\cdot\frac{1}{r'}\frac{\partial h'}{\partial r'} + \int_0^{h'}\left[\frac{1}{r'}\frac{\partial}{\partial r'}(r'u')\right]dz' , \tag{2.158}$$

$$= u'_{z'=h'}\cdot\frac{\partial h'}{\partial r'} + \int_0^{h'}\left[\frac{1}{r'}\frac{\partial}{\partial r'}(r'u')\right]dz' . \tag{2.159}$$

Thus, we replace the second and third terms in Eq. (2.157) with left hand side of the Eq. (2.158). The kinematic boundary condition can be written as

$$\frac{\partial h'}{\partial t'} + \frac{1}{r'}\frac{\partial}{\partial r'}\left(\int_0^{h'(r',t')} r'u'\cdot dz'\right) - w'_{z'=0} = 0 , \tag{2.160}$$

or

$$\frac{\partial h'}{\partial t'} + \frac{1}{r'}\frac{\partial}{\partial r'}\left(r'h'\cdot\overline{u}'\right) - w'_{z'=0} = 0 . \tag{2.161}$$

The vertically averaged horizontal velocity $\overline{u}'$ can be determined by integrating Eq. (2.152),

$$\overline{u}' = \frac{1}{h'}\int_0^{h'} u'dz' \tag{2.162}$$

$$= \frac{1}{h'}\frac{\partial p'}{\partial r'}\int_0^{h'}\left[\frac{1}{2}z'^2 - h'z' - \left(\frac{\sqrt{\kappa}}{\beta H}h' + \frac{\kappa p_c}{\mu u_c L}\right)\right]dz' \tag{2.163}$$

$$= \frac{1}{h'}\frac{\partial p'}{\partial r'}\left[-\frac{1}{3}h'^3 - \frac{\sqrt{\kappa}}{\beta H}h'^2 - \frac{\kappa p_c}{\mu u_c L}h'\right] . \tag{2.164}$$

The absorption velocity $w'|_{z'=0}$ can be calculated from the continuity condition for the normal velocity (Eq. (2.109))

$$w'_{z=0} = w'_{p\,z'=0} = -\frac{\kappa}{\mu}\left(\frac{p_c}{Hw_c}\frac{\partial p_p}{\partial z'}_{z'=0} + \frac{\rho g}{w_c}\right) \tag{2.165}$$

$$= -\frac{\kappa}{\mu}\left(\frac{p_c}{Hw_c}C_3(r',t') + \frac{\rho g}{w_c}\right) \tag{2.166}$$

$$= -\frac{\kappa}{\mu}\left\{\frac{p_c}{Hw_c}\left[\frac{\rho g\epsilon^3 L^2}{\mu u_c}\frac{h'}{h'_p} - \frac{\sigma H^3}{\mu L^3 u_c}\frac{1}{h'_p}\frac{1}{r}\frac{\partial}{\partial r'}\left(r'\frac{\partial h'}{\partial r'}\right) + \frac{p'_{ca}}{h'_p}\right] + \frac{\rho g}{w_c}\right\} . \tag{2.167}$$

After substituting Eq. (2.162) and Eq. (2.165) into Eq. (2.161), we can obtain the equation that governs the profile of the droplet ;

$$\frac{\partial h'}{\partial t'} + \frac{1}{r'}\frac{\partial}{\partial r'}\left[r'\frac{\partial p'}{\partial r'}\left(-\frac{1}{3}h'^3 - \frac{\sqrt{\kappa}}{\beta H}h'^2 - \frac{\kappa p_c}{\mu u_c L}h'\right)\right] = \\ -\frac{\kappa}{\mu}\left\{\frac{p_c}{H w_c}\left[\frac{\rho g \epsilon^3 L^2}{\mu u_c}\frac{h'}{h'_p} - \frac{\sigma H^3}{\mu L^3 u_c}\frac{1}{h'_p}\frac{1}{r}\frac{\partial}{\partial r'}\left(r'\frac{\partial h'}{\partial r'}\right) + \frac{p'_{ca}}{h'_p}\right] + \frac{\rho g}{w_c}\right\} . \quad (2.168)$$

Then, we let

$$p_c = \frac{\mu u_c}{L}\frac{1}{\epsilon^2} . \quad (2.169)$$

The factors can be rewritten as

$$\frac{p_c}{H w_c} = \frac{\mu}{\epsilon^2}\cdot\frac{1}{H^2} , \quad (2.170)$$

$$\frac{p_c}{L u_c} = \frac{\mu}{\epsilon^2}\cdot\frac{1}{L^2} . \quad (2.171)$$

After plugging above two relations into Eq. (2.168), we can rewrite the final form of the droplet profile evolution equation :

$$\frac{\partial h'}{\partial t'} + \frac{1}{r'}\frac{\partial}{\partial r'}\left[r'\frac{\partial p'}{\partial r'}\left(-\frac{1}{3}h'^3 - \frac{\sqrt{\kappa}}{\beta H}h'^2 - \frac{\kappa}{\epsilon^2\cdot L^2}h'\right)\right] = \\ -Pm\left[Bo\cdot h' - \frac{1}{Ca}\frac{1}{r'}\frac{\partial}{\partial r'}\left(r'\frac{\partial h'}{\partial r'}\right) + p_{ca}\right]\Big/ h'_p - Pm\cdot Bo , \quad (2.172)$$

or (after dropping primes)

$$\frac{\partial h}{\partial t} + \frac{1}{r}\frac{\partial}{\partial r}\left[r\frac{\partial p}{\partial r}\left(-\frac{1}{3}h^3 - \frac{\sqrt{\kappa}}{\beta H}h^2 - \frac{\kappa}{\epsilon^2\cdot L^2}h\right)\right] \\ + Pm\left[Bo\cdot\left(1+\frac{h}{h_p}\right) - \frac{1}{Ca}\frac{1}{h_p}\frac{1}{r}\frac{\partial}{\partial r}\left(r\frac{\partial h}{\partial r}\right) + \frac{p'_{ca}}{h_p}\right] = 0 , \quad (2.173)$$

where β is the slip coefficient and the dimensionless groups are defined as follows:

$$Pm \equiv \frac{\kappa\cdot L^2}{H^4},\ Bo \equiv \frac{\rho g\epsilon^3 L^2}{\mu u_c},\ Ca \equiv \frac{\mu u_c}{\sigma\epsilon^3},\ \text{and } p'_{ca} \equiv \frac{P_{ca}L^2}{\sigma H} .$$

To find out the evolution equation for the wetting front, we start our derivation from dimensionless form of the continuity equation inside the porous substrate (Eq. (2.122)),

$$\frac{1}{r'}\frac{\partial(r'u'_p)}{\partial r'} + \frac{\partial w'_p}{\partial z'} = 0 . \quad (2.174)$$

We integrate Eq. (2.174) with respect to z,

$$\int_{-h'_p}^{0} \frac{1}{r'}\frac{\partial}{\partial r'}(r'u'_p)\ dz' + w_p \Big|_{-h'_p}^{0} = 0\ , \tag{2.175}$$

or

$$w'_p \Big|_{z'=-h'_p} = \int_{-h'_p}^{0} \frac{1}{r'}\frac{\partial}{\partial r'}(r'u'_p)\ dz' + w_p \Big|_{z'=0}\ . \tag{2.176}$$

After substituting Eq. (2.176) into dimensionless form of kinematic boundary condition for the wetting front, we rewrite Eq. (2.124),

$$\phi\frac{\partial h'_p}{\partial t'} + u'_p \Big|_{z'=-h'_p}\frac{\partial h'_p}{\partial r'} + \int_{-h'_p}^{0} \frac{1}{r'}\frac{\partial}{\partial r'}(r'u'_p)\ dz' + w'_p \Big|_{z'=0} = 0\ . \tag{2.177}$$

Similarly, after applying the Leibniz integral rule, we have

$$\phi\frac{\partial h'_p}{\partial t'} + \frac{1}{r'}\frac{\partial}{\partial r'}\int_{-h'_p}^{0} r'u'_p\ dz' + w'_p \Big|_{z'=0} = 0\ . \tag{2.178}$$

The tangential velocity inside the porous medium is given by

$$u'_p = -\frac{\kappa p_c}{\mu u_c L}\left(\frac{\partial C_3}{\partial r'}z' + \frac{\partial C_4}{\partial r'}\right) \tag{2.179}$$

Then, we can write the vertically averaged horizontal velocity by integrating Eq. (2.179)

$$\int_{-h'_p}^{0} r'u'_p\ dz' = r'\int_{-h'_p}^{0}\left(-\frac{\kappa p_c}{\mu u_c L}\right)\cdot\left(\frac{\partial C_3}{\partial r'}z + \frac{\partial C_4}{\partial r}\right)\ dz' \tag{2.180}$$

$$= -\frac{\kappa p_c}{\mu u_c L}\cdot r'\left(\frac{1}{2}\frac{\partial C_3}{\partial r'}z'^2 + \frac{\partial C_4}{\partial r'}z'\right)\Big|_{-h'_p}^{0} \tag{2.181}$$

$$= -\frac{\kappa p_c}{\mu u_c L}\cdot r'\left(-\frac{1}{2}\frac{\partial C_3}{\partial r'}h_p'^{\,2} + \frac{\partial C_4}{\partial r'}h'_p\right) \tag{2.182}$$

After substituting Eq. (2.165) and Eq. (2.180) into Eq. (2.177), we determine the evolution equation of the wetting front

$$\phi\frac{\partial h'_p}{\partial t'} - \frac{\kappa}{L^2\cdot\epsilon^2}\frac{1}{r'}\frac{\partial}{\partial r'}\left[r'\left(-\frac{1}{2}\frac{\partial C_3}{\partial r'}h_p'^{\,2} + \frac{\partial C_4}{\partial r'}h'_p\right)\right] =$$
$$\frac{\kappa}{\mu}\left\{\frac{p_c}{Hw_c}\left[\frac{\rho g\epsilon^3 L^2}{\mu u_c}\frac{h'}{h'_p} - \frac{\sigma H^3}{\mu L^3 u_c}\frac{1}{h'_p}\frac{1}{r}\frac{\partial}{\partial r'}\left(r'\frac{\partial h'}{\partial r'}\right) + \frac{p'_{ca}}{h'_p}\right] + \frac{\rho g}{w_c}\right\}\ , \tag{2.183}$$

or (after dropping primes)

$$\frac{\partial h_p}{\partial t} - \frac{Pm \cdot \epsilon^2}{\phi}\frac{1}{r}\frac{\partial}{\partial r}\left[r\left(-\frac{1}{2}\frac{\partial C_3}{\partial r}{h_p}^2 + \frac{\partial C_4}{\partial r}h_p\right)\right] = \frac{Pm}{\phi}\left[Bo \cdot \left(1 + \frac{h}{h_p}\right) - \frac{1}{Ca}\frac{1}{h_p}\frac{1}{r}\frac{\partial}{\partial r}\left(r\frac{\partial h}{\partial r}\right) + \frac{p'_{ca}}{h_p}\right] , \quad (2.184)$$

where

$$C_3(r,t) = \frac{p'_{ca}}{h_p} + Bo \cdot \frac{h}{h_p} - \frac{1}{Ca}\frac{1}{h_p}\frac{1}{r}\frac{\partial}{\partial r}\left(r\frac{\partial h}{\partial r}\right) , \quad (2.185)$$

$$C_4(r,t) = P_a + Bo \cdot h - \frac{1}{Ca}\frac{1}{r}\frac{\partial}{\partial r}\left(r\frac{\partial h}{\partial r}\right) . \quad (2.186)$$

Eq. (2.173) and Eq. (2.184) are two coupled lubrication equations describing both the droplet profile and wetting front.

2.3 Mathematical Formulation (Power-Law Droplet)

An important type of non-Newtonian fluids is the so-called power-law fluids following the Ostwaldde Waele relation. The power-law dependence of viscosity μ on the deformation rate $\dot{\gamma}$ is given by

$$\mu(\dot{\gamma}) = \mu_0 |\dot{\gamma}|^{n-1} \ , \tag{2.187}$$

$$\tau_{ij} = \mu S_{ij} \ , \tag{2.188}$$

Here, μ_0 is the zero-shear-rate viscosity, and n is the power-law exponent ($n = 1$ corresponds to a Newtonian liquid). The shear rate $\dot{\gamma}$ in Eq. (2.187) is defined using this the rate-of-deformation tensor $\underline{\underline{S}}$

$$\underline{\underline{S}} = \nabla \vec{u} + \nabla \vec{u}^T \ , \tag{2.189}$$

$$\dot{\gamma} = \sqrt{\frac{1}{2}(\underline{\underline{S}} : \underline{\underline{S}})} \ . \tag{2.190}$$

The components of rate-of-deformation tensor are give by

$$S_{rr} = 2\frac{\partial u}{\partial r}, \ S_{\theta\theta} = 2\frac{u}{r} \ , \tag{2.191}$$

$$S_{rz} = S_{zr} = \left(\frac{\partial w}{\partial r} + \frac{\partial u}{\partial z}\right), \ S_{zz} = 2\frac{\partial w}{\partial z} \ . \tag{2.192}$$

In this section, steps of the derivation for the evolution equations are similar to those in the previous section except using the rate-dependent viscosity in the derivation.

2.3.1 Spreading Over a Solid Substrate

We start from the continuity and Cauchy momentum equations in a cylindrical coordinate:

$$\frac{1}{r}\frac{\partial}{\partial r}(ru) + \frac{\partial w}{\partial z} = 0 \ , \tag{2.193}$$

$$\rho\left(\frac{\partial u}{\partial t} + u\frac{\partial u}{\partial r} + w\frac{\partial u}{\partial z}\right) = -\frac{\partial p}{\partial r} + \left[\frac{1}{r}\frac{\partial}{\partial r}(r\tau_{rr}) + \frac{\partial}{\partial z}\tau_{zr} - \frac{\tau_{\theta\theta}}{r}\right] \ , \tag{2.194}$$

$$\rho\left(\frac{\partial w}{\partial t}+u\frac{\partial w}{\partial r}+w\frac{\partial w}{\partial z}\right)=-\frac{\partial p}{\partial z}+\left[\frac{1}{r}\frac{\partial}{\partial r}(r\tau_{rz})+\frac{\partial}{\partial z}\tau_{zz}\right]-\rho g\ . \tag{2.195}$$

After substituting Eq. (2.187), Eq. (2.191), and Eq. (2.192) into the momentum equations, we can write the r-direction momentum equation as

$$\rho\left(\frac{\partial u}{\partial t}+u\frac{\partial u}{\partial r}+w\frac{\partial u}{\partial z}\right)=-\frac{\partial p}{\partial r}+\left[\frac{1}{r}\frac{\partial}{\partial r}(r\cdot 2\mu\frac{\partial u}{\partial r})+\frac{\partial}{\partial z}\left[\mu\left(\frac{\partial w}{\partial r}+\frac{\partial u}{\partial z}\right)\right]-2\frac{\mu u}{r^2}\right]\ , \tag{2.196}$$

or

$$\begin{aligned}&\rho\left(\frac{\partial u}{\partial t}+u\frac{\partial u}{\partial r}+w\frac{\partial u}{\partial z}\right)\\&=-\frac{\partial p}{\partial r}+\frac{2\mu}{r}\frac{\partial u}{\partial r}+2\frac{\partial \mu}{\partial r}\frac{\partial u}{\partial r}+2\mu\frac{\partial^2 u}{\partial r^2}+\frac{\partial \mu}{\partial z}\left[\left(\frac{\partial w}{\partial r}+\frac{\partial u}{\partial z}\right)\right]+\mu\left(\frac{\partial^2 w}{\partial r\partial z}+\frac{\partial^2 u}{\partial z^2}\right)-2\frac{\mu u}{r^2}\ .\end{aligned} \tag{2.197}$$

Similarly, we can write the z-direction momentum equation as

$$\rho\left(\frac{\partial w}{\partial t}+u\frac{\partial w}{\partial r}+w\frac{\partial w}{\partial z}\right)=-\frac{\partial p}{\partial z}+\frac{1}{r}\frac{\partial}{\partial r}\left[r\cdot\mu\left(\frac{\partial w}{\partial r}+\frac{\partial u}{\partial z}\right)\right]+\frac{\partial}{\partial z}\left(\mu\cdot 2\frac{\partial w}{\partial z}\right)-\rho g\ , \tag{2.198}$$

or

$$\begin{aligned}&\rho\left(\frac{\partial w}{\partial t}+u\frac{\partial w}{\partial r}+w\frac{\partial w}{\partial z}\right)\\&=-\frac{\partial p}{\partial z}+\frac{\mu}{r}\left(\frac{\partial w}{\partial r}+\frac{\partial u}{\partial z}\right)+\frac{\partial \mu}{\partial r}\left(\frac{\partial w}{\partial r}+\frac{\partial u}{\partial z}\right)+\mu\left(\frac{\partial^2 w}{\partial r^2}+\frac{\partial^2 u}{\partial r\partial z}\right)+2\frac{\partial \mu}{\partial z}\frac{\partial w}{\partial z}+2\mu\frac{\partial^2 w}{\partial z^2}-\rho g\ .\end{aligned} \tag{2.199}$$

At surface of the substrate, the no-slip and no-penetration boundary conditions are given by

$$u\underset{z=0}{\ }=w\underset{z=0}{\ }=0\ . \tag{2.200}$$

At the liquid-gas surface ($z=h$), the kinematic and traction boundary conditions (normal and shear stress balance conditions) are applied to enforce no mass transfer across the free surface $h(r,t)$. The kinematic boundary condition is given by

$$\vec{u}\cdot\vec{n}=-\frac{1}{|\nabla F|}\frac{\partial F}{\partial t}\ . \tag{2.201}$$

The normal stress balance condition is given by

$$P-P_a-2\mu(\underline{\underline{S}}\cdot\vec{n}\cdot\vec{n})=\sigma(\nabla\cdot\vec{n})\ . \tag{2.202}$$

The shear stress balance condition is given by

$$2\mu(\underline{\underline{S}} \cdot \vec{n} \cdot \vec{t_i}) - (\nabla_s \sigma) \cdot \vec{t_i} = 0 \ . \tag{2.203}$$

The definition of F and the steps of simplification are documented in section 2.1. The kinematic boundary condition in terms of the profile of a droplet is written as

$$\frac{\partial h}{\partial t} + u\Big|_{z=0} \frac{\partial h}{\partial r} - w\Big|_{z=0} = 0 \ . \tag{2.204}$$

After substituting expressions for normal vector $\vec{n}$ and tangential vector $\vec{t_i}$ and following the same idea, we can rewrite Eq. (2.202) and Eq. (2.203)

$$P - P_a - \frac{2\mu}{1 + (\frac{\partial h}{\partial r})^2}\left[\frac{\partial u}{\partial r}\left(\frac{\partial h}{\partial r}\right)^2 - \frac{\partial h}{\partial r}\left(\frac{\partial u}{\partial z} + \frac{\partial w}{\partial r}\right) + \frac{\partial w}{\partial z}\right] = \sigma\left\{ -\frac{1}{r}\frac{\partial}{\partial r}\left[\frac{r\frac{\partial h}{\partial r}}{\sqrt{1 + (\frac{\partial h}{\partial r})^2}}\right] + \frac{\partial}{\partial z}\left[\frac{1}{\sqrt{1 + (\frac{\partial h}{\partial r})^2}}\right]\right\} , \tag{2.205}$$

$$\left[-\frac{\partial u}{\partial r}\frac{\partial h}{\partial r} + \frac{1}{2}\left(\frac{\partial u}{\partial z} + \frac{\partial w}{\partial r}\right) - \frac{1}{2}\left(\frac{\partial u}{\partial z} + \frac{\partial w}{\partial r}\right)\left(\frac{\partial h}{\partial r}\right)^2 + \frac{\partial w}{\partial z}\frac{\partial h}{\partial r}\right] = 0 \ . \tag{2.206}$$

The continuity equation, the Cauchy momentum equations and all boundary conditions are made dimensionless by the following relations

$$u \equiv u_c \cdot u', h \equiv H \cdot h', r \equiv L \cdot r', p \equiv p_c \cdot p'$$

$$w \equiv w_c \cdot w', z \equiv H \cdot z', t \equiv \left(\frac{L}{u_c}\right) t'$$

Here, the variables with primes denotes the dimensionless ones. The dimensionless form of Eq. (2.193) is

$$\frac{1}{L \cdot r'}\frac{\partial(L \cdot r' \cdot u_c \cdot u')}{L \partial r'} + \frac{\partial(w_c \cdot w')}{H \partial z'} = 0 \ , \tag{2.207}$$

$$\frac{u_c}{L}\frac{1}{r'}\frac{\partial(r'u')}{\partial r'} + \frac{w_c}{H}\frac{\partial w'}{\partial z'} = 0 \ . \tag{2.208}$$

From the continuity condition, we should enforce

$$\frac{u_c}{L} = \frac{w_c}{H} \ , \tag{2.209}$$

or

$$\epsilon \equiv \frac{H}{L} = \frac{w_c}{u_c} \ll 1 \ . \tag{2.210}$$

The r-direction momentum equation is written as

$$\begin{aligned}
&\rho\left(\frac{u_c}{L/u_c}\frac{\partial u'}{\partial t'} + u_c u'\frac{u_c}{L}\frac{\partial u'}{\partial r'} + w_c w'\frac{u_c}{H}\frac{\partial u'}{\partial z'}\right) \\
&\qquad = -\frac{p_c}{L}\frac{\partial p'}{\partial r'} + \frac{\mu_0 u_c}{L^2}\frac{2\mu'}{r'}\frac{\partial u'}{\partial r'} + 2\frac{\mu_0 u_c}{L^2}\frac{\partial \mu'}{\partial r'}\frac{\partial u'}{\partial r'} + 2\frac{\mu_0 u_c}{L^2}\mu'\frac{\partial^2 u'}{\partial r'^2} - 2\frac{\mu_0 u_c}{L^2}\frac{\mu' u'}{r'^2} \\
&\qquad\quad + \frac{\mu_0}{H}\frac{\partial \mu'}{\partial z'}\left[\left(\frac{w_c}{L}\frac{\partial w'}{\partial r'} + \frac{u_c}{H}\frac{\partial u'}{\partial z'}\right)\right] + \mu_0\mu'\left(\frac{w_c}{LH}\frac{\partial^2 w'}{\partial r'\partial z'} + \frac{u_c}{H^2}\frac{\partial^2 u'}{\partial z'^2}\right) ,
\end{aligned} \tag{2.211}$$

or

$$\begin{aligned}
&\frac{\partial u'}{\partial t'} + u'\frac{\partial u'}{\partial r'} + w'\frac{\partial u'}{\partial z'} \\
&\qquad = -\frac{p_c}{\rho u_c^2}\frac{\partial p'}{\partial r'} + 2\frac{\mu_0}{\rho u_c L}\left(\frac{\mu'}{r'}\frac{\partial u'}{\partial r'} + \frac{\partial \mu'}{\partial r'}\frac{\partial u'}{\partial r'} + \mu'\frac{\partial^2 u'}{\partial r'^2} - \frac{\mu' u}{r'^2}\right) \\
&\qquad\quad + \frac{\partial \mu'}{\partial z'}\left[\left(\frac{\mu_0}{\rho u_c L}\frac{\partial w'}{\partial r'} + \frac{\mu_0 L}{\rho u_c H^2}\frac{\partial u'}{\partial z'}\right)\right] + \mu'\left(\frac{\mu_0}{\rho u_c L}\frac{\partial^2 w'}{\partial r'\partial z'} + \frac{\mu_0 L}{\rho u_c H^2}\frac{\partial^2 u'}{\partial z'^2}\right) .
\end{aligned} \tag{2.212}$$

The z-direction momentum equation is written as

$$\begin{aligned}
&\rho\left(\frac{w_c}{L/u_c}\frac{\partial w'}{\partial t'} + \frac{u_c w_c}{L}u'\frac{\partial w'}{\partial r'} + \frac{w_c^2}{H}w'\frac{\partial w'}{\partial z'}\right) \\
&\qquad = -\frac{p_c}{H}\frac{\partial p'}{\partial z'} + \frac{\mu_0}{L}\frac{\mu'}{r'}\left(\frac{w_c}{L}\frac{\partial w'}{\partial r'} + \frac{u_c}{H}\frac{\partial u'}{\partial z'}\right) + \frac{\mu_0}{L}\frac{\partial \mu'}{\partial r'}\left(\frac{w_c}{L}\frac{\partial w'}{\partial r'} + \frac{u_c}{H}\frac{\partial u'}{\partial z'}\right) \\
&\qquad\quad + \mu_0\mu'\left(\frac{w_c}{L^2}\frac{\partial^2 w'}{\partial r'^2} + \frac{u_c}{LH}\frac{\partial^2 u'}{\partial r'\partial z'}\right) + 2\frac{\mu_0 w_c}{H^2}\frac{\partial \mu'}{\partial z'}\frac{\partial w'}{\partial z'} + 2\frac{\mu_0 w_c}{H^2}\mu'\frac{\partial^2 w}{\partial z^2} - \rho g \ ,
\end{aligned} \tag{2.213}$$

or

$$\begin{aligned}
&\frac{\partial w'}{\partial t'} + u'\frac{\partial w'}{\partial r'} + w'\frac{\partial w'}{\partial z'} \\
&\quad = -\frac{p_c L}{\rho u_c^2 \epsilon H}\frac{\partial p'}{\partial z'} + \frac{\mu'}{r'}\left(\frac{\mu_0}{\rho u_c L}\frac{\partial w'}{\partial r'} + \frac{\mu_0}{\rho u_c \epsilon H}\frac{\partial u'}{\partial z'}\right) + \frac{\partial \mu'}{\partial r'}\left(\frac{\mu_0}{\rho u_c L}\frac{\partial w'}{\partial r'} + \frac{\mu_0}{\rho u_c \epsilon H}\frac{\partial u'}{\partial z'}\right) \\
&\qquad + \mu'\left(\frac{\mu_0}{\rho u_c L}\frac{\partial^2 w'}{\partial r'^2} + \frac{\mu_0}{\rho u_c H\epsilon}\frac{\partial^2 u'}{\partial r'\partial z'}\right) + 2\frac{\mu_0 L}{\rho u_c H^2}\frac{\partial \mu'}{\partial z'}\frac{\partial w'}{\partial z'} + 2\frac{\mu_0 L}{\rho u_c H^2}\mu'\frac{\partial^2 w}{\partial z^2} - \frac{gL}{\epsilon u_c^2} \ .
\end{aligned} \tag{2.214}$$

After defining $Re \equiv \rho u_c L/\mu_0$ and $p_c = \mu_0 u_c/(L\epsilon^2)$, we can rewrite Eq. (2.212) and Eq. (2.214) as

$$\begin{aligned}\frac{\partial u'}{\partial t'} + u'\frac{\partial u'}{\partial r'} + w'\frac{\partial u'}{\partial z'} \\ = -\frac{1}{Re}\frac{1}{\epsilon^2}\frac{\partial p'}{\partial r'} + \frac{2}{Re}\left(\frac{\mu'}{r'}\frac{\partial u'}{\partial r'} + \frac{\partial \mu'}{\partial r'}\frac{\partial u'}{\partial r'} + \mu'\frac{\partial^2 u'}{\partial r'^2} - \frac{\mu' u}{r'^2}\right) \\ + \frac{1}{Re}\frac{1}{\epsilon^2}\frac{\partial \mu'}{\partial z'}\left[\left(\epsilon^2\frac{\partial w'}{\partial r'} + \frac{\partial u'}{\partial z'}\right)\right] + \frac{1}{Re}\frac{1}{\epsilon^2}\mu'\left(\epsilon^2\frac{\partial^2 w'}{\partial r'\partial z'} + \frac{\partial^2 u'}{\partial z'^2}\right),\end{aligned} \tag{2.215}$$

$$\begin{aligned}\frac{\partial w'}{\partial t'} + u'\frac{\partial w'}{\partial r'} + w'\frac{\partial w'}{\partial z'} \\ = -\frac{1}{Re}\frac{1}{\epsilon^4}\frac{\partial p'}{\partial z'} + \frac{1}{Re}\frac{1}{\epsilon^2}\frac{\mu'}{r'}\left(\epsilon^2\frac{\partial w'}{\partial r'} + \frac{\partial u'}{\partial z'}\right) + \frac{1}{Re}\frac{1}{\epsilon^2}\frac{\partial \mu'}{\partial r'}\left(\epsilon^2\frac{\partial w'}{\partial r'} + \frac{\partial u'}{\partial z'}\right) \\ + \frac{1}{Re}\frac{1}{\epsilon^2}\mu'\left(\epsilon^2\frac{\partial^2 w'}{\partial r'^2} + \frac{\partial^2 u'}{\partial r'\partial z'}\right) + \frac{2}{Re}\frac{1}{\epsilon^2}\frac{\partial \mu'}{\partial z'}\frac{\partial w'}{\partial z'} + \frac{2}{Re}\frac{1}{\epsilon^2}\mu'\frac{\partial^2 w}{\partial z^2} - \frac{gL}{\epsilon u_c^2}.\end{aligned} \tag{2.216}$$

We multiply Eq. (2.215) by $Re \cdot \epsilon^2$ and Eq. (2.216) by $Re \cdot \epsilon^4$

$$\begin{aligned}Re\cdot\epsilon^2\left(\frac{\partial u'}{\partial t'} + u'\frac{\partial u'}{\partial r'} + w'\frac{\partial u'}{\partial z'}\right) \\ = -\frac{\partial p'}{\partial r'} + 2\epsilon^2\left(\frac{\mu'}{r'}\frac{\partial u'}{\partial r'} + \frac{\partial \mu'}{\partial r'}\frac{\partial u'}{\partial r'} + \mu'\frac{\partial^2 u'}{\partial r'^2} - \frac{\mu' u}{r'^2}\right) \\ + \frac{\partial \mu'}{\partial z'}\left[\left(\epsilon^2\frac{\partial w'}{\partial r'} + \frac{\partial u'}{\partial z'}\right)\right] + \mu'\left(\epsilon^2\frac{\partial^2 w'}{\partial r'\partial z'} + \frac{\partial^2 u'}{\partial z'^2}\right)\end{aligned} \tag{2.217}$$

$$\begin{aligned}Re\cdot\epsilon^4\left(\frac{\partial w'}{\partial t'} + u'\frac{\partial w'}{\partial r'} + w'\frac{\partial w'}{\partial z'}\right) \\ = -\frac{\partial p'}{\partial z'} + \epsilon^2\frac{\mu'}{r'}\left(\epsilon^2\frac{\partial w'}{\partial r'} + \frac{\partial u'}{\partial z'}\right) + \epsilon^2\frac{\partial \mu'}{\partial r'}\left(\epsilon^2\frac{\partial w'}{\partial r'} + \frac{\partial u'}{\partial z'}\right) \\ + \epsilon^2\mu'\left(\epsilon^2\frac{\partial^2 w'}{\partial r'^2} + \frac{\partial^2 u'}{\partial r'\partial z'}\right) + \epsilon^2\frac{\partial \mu'}{\partial z'}\frac{\partial w'}{\partial z'} + \epsilon^2\mu'\frac{\partial^2 w}{\partial z^2} - \frac{\rho g L^2\epsilon^3}{\mu_0 u_c}\end{aligned} \tag{2.218}$$

We can write down Eq. (2.197) and Eq. (2.218) to the leading order approximation

$$0 = -\frac{\partial p'}{\partial r'} + \frac{\partial \mu'}{\partial z'}\frac{\partial u'}{\partial z'} + \mu'\frac{\partial^2 u'}{\partial z'^2} + \cancelto{0}{\mathcal{O}(Re\cdot\epsilon^2, \epsilon^2)}, \tag{2.219}$$

$$0 = -\frac{\partial p'}{\partial z'} - \frac{\rho g \epsilon^3 L^2}{\mu_0 u_c} + \cancelto{0}{\mathcal{O}(Re \cdot \epsilon^4, \epsilon^4, \epsilon^2)} \ , \tag{2.220}$$

$$\frac{1}{r'}\frac{\partial}{\partial r'}(r'u') + \frac{\partial w'}{\partial z'} = 0 \ , \tag{2.221}$$

where

$$\mu' = |\dot{\gamma}|^{n-1} \ . \tag{2.222}$$

In the next step, we substitute Eq. (2.191) and Eq. (2.192) into Eq. (2.190), then into Eq. (2.187) to find the dominant rate-of-deformation term in viscosity:

$$S_{rr} = \frac{2u_c}{L}\frac{\partial u'}{\partial r'}, \ S_{\theta\theta} = \frac{2u_c}{L}\frac{u'}{r'} \ , \tag{2.223}$$

$$S_{rz} = S_{zr} = \left(\frac{w_c}{L}\frac{\partial w'}{\partial r'} + \frac{u_c}{H}\frac{\partial u'}{\partial z'}\right), \ S_{zz} = \frac{2w_c}{H}\frac{\partial w'}{\partial z'} \ , \tag{2.224}$$

$$\dot{\gamma} = \left\{\frac{1}{2}\left[4\frac{u_c^2}{L^2}\left(\frac{\partial u'}{\partial r'}\right)^2 + 4\frac{w_c^2}{H^2}\left(\frac{\partial w'}{\partial z'}\right)^2 + 4\frac{u_c^2}{L^2}\left(\frac{u'}{r'}\right)^2 + 2\frac{u_c^2}{H^2}\left(\frac{\partial u'}{\partial z'}\right)^2 + 4\frac{u_c w_c}{LH}\frac{\partial u'}{\partial z'}\frac{\partial w'}{\partial r'} + 2\frac{w_c^2}{L^2}\left(\frac{\partial w'}{\partial r'}\right)^2\right]\right\}^{1/2} \ ,$$

$$= \left\{\frac{1}{2}\frac{u_c^2}{L^2}\left[4\left(\frac{\partial u'}{\partial r'}\right)^2 + 4\left(\frac{\partial w'}{\partial z'}\right)^2 + 4\left(\frac{u'}{r'}\right)^2 + \frac{2}{\epsilon^2}\left(\frac{\partial u'}{\partial z'}\right)^2 + 4\frac{\partial u'}{\partial z'}\frac{\partial w'}{\partial r'} + 2\epsilon^2\left(\frac{\partial w'}{\partial r'}\right)^2\right]\right\}^{1/2} \ . \tag{2.225}$$

Eq. (2.225) to the leading order approximation is given by

$$\dot{\gamma} = \left\{\frac{1}{2}\frac{u_c^2}{L^2}\left[\frac{2}{\epsilon^2}\left(\frac{\partial u'}{\partial z'}\right)^2 + \cancelto{0}{\mathcal{O}(1, \epsilon^2)}\right]\right\}^{1/2} \tag{2.226}$$

$$\approx \frac{u_c}{H}\frac{\partial u'}{\partial z'} \ . \tag{2.227}$$

Therefore,

$$\mu' = \left(m \ \frac{\partial u'}{\partial z'} \ \right)^{n-1} \ . \tag{2.228}$$

Here, the characteristic deformation rate m is defined by

$$m \equiv \frac{u_c}{H} \tag{2.229}$$

Thus, we summarize the dimensionless forms of the boundary conditions :

(i)**The no slip and no penetration** at the surface of the substrate ($z = 0$)

$$u'_{z'=0} = w'_{z'=0} = 0 \tag{2.230}$$

(ii)**The kinematic boundary condition** at the liquid-gas interface ($z = h$)

$$\frac{\partial h'}{\partial t'} + u'_{z'=h'} \frac{\partial h'}{\partial r'} - w'_{z'=h'} = 0 \tag{2.231}$$

(iii)**The normal stress balance condition** at the liquid-gas interface ($z = h$)

$$p' - P'_a = -\frac{\sigma H^3}{\mu_0 u_c L^3} \frac{1}{r'} \frac{\partial}{\partial r'} \left[r' \frac{\partial h'}{\partial r'} \right] \tag{2.232}$$

(iv)**The shear stress balance condition** at the liquid-gas interface ($z = h$)

$$\mu' \frac{\partial u'}{\partial z'} = 0 \tag{2.233}$$

The system of dimensionless governing equations is rewritten as (after dropping primes),

$$-\frac{\partial p}{\partial r} + \frac{\partial \mu}{\partial z}\frac{\partial u}{\partial z} + \mu \frac{\partial^2 u}{\partial z^2} = 0 \ , \tag{2.234}$$

$$\frac{\partial p}{\partial z} + \frac{\rho g \epsilon^3 L^2}{\mu_0 u_c} = 0 \ , \tag{2.235}$$

$$\frac{1}{r}\frac{\partial}{\partial r}(ru) + \frac{\partial w}{\partial z} = 0 \ , \tag{2.236}$$

with boundary conditions

$$u_{z=0} = w_{z=0} = 0 \ , \tag{2.237}$$

$$\frac{\partial h}{\partial t} + u_{z=h} \frac{\partial h}{\partial r} - w_{z=h} = 0 \ , \tag{2.238}$$

$$p_{z=h} - P_a = -\frac{\sigma H^3}{\mu_0 u_c L^3} \frac{1}{r} \frac{\partial}{\partial r} \left[r \frac{\partial h}{\partial r} \right] \ , \tag{2.239}$$

$$\mu \frac{\partial u}{\partial z}_{z=h} = 0 \ . \tag{2.240}$$

The derivation for pressure p is exactly the same as that in section 2.4.1. One can follow the steps described there to obtain the expression for p

$$p(r, z, t) = P_a + \frac{\epsilon^3 L^2 \rho g}{\mu u_c} \cdot (h - z) - \frac{\sigma H^3}{\mu_0 u_c L^3} \left[\frac{1}{r} \frac{\partial}{\partial r} \left(r \frac{\partial h}{\partial r} \right) \right] \ . \tag{2.241}$$

Eq. (2.234) can be rewritten as

$$-\frac{\partial p}{\partial r}+\frac{\partial}{\partial z}\left(\mu\frac{\partial u}{\partial z}\right)=0\ . \tag{2.242}$$

We integrate Eq. (2.242) over z,

$$\mu\frac{\partial u}{\partial z}=\frac{\partial p}{\partial r}z+g(r)\ . \tag{2.243}$$

After applying the boundary condition (Eq. (2.237)), we can determine the unknown coefficient,

$$\mu\frac{\partial u}{\partial z}_{z=h}=\frac{\partial p}{\partial r}h+g(r)=0\ , \tag{2.244}$$

$$g(r)=-\frac{\partial p}{\partial r}h\ . \tag{2.245}$$

By substituting Eq. (2.245) and Eq. (2.228) into Eq. (2.243), we can compute the z derivative of the horizontal velocity,

$$\left(m\ \frac{\partial u}{\partial z}\ \right)^{n-1}\frac{\partial u}{\partial z}=-\frac{\partial p}{\partial r}(h-z)\ , \tag{2.246}$$

or

$$\frac{\partial u}{\partial z}=-\left(\frac{1}{m}\right)^{n-1}\ \frac{\partial p}{\partial r}^{\ 1/n-1}\frac{\partial p}{\partial r}\cdot(h-z)^{1/n}\ . \tag{2.247}$$

Therefore, tangential velocity $u(r,z,t)$ can be obtained by integrating Eq. (2.247) over z:

$$u(r,z,t)=\frac{n}{1+n}\left(\frac{1}{m}\right)^{n-1}\ \frac{\partial p}{\partial r}^{\ 1/n-1}\frac{\partial p}{\partial r}\cdot(h-z)^{1/n+1}+u_0(r,t)\ . \tag{2.248}$$

After applying no slip boundary condition to Eq. (2.248), we can determine the integration constant,

$$u_0(r,t)=-\frac{n}{1+n}\left(\frac{1}{m}\right)^{n-1}\ \frac{\partial p}{\partial r}^{\ 1/n-1}\frac{\partial p}{\partial r}\cdot h^{1/n+1}\ . \tag{2.249}$$

Thus, the tangential velocity is given by

$$u=\frac{n}{1+n}\left(\frac{1}{m}\right)^{n-1}\ \frac{\partial p}{\partial r}^{\ 1/n-1}\frac{\partial p}{\partial r}\cdot\left[(h-z)^{1/n+1}-h^{1/n+1}\right] \tag{2.250}$$

The vertically averaged horizontal velocity $\overline{u}$ is determined by integrating Eq. (2.250)

$$\overline{u} = \frac{1}{h}\left(\int_0^h u \; dz \right) \tag{2.251}$$

$$= \frac{1}{h}\frac{n}{1+n}\left(\frac{1}{m}\right)^{n-1} \left|\frac{\partial p}{\partial r}\right|^{1/n-1}\frac{\partial p}{\partial r} \cdot \int_0^h \left[(h-z)^{1/n+1} - h^{1/n+1} \right] dz \tag{2.252}$$

$$= -\frac{n}{1+2n}\left(\frac{1}{m}\right)^{n-1} \left|\frac{\partial p}{\partial r}\right|^{1/n-1}\frac{\partial p}{\partial r} \cdot h^{1/n+1} \; . \tag{2.253}$$

After following the same steps as those in section 2.4.1 from Eq. (2.87) to Eq. (2.92), we can obtain the lubrication equation,

$$\frac{\partial h}{\partial t} + \frac{1}{r}\frac{\partial}{\partial r}\left(\int_0^{h(r,t)} ru \cdot dz \right) = 0 \; , \tag{2.254}$$

or

$$\frac{\partial h}{\partial t} + \frac{1}{r}\frac{\partial}{\partial r}\left(rh \cdot \overline{u} \right) = 0 \; . \tag{2.255}$$

By substituting Eq. (2.251) into Eq. (2.255), we can have the final form of lubrication equation,

$$\frac{\partial h}{\partial t} - \frac{n}{1+2n}\left(\frac{1}{m}\right)^{n-1}\frac{1}{r}\frac{\partial}{\partial r}\left(r \left|\frac{\partial p}{\partial r}\right|^{1/n-1}\frac{\partial p}{\partial r} \cdot h^{\frac{1+2n}{n}} \right) = 0 \; , \tag{2.256}$$

where

$$\frac{\partial p}{\partial r} = Bo \cdot \frac{\partial h}{\partial r} - \frac{1}{Ca}\frac{\partial}{\partial r}\left[\frac{1}{r}\frac{\partial}{\partial r}\left(r\frac{\partial h}{\partial r} \right) \right] .$$

$$m \equiv \frac{u_c}{H}, \; Ca \equiv \frac{\mu_0 u_c}{\sigma \epsilon^3}, \text{ and } Bo \equiv \frac{\rho g \epsilon^3 L^2}{\mu_0 u_c}$$

By substituting $n = 1$ into Eq. (2.256), we can verify Eq. (2.256) is the same as Eq. 2.95 in section 2.4.1 for the Newtonian case.

2.3.2 Spreading Over a Porous Substrate with the Beavers and Joseph Condition

The mathematical model for a power-law droplet spreading over a porous substrate is investigated in this section. The surface of porous substrate is assumed to be perfectly smooth. The Beavers and Joseph boundary condition has been implemented in our derivation to have a more realistic and accurate model.

For flow above the surface of substrate, we start from dimensionless governing equations and boundary conditions we obtained in section 2.3.1. Note that the variables with subscript "p" denote the variables in the porous media and the variables with primes denote the dimensionless variables.

$$-\frac{\partial p'}{\partial r'}+\frac{\partial \mu'}{\partial z'}\frac{\partial u'}{\partial z'}+\mu'\frac{\partial^2 u'}{\partial z'^2}=0\ , \tag{2.257}$$

$$\frac{\partial p'}{\partial z'}+\frac{\rho g\epsilon^3 L^2}{\mu_0 u_c}=0\ , \tag{2.258}$$

$$\frac{1}{r'}\frac{\partial}{\partial r'}(r'u')+\frac{\partial w'}{\partial z'}=0\ , \tag{2.259}$$

with the boundary conditions at the liquid-gas interface

$$\frac{\partial h'}{\partial t'}+u'_{z'=h'}\frac{\partial h'}{\partial r'}-w'_{z'=h'}=0\ , \tag{2.260}$$

$$p'_{z'=h'}-P'_a=-\frac{\sigma H^3}{\mu_0 u_c L^3}\frac{1}{r'}\frac{\partial}{\partial r'}\left[r'\frac{\partial h'}{\partial r'}\right]\ , \tag{2.261}$$

$$\mu'\frac{\partial u'}{\partial z'}_{z'=h'}=0\ . \tag{2.262}$$

The continuity conditions connecting flow above the surface and inside the substrate are given by

$$w'_{z'=0}=w'_{p\,z'=0}\ , \tag{2.263}$$

$$p'_{z'=0}=p'_{p\,z'=0}\ , \tag{2.264}$$

$$\frac{du'}{dz'}_{z'=0}=\frac{\beta\cdot H}{\sqrt{\kappa}}(u'|_{z'=0}-u'_p|_{z'=0})\ , \tag{2.265}$$

where β is the slip coefficient and κ is the permeability of the porous substrate. By recognizing that there is a wetting front separating the saturated domain from unsaturated porous medium, we can write down a pressure-jump boundary condition at that boundary ($z = -h_p$),

$$p_p|_{z=-h_p} = P_a - P_{ca} \ . \tag{2.266}$$

For a power-law liquid inside the porous substrate, we assume that the flow is governed by the continuity equation and the modified Darcy's law,

$$\frac{1}{r}\frac{\partial}{\partial r}(ru_p) + \frac{\partial w_p}{\partial z} = 0 \ , \tag{2.267}$$

$$u_p = -\left(\frac{\kappa}{\mu_0}\right)^{1/n}\left(\frac{\partial p_p}{\partial r}\ \frac{\partial p_p}{\partial r}^{1/n-1}\right) \ , \tag{2.268}$$

$$w_p = -\left(\frac{\kappa}{\mu_0}\right)^{1/n}\left(\frac{\partial p_p}{\partial z}\ \frac{\partial p_p}{\partial z}^{1/n-1} + \rho g\right) \ . \tag{2.269}$$

After substituting Eq. (2.268) and Eq. (2.269) into Eq. (2.267), we make Eq. (2.267) dimensionless by using the following relations,

$$u \equiv u_c \cdot u',\ h \equiv H \cdot h',\ r \equiv L \cdot r',\ p \equiv p_c \cdot p',\ p_c = \mu_0 u_c/(L\epsilon^2),$$

$$w \equiv w_c \cdot w',\ z \equiv H \cdot z',\ \text{and } t \equiv \left(\frac{L}{u_c}\right)t'.$$

Thus, the continuity equation in dimensionless form is given by

$$\epsilon^{1+1/n}\frac{1}{r'}\frac{\partial}{\partial r'}\left(r'\frac{\partial p'_p}{\partial r'}\ \frac{\partial p'_p}{\partial r'}^{1/n-1}\right) + \frac{\partial}{\partial z'}\left(\frac{\partial p'_p}{\partial z'}\ \frac{\partial p'_p}{\partial z'}^{1/n-1}\right) = 0 \ . \tag{2.270}$$

Eq. (2.270) to the leading order approximation is written as

$$\frac{\partial}{\partial z'}\left(\frac{\partial p'_p}{\partial z'}\ \frac{\partial p'_p}{\partial z'}^{1/n-1}\right) + \cancelto{0}{\mathcal{O}(\epsilon^{1+1/n})} = 0 \ . \tag{2.271}$$

We integrate Eq. (2.271) over z,

$$\frac{\partial p'_p}{\partial z'}\ \frac{\partial p'_p}{\partial z'}^{1/n-1} = C_1(r', t') \ . \tag{2.272}$$

Therefore, the z derivative of the pressure for flow inside the porous substrate is given by

$$\frac{\partial p'_p}{\partial z'} = C_1(r',t')\ C_1(r',t')^{\,n-1} . \tag{2.273}$$

We compute the pressure p'_p by integrating Eq (2.273) over z,

$$p'_p = C_1(r',t')\ C_1(r',t')^{\,n-1} \cdot z' + C_2(r',t') . \tag{2.274}$$

The unknown coefficient $C_2(r',t')$ can be determined by applying the continuity equation for the pressure (Eq. (2.264)),

$$C_2(r',t') = p'^{\,z=0} \tag{2.275}$$

$$= \frac{\rho g L^2 \epsilon^3}{\mu_0 u_c} h' - \frac{\sigma H^3}{\mu_0 L^3 u_c} \frac{1}{r'} \frac{\partial}{\partial r'} \left(r \frac{\partial h'}{\partial r'} \right) , \tag{2.276}$$

where the ambient pressure P'_a is set to be zero. The unknown coefficient $C_1(r',t')$ is computed by applying the pressure-jump boundary condition at the wetting front.

$$C_1(r',t')\ C_1(r',t')^{\,n-1} (-h'_p) + P'_a + \frac{\rho g L^2 \epsilon^3}{\mu_0 u_c} h' - \frac{\sigma H^3}{\mu_0 L^3 u_c} \frac{1}{r'} \frac{\partial}{\partial r'} \left(r \frac{\partial h'}{\partial r'} \right) = P'_a - P'_{ca} , \tag{2.277}$$

$$C_1(r',t')\ C_1(r',t')^{\,n-1} = \frac{\rho g L^2 \epsilon^3}{\mu_0 u_c} \frac{h'\,'}{h'_p} - \frac{\sigma H^3}{\mu_0 L^3 u_c} \frac{1}{r'} \frac{1}{h'_p} \frac{\partial}{\partial r'} \left(r \frac{\partial h'}{\partial r'} \right) + \frac{P'_{ca}}{h'_p} . \tag{2.278}$$

After substituting Eq. (2.275) and Eq. (2.278) into Eq. (2.274), we obtain the expression for pressure,

$$p'_p = \left[\frac{\rho g L^2 \epsilon^3}{\mu_0 u_c} \frac{h'}{h'_p} - \frac{\sigma H^3}{\mu_0 L^3 u_c} \frac{1}{r'} \frac{1}{h'_p} \frac{\partial}{\partial r'} \left(r \frac{\partial h'}{\partial r'} \right) + \frac{P'_{ca}}{h'_p} \right] \cdot z + \frac{\rho g L^2 \epsilon^3}{\mu_0 u_c} h' - \frac{\sigma H^3}{\mu_0 L^3 u_c} \frac{1}{r'} \frac{\partial}{\partial r'} \left(r \frac{\partial h'}{\partial r'} \right) . \tag{2.279}$$

Because we already had the dimensionless expression for the pressure field inside the substrate p_p, the tangential and vertical velocities inside the medium, u_p and w_p, can be computed by applying the pressure to the modified Darcy's law,

$$u'_p = -\left(\frac{\kappa p_c}{\mu_0 {u_c}^n L} \right)^{1/n} \left(\frac{\partial p'_p}{\partial r'} \left| \frac{\partial p'_p}{\partial r'} \right|^{1/n-1} \right) , \tag{2.280}$$

$$w'_p = -\frac{1}{w_c}\left(\frac{\kappa p_c}{\mu_0 H}\right)^{1/n}\left(\frac{\partial p'_p}{\partial z'}\,\frac{\partial p'_p}{\partial z'}^{\,1/n-1} + \frac{\rho g L^{2/n}\epsilon^{3/n}}{\mu_0^{1/n}u_c^{1/n}}\right) . \tag{2.281}$$

The pressure gradient in the r-direction at surface of the substrate is given by

$$\frac{\partial p'_p}{\partial r'}_{z'=0} = \frac{\partial C_2}{\partial r'} \tag{2.282}$$

$$= \frac{\rho g L^2\epsilon^3}{\mu_0 u_c}\frac{\partial h'}{\partial r'} - \frac{\sigma H^3}{\mu_0 L^3 u_c}\frac{\partial}{\partial r'}\left[\frac{1}{r'}\frac{\partial}{\partial r'}\left(r\frac{\partial h'}{\partial r'}\right)\right] . \tag{2.283}$$

The pressure gradient in the z-direction at surface of the substrate is given by

$$\frac{\partial p'_p}{\partial z'}_{z'=0} = C_1(r',t')\;C_1(r',t')^{n-1} \tag{2.284}$$

$$= \frac{\rho g L^2\epsilon^3}{\mu_0 u_c}\frac{h'\,'}{h'_p} - \frac{\sigma H^3}{\mu_0 L^3 u_c}\frac{1}{r'}\frac{1}{h'_p}\frac{\partial}{\partial r'}\left(r\frac{\partial h'}{\partial r'}\right) + \frac{p'_{ca}}{h'_p} . \tag{2.285}$$

Thus, we have the tangential and the normal velocities at the surface of the porous medium,

$$u'_p{}_{z'=0} = -\left(\frac{\kappa p_c}{\mu_0 {u_c}^n L}\right)^{1/n}\left\{\left[\frac{\rho g L^2\epsilon^3}{\mu_0 u_c}\frac{\partial h'}{\partial r'} - \frac{\sigma H^3}{\mu_0 L^3 u_c}\frac{\partial}{\partial r'}\left[\frac{1}{r'}\frac{\partial}{\partial r'}\left(r\frac{\partial h'}{\partial r'}\right)\right]\right]\times \right.$$
$$\left.\frac{\rho g L^2\epsilon^3}{\mu_0 u_c}\frac{\partial h'}{\partial r'} - \frac{\sigma H^3}{\mu_0 L^3 u_c}\frac{\partial}{\partial r'}\left[\frac{1}{r'}\frac{\partial}{\partial r'}\left(r\frac{\partial h'}{\partial r'}\right)\right]^{1/n-1}\right\} , \tag{2.286}$$

$$w'_p{}_{z'=0} = -\left(\frac{\kappa p_c}{\mu_0 w_c^n H}\right)^{1/n}\left\{\left[\frac{\rho g L^2\epsilon^3}{\mu u_c}\frac{h'}{h'_p} - \frac{\sigma H^3}{\mu L^3 u_c}\frac{1}{r'}\frac{1}{h'_p}\frac{\partial}{\partial r'}\left(r\frac{\partial h'}{\partial r'}\right) + \frac{P'_{ca}}{h'_p}\right]\times \right.$$
$$\left.\frac{\rho g L^2\epsilon^3}{\mu u_c}\frac{h'\,'}{h'_p} - \frac{\sigma H^3}{\mu L^3 u_c}\frac{1}{r'}\frac{1}{h'_p}\frac{\partial}{\partial r'}\left(r\frac{\partial h'}{\partial r'}\right) + \frac{P'_{ca}}{h'_p}^{\,1/n-1} + \frac{\rho g L^{2/n}\epsilon^{3/n}}{\mu_0^{1/n}u_c^{1/n}}\right\} . \tag{2.287}$$

We can follow the same steps as those in section 2.2 to obtain the expression for p,

$$p'(r',t') = \frac{\epsilon^3 L^2\rho g}{\mu_0 u_c}\cdot(h'-z') - \frac{\sigma H^3}{\mu_0 u_c L^3}\left[r'\frac{\partial}{\partial r'}\left(r'\frac{\partial h'}{\partial r'}\right)\right] . \tag{2.288}$$

To find out the flow field inside the droplet, we start from Eq. (2.257)

$$-\frac{\partial p'}{\partial r'} + \frac{\partial}{\partial z'}\left(\mu'\frac{\partial u'}{\partial z'}\right) = 0 . \tag{2.289}$$

We integrate Eq. (2.289) over z,

$$\mu'\frac{\partial u'}{\partial z'} = \frac{\partial p'}{\partial r'}z' + g(r') . \tag{2.290}$$

After applying boundary condition (Eq. (2.262)) to Eq. (2.290), we determine the unknown coefficient,

$$\mu' \frac{\partial u'}{\partial z'}_{z'=h'} = \frac{\partial p'}{\partial r'} h' + g(r') = 0 \ , \tag{2.291}$$

$$g(r') = -\frac{\partial p'}{\partial r'} h' \ . \tag{2.292}$$

By substituting expression for viscosity (Eq. (2.228)) and Eq. (2.292) into Eq. (2.290), we rewrite Eq. (2.290),

$$\left(m \ \frac{\partial u'}{\partial z'} \right)^{n-1} \frac{\partial u'}{\partial z'} = -\frac{\partial p'}{\partial r'} (h' - z') \ . \tag{2.293}$$

Thus, we compute the z derivative of the horizontal velocity,

$$\frac{\partial u'}{\partial z'} = -\left(\frac{1}{m} \right)^{n-1} \ \frac{\partial p'}{\partial r'}^{\ 1/n-1} \frac{\partial p'}{\partial r'} \cdot (h' - z')^{1/n} \ . \tag{2.294}$$

The tangential velocity $u(r, z, t)$ is determined by integrating Eq. (2.294) over z,

$$u'(r', z', t') = \frac{n}{1+n} \left(\frac{1}{m} \right)^{n-1} \ \frac{\partial p'}{\partial r'}^{\ 1/n-1} \frac{\partial p'}{\partial r'} \cdot (h' - z')^{1/n+1} + u_0(r', t') \ . \tag{2.295}$$

The shear rate and horizontal velocity at the surface of the substrate are determined based on Eq. (2.295)

$$\frac{\partial u'}{\partial z'}_{z'=0} = -\left(\frac{1}{m} \right)^{n-1} \ \frac{\partial p'}{\partial r'}^{\ 1/n-1} \frac{\partial p'}{\partial r'} \cdot h'^{1/n} \ , \tag{2.296}$$

$$u'_{z'=0} = \frac{n}{1+n} \left(\frac{1}{m} \right)^{n-1} \ \frac{\partial p'}{\partial r'}^{\ 1/n-1} \frac{\partial p'}{\partial r'} \cdot h'^{1/n+1} + u_0(r', t') \ . \tag{2.297}$$

The unknown coefficient $u_0(r', t')$ is determined by the Beavers and Joseph boundary conditions at the fluid-porous medium interface. By substituting Eq. (2.286), Eq. (2.296), and Eq. (2.297) into Eq. (2.265), the equation is written as

$$\begin{aligned} -\left(\frac{1}{m} \right)^{n-1} \ \frac{\partial p'}{\partial r'}^{\ 1/n-1} \frac{\partial p'}{\partial r'} \cdot h'^{1/n} = \frac{\beta \cdot H}{\sqrt{\kappa}} \Bigg\{ & \frac{n}{1+n} \left(\frac{1}{m} \right)^{n-1} \ \frac{\partial p'}{\partial r'}^{\ 1/n-1} \frac{\partial p'}{\partial r'} \cdot h'^{1/n+1} \\ & + u_0(r', t') + \left(\frac{\kappa p_c}{\mu_0 {u_c}^n L} \right)^{1/n} \left[\frac{\partial p'}{\partial r'} \ \frac{\partial p'}{\partial r'}^{\ 1/n-1} \right] \Bigg\} \ . \end{aligned} \tag{2.298}$$

Thus, the unknown coefficient is given by

$$u_0(r',t') = -\frac{\partial p'}{\partial r'}\,\frac{\partial p'}{\partial r'}^{1/n-1}\left[\frac{n}{1+n}\left(\frac{1}{m}\right)^{n-1}h'^{1/n+1}+\frac{\sqrt{\kappa}}{\beta\cdot H}\left(\frac{1}{m}\right)^{n-1}h'^{1/n}+\left(\frac{\kappa}{H^2{u_c}^{n-1}}\right)^{1/n}\right]. \tag{2.299}$$

By substituting Eq. (2.299) into Eq. (2.295), we obtain the horizontal velocity,

$$u'(r',z',t') = -\frac{\partial p'}{\partial r'}\,\frac{\partial p'}{\partial r'}^{1/n-1}\left[-\frac{n}{1+n}\left(\frac{1}{m}\right)^{n-1}\cdot(h'-z')^{1/n+1}\right.$$
$$\left.\frac{n}{1+n}\left(\frac{1}{m}\right)^{n-1}h'^{1/n+1}+\frac{\sqrt{\kappa}}{\beta\cdot H}\left(\frac{1}{m}\right)^{n-1}h'^{1/n}+\left(\frac{\kappa}{H^2{u_c}^{n-1}}\right)^{1/n}\right]. \tag{2.300}$$

To form the lubrication equation, we need to determine the vertical velocity $w'|_{z'=h'}$ at the free surface in Eq. (2.260). By integrating the continuity equation over z, the vertical velocity is determined,

$$-w'_{z'=h'} = \int_0^{h'}\left[\frac{1}{r'}\frac{\partial}{\partial r'}(r'u')\right]dz' - w_{z'=0}. \tag{2.301}$$

After substituting the vertical velocity into the kinematic boundary condition and applying Leibniz integral rule to the kinematic boundary condition, we can rewrite Eq. (2.260),

$$\frac{\partial h'}{\partial t'}+\frac{1}{r'}\frac{\partial}{\partial r'}\left(\int_0^{h'(r',t')} r'u'\cdot dz'\right)-w'_{z'=0}=0\,, \tag{2.302}$$

or

$$\frac{\partial h'}{\partial t'}+\frac{1}{r'}\frac{\partial}{\partial r'}\left(r'h'\overline{u}'\right)-w'_{z'=0}=0\,. \tag{2.303}$$

Here, the vertically averaged horizontal velocity is given by

$$\overline{u}' = \frac{1}{h'}\int_0^{h'(r',t')} u' \cdot dz' \tag{2.304}$$

$$= -\frac{1}{h'}\frac{\partial p'}{\partial r'}\left|\frac{\partial p'}{\partial r'}\right|^{1/n-1}\int_0^{h'(r',t')}\left[-\frac{n}{1+n}\left(\frac{1}{m}\right)^{n-1}\cdot(h'-z')^{1/n+1}\right.$$
$$\left.+\frac{n}{1+n}\left(\frac{1}{m}\right)^{n-1}h'^{1/n+1}+\frac{\sqrt{\kappa}}{\beta\cdot H}\left(\frac{1}{m}\right)^{n-1}h'^{1/n}+\left(\frac{\kappa}{\epsilon^2L^2{u_c}^{n-1}}\right)^{1/n}\right]dz'$$
$$= -\frac{1}{h'}\frac{\partial p'}{\partial r'}\left|\frac{\partial p'}{\partial r'}\right|^{1/n-1}\left[-\frac{n^2}{(1+n)(1+2n)}\left(\frac{1}{m}\right)^{n-1}\cdot h'^{1/n+2}\right.$$
$$\left.+\frac{n}{1+n}\left(\frac{1}{m}\right)^{n-1}h'^{1/n+2}+\frac{\sqrt{\kappa}}{\beta\cdot H}\left(\frac{1}{m}\right)^{n-1}h'^{1/n+1}+\left(\frac{\kappa}{\epsilon^2L^2{u_c}^{n-1}}\right)^{1/n}h'\right]. \tag{2.305}$$

After substituting Eq. (2.305) and Eq. (2.287) into Eq. (2.303), we have the final form of lubrication equation,

$$\frac{\partial h'}{\partial t'}+\frac{1}{r'}\frac{\partial}{\partial r'}\left\{r'\frac{\partial p'}{\partial r'}\left|\frac{\partial p'}{\partial r'}\right|^{1/n-1}W\right\}$$
$$= -\left(\frac{\kappa}{\epsilon^{n+3}L^2u_c^{n-1}}\right)^{1/n}\left\{\left[\frac{\rho gL^2\epsilon^3}{\mu_0u_c}\frac{h'}{h'_p}-\frac{\sigma H^3}{\mu_0L^3u_c}\frac{1}{r'}\frac{1}{h'_p}\frac{\partial}{\partial r'}\left(r'\frac{\partial h'}{\partial r'}\right)+\frac{p'_{ca}}{h'_p}\right]\right.$$
$$\left.\frac{\rho gL^2\epsilon^3}{\mu_0u_c}\frac{h'}{h'_p}-\frac{\sigma H^3}{\mu_0L^3u_c}\frac{1}{r'}\frac{1}{h'_p}\frac{\partial}{\partial r'}\left(r'\frac{\partial h'}{\partial r'}\right)+\frac{p'_{ca}}{h'_p}\left|\frac{p'_{ca}}{h'_p}\right|^{1/n-1}+\frac{\rho gL^{2/n}\epsilon^{3/n}}{\mu_0^{1/n}u_c^{1/n}}\right\}, \tag{2.306}$$

or (after dropping primes)

$$\frac{\partial h}{\partial t}+\frac{1}{r}\frac{\partial}{\partial r}\left\{r\frac{\partial p}{\partial r}\left|\frac{\partial p}{\partial r}\right|^{1/n-1}W\right\} = -Pm^{1/n}\left\{\left[Bo\frac{h}{h_p}-\frac{1}{Ca}\frac{1}{r}\frac{1}{h_p}\frac{\partial}{\partial r}\left(r\frac{\partial h}{\partial r}\right)+\frac{p'_{ca}}{h_p}\right]\right.$$
$$\left.\times\ Bo\frac{h}{h_p}-\frac{1}{Ca}\frac{1}{r}\frac{1}{h_p}\frac{\partial}{\partial r}\left(r\frac{\partial h}{\partial r}\right)+\frac{p'_{ca}}{h_p}\left|\frac{p'_{ca}}{h_p}\right|^{1/n-1}+BoP\right\}, \tag{2.307}$$

where

$$W \equiv \left[\frac{n^2}{(1+n)(1+2n)}\left(\frac{1}{m}\right)^{n-1}\cdot h'^{1/n+2}\right.$$
$$\left.-\frac{n}{1+n}\left(\frac{1}{m}\right)^{n-1}h^{1/n+2}-\frac{\sqrt{\kappa}}{\beta\cdot H}\left(\frac{1}{m}\right)^{n-1}h^{1/n+1}-\left(\frac{\kappa}{\epsilon^2L^2{u_c}^{n-1}}\right)^{1/n}h\right], \tag{2.308}$$

$$\frac{\partial p}{\partial r} = Bo \cdot \frac{\partial p}{\partial r} - \frac{1}{Ca}\frac{\partial}{\partial r}\left[r\frac{\partial}{\partial r}\left(r\frac{\partial h}{\partial r}\right)\right], \tag{2.309}$$

$$Pm \equiv \frac{\kappa}{\epsilon^{n+3}L^2 u_c^{n-1}},\ Ca \equiv \frac{\mu u_c}{\sigma\epsilon^3},\ Bo \equiv \frac{\rho g L^2\epsilon^3}{\mu_0 u_c},\ BoP \equiv \frac{\rho g L^{2/n}\epsilon^{3/n}}{\mu_0^{1/n} u_c^{1/n}},$$

$$\text{and}\ \ p'_{ca} \equiv \frac{P_{ca}L^2}{\sigma H}\ .$$

We can quickly verify that Eq. (2.307), Eq. (2.308), and Eq. (2.309) are exactly the same as Eq. (2.173) for the Newtonian fluid ($n = 1$).

For the evolution equation of wetting front, we follow the same steps as those in Section 2.2.2 from Eq (2.174) to Eq. (2.178) to rewrite the kinematic boundary condition for the wetting front,

$$\phi\frac{\partial h'_p}{\partial t'} + \frac{1}{r'}\frac{\partial}{\partial r'}\left(r' h'_p \overline{u_p}'\right) + w'_p\Big|_{z'=0} = 0 \tag{2.310}$$

To find the expression for the vertically averaged tangential velocity $\overline{u_p}'$, we need to determine the pressure gradient inside the porous medium first. The pressure is given by

$$p'_p = \left[Bo\frac{h'}{h'_p} - \frac{1}{Ca}\frac{1}{r'}\frac{1}{h'_p}\frac{\partial}{\partial r'}\left(r'\frac{\partial h'}{\partial r'}\right) + \frac{p'_{ca}}{h'_p}\right]\cdot z + Bo\cdot h' - \frac{1}{Ca}\frac{1}{r'}\frac{\partial}{\partial r'}\left(r\frac{\partial h'}{\partial r'}\right) \tag{2.311}$$

Thus, the pressure gradient in r-direction is given by

$$\frac{\partial p'_p}{\partial r'} = \frac{\partial}{\partial r'}\left[Bo\frac{h'}{h'_p} - \frac{1}{Ca}\frac{1}{r'}\frac{1}{h'_p}\frac{\partial}{\partial r'}\left(r'\frac{\partial h'}{\partial r'}\right) + \frac{p'_{ca}}{h'_p}\right]\cdot z + Bo\frac{\partial h'}{\partial r'} - \frac{1}{Ca}\frac{\partial}{\partial r'}\left[\frac{1}{r'}\frac{\partial}{\partial r'}\left(r\frac{\partial h'}{\partial r'}\right)\right] \tag{2.312}$$

The vertically averaged tangential velocity $\overline{u_p}'$ is given by substituting Eq. (2.313)

$$\overline{u_p}' = \frac{1}{h'_p}\int_{-h'_p}^{0} u'_p\, dz' \tag{2.313}$$

$$= -\frac{1}{h'_p}\left(\frac{\kappa p_c}{\mu_0 {u_c}^n L}\right)^{1/n}\int_{-h'_p}^{0}\frac{\partial p'_p}{\partial r'}\left|\frac{\partial p'_p}{\partial r'}\right|^{1/n-1} dz'$$

$$= -\frac{\epsilon^{1+n}}{h'_p}\left(\frac{\kappa}{\epsilon^{3+n}L^2 {u_c}^{n-1}}\right)^{1/n}\left\{\frac{n}{1+n}\frac{{K_2}^{1/n+1} - \left|K_2 - h'_p K_1\right|^{1/n+1}}{K_1}\right\}$$

$$= -\frac{1}{h'_p}Pm^{1/n}\epsilon^{1+n}\left\{\frac{n}{1+n}\frac{{K_2}^{1/n+1} - \left|K_2 - h'_p K_1\right|^{1/n+1}}{K_1}\right\} \tag{2.314}$$

The integration has been computed by doing symbolic evaluation in *Mathematica* and the results are verified by *Maple*. Here, the components for the pressure gradient are given by

$$K_1(r',t') = \frac{\partial}{\partial r'}\left[Bo\frac{h'}{h'_p} - \frac{1}{Ca}\frac{1}{r'}\frac{1}{h'_p}\frac{\partial}{\partial r'}\left(r'\frac{\partial h'}{\partial r'}\right) + \frac{p'_{ca}}{h'_p}\right] \tag{2.315}$$

$$K_2(r',t') = Bo\frac{\partial h'}{\partial r'} - \frac{1}{Ca}\frac{\partial}{\partial r'}\left[\frac{1}{r'}\frac{\partial}{\partial r'}\left(r\frac{\partial h'}{\partial r'}\right)\right] \tag{2.316}$$

After substituting Eq. (2.314) and Eq. (2.287) into Eq. (2.310), we obtain the final form of lubrication equation (after dropping primes):

$$\begin{aligned}\frac{\partial h_p}{\partial t} - \frac{n}{1+n}\frac{Pm^{1/n}\epsilon^{1+n}}{\phi}\frac{1}{r}\frac{\partial}{\partial r}\left\{r\left[\frac{K_2{}^{1/n+1} - K_2 - h_p\cdot K_1{}^{1/n+1}}{K_1}\right]\right\} \\ = \frac{Pm^{1/n}}{\phi}\left\{\left[Bo\frac{h}{h_p} - \frac{1}{Ca}\frac{1}{r}\frac{1}{h_p}\frac{\partial}{\partial r}\left(r\frac{\partial h}{\partial r}\right) + \frac{p'_{ca}}{h_p}\right]\right. \\ \left.\times\ Bo\frac{h}{h_p} - \frac{1}{Ca}\frac{1}{r}\frac{1}{h_p}\frac{\partial}{\partial r}\left(r\frac{\partial h}{\partial r}\right) + \frac{p'_{ca}}{h_p}{}^{1/n-1} + BoP\right\}\end{aligned} \tag{2.317}$$

where

$$Pm \equiv \frac{\kappa}{\epsilon^{n+3}L^2u_c^{n-1}},\ Ca \equiv \frac{\mu u_c}{\sigma\epsilon^3},\ Bo \equiv \frac{\rho g L^2\epsilon^3}{\mu_0 u_c},\ BoP \equiv \frac{\rho g L^{2/n}\epsilon^{3/n}}{\mu_0^{1/n}u_c^{1/n}},$$

$$\text{and } p'_{ca} \equiv \frac{P_{ca}L^2}{\sigma H}$$

Eq. (2.307) and Eq. (2.317) are two coupled lubrication equations. We will numerically solve them to obtain the droplet profile and wetting front inside the porous medium.

2.4 Boundary Conditions for Lubrication Equation

In this section, we will discuss the boundary conditions for the governing equations derived in the previous four subsections. The order of the partial differential equation mainly depends on the order of the pressure term. To form a well-posed boundary value problem, the number of required boundary conditions should be equal to the order of the highest derivative in the equation. Besides, the radius of droplet remains unknown during the computation. Therefore, we need one more condition to determine the moving boundary. For capillary spreading over a solid substrate (Eq. (2.97)), we have zero-slope and axisymmetric conditions at $r = 0$,

$$\frac{\partial h}{\partial r}\Big|_{r=0} = 0 \ , \tag{2.318}$$

$$\frac{\partial^3 h}{\partial r^3}\Big|_{r=0} = 0 \ . \tag{2.319}$$

At the edge of droplet, we enforce the height of contact point to be zero,

$$h\big(R(t), t\big) = 0 \ . \tag{2.320}$$

The volume constraint is applied to enforce the volume of drop to be constant:

$$V = 2\pi \int_0^R rh(r,t) \cdot dr \ . \tag{2.321}$$

One common way to provide the contact-line condition is to use the relationship between the contact angle and the slip velocity reported by Haley and Miksis [11] :

$$\frac{dR}{dt} = Caf\Big(- \frac{\partial h}{\partial r}\Big|_{r=R}\Big) \tag{2.322}$$

$$= Caf\big(\theta_D\big) \ . \tag{2.323}$$

Here, the function f can be assumed to be linear, quadratic or cubic function of "$\theta_D - \theta_S$". θ_S is the static contact angle for a given liquid-solid system and θ_D is the dynamic contact angle which is composed of unknown height profile at the rim of the droplet:

$$\theta_D = -tan^{-1}\Big(\frac{\partial h}{\partial r}\Big|_{r=R}\Big) \ . \tag{2.324}$$

Another model is based on the molecular kinematic theory. The driving force for the wetting line is resulted from the unbalanced surface tension force that arises in the non-equilibrium situation. This model (Blake [17]) can be reduced to

$$\frac{dR}{dt} = \frac{\sigma}{\zeta}\big(Cos(\theta_S) - Cos(\theta_D)\big) \ , \tag{2.325}$$

where $\zeta = k_B T/(\kappa^0 \Lambda^3)$ is the coefficient of wetting-line friction and k_B is the Boltzmann constant. κ^0 is the equilibrium frequency of the random molecular displacements occurring within the three-phase zone and Λ is the average distance of each displacement. The detailed discussion of these molecular-related parameters can be found in Blake [17]. The contact-line friction for specific liquid-solid system can be found from the tables provided by Blake [17] as well.

Two ways described above are based on numerical simulations. If we are given the initial geometries of a droplet as well as the experimental data like contact angle versus time (Chen [15]), we are able to carry out the simulation by treating these data as the boundary conditions to solve the system of equations. This so-called "hybrid model" can be used as a check on the accuracy of numerical scheme.

3. METHODOLOGY AND RESULTS

In this chapter, scaling arguments for spreading exponent (Warren [34]) and analytical method (Leal [33]) to simpler problem will be provided to support the computational results reported in the present study. The governing equations that were developed in the previous chapter were discretized and solved using the boundary conditions described therein by following the classical finite difference method. Detailed algorithms, discretization and formulation of linear system of equations are discussed in the following subsections. Finally, the numerical results for a Newtonian and non-Newtonian droplet spreading over a solid and porous substrate are reported and compared.

3.1 Scaling Argument and Analytical Investigation

Let us consider (Warren [34]) a liquid meniscus being drawn into a tube with internal diameter d. After the fluid reaches a sufficient distance from the initial position $L \gg d$, the velocity can be described well by the Poiseuille's flow:

$$\frac{dL}{dt} \approx \frac{d^2}{\mu}\frac{\Delta P}{L} \tag{3.1}$$

Consider a thin droplet spreading over a solid and smooth substrate for complete wetting case. Let R and H to be the characteristic radius and height of a droplet. When $R \gg H$, the lubrication approximation can be performed using this key condition. The spreading velocity can be scaled using the above relation:

$$\frac{dR}{dt} \approx \frac{H^2}{\mu}\frac{\Delta P}{L} \tag{3.2}$$

The scale for pressure drop ΔP can be obtained from Eq. (2.93)

$$\Delta P \sim \frac{\sigma H}{R^2} \tag{3.3}$$

Thus,

$$\frac{dR}{dt} \sim \frac{H^3}{R^3}\frac{\sigma}{\mu} \tag{3.4}$$

The volume constraint condition in a cylindrical coordinate is given by

$$\begin{aligned} V &= 2\pi \int_0^R rh \cdot dr \\ &\approx H \cdot R^2 \end{aligned} \tag{3.5}$$

and hence,

$$\frac{dR}{dt} \sim \frac{\sigma}{\mu}\frac{V^3}{R^9} \tag{3.6}$$

We integrate Eq. (3.6), thus, we have

$$R \sim \left(\frac{\sigma V^3 t}{\mu}\right)^{1/10} \tag{3.7}$$

$$\sim V^{0.3} t^{0.1} \tag{3.8}$$

We can observe that the scaling follows the Tanner's law (Chen [15]) for capillary dominant spreading. For the gravity dominant spreading, the scale for pressure drop ΔP is given by

$$\Delta P \sim \rho g H \tag{3.9}$$

Substituting Eq. (3.9) into Eq. (3.2) and integrating it, the result becomes

$$R \sim \left(\frac{\rho g V^3 t}{\mu}\right)^{1/8} \tag{3.10}$$

$$\sim V^{3/8} t^{1/8} \tag{3.11}$$

The scaling relation for gravitational spreading is well reported and verified by Lopez, Miller & Ruckenstein [19] and Cazabat & Cohen Stuart [35]. The results for above two cases can also be derived by using the similarity method. The detailed derivation won't be presented here. The formal procedures for the mathematical investigation are reported in Leal [33]. For case of gravitational spreading, the governing equation is given by Eq. (2.97) with $Bo = 1$. The final solution to the droplet profile is given by

$$h = \left[q\left(\frac{9}{16}\right)\frac{\Gamma(7/3)}{\pi\Gamma(4/3)}\right]^{1/4} t^{-1/4} f(\eta) \ , \tag{3.12}$$

$$f(\eta) = (1-\eta^2)^{1/3} \ , \tag{3.13}$$

$$\eta = (9/16)^{1/8}(r/t^{1/8}) \Big/ \left[q\frac{\Gamma(7/3)}{\pi\Gamma(4/3)}\right]^{3/8} \ . \tag{3.14}$$

Here, q, a characteristic volume of the droplet, is equal to HR^2. In this case, the height of the droplet decreases as $t^{-1/4}$ and the radius increases as $t^{1/8}$. For the case of capillary spreading, the governing equation is given by Eq. (2.100) with $Ca = 1$ for simplicity. The final ordinary differential equation we obtain is

$$G^2\frac{d}{d\eta}\left[\frac{1}{\eta}\frac{d}{d\eta}\left(\eta\frac{dG}{d\eta}\right)\right] = -\frac{0.3}{A^3B^4}\eta \ , \tag{3.15}$$

which is third-order and non-linear ODE for the unknown function $G(\eta)$. The profile of the droplet and the similarity variable are given by

$$h(r,t) = At^{-2\beta}G(\eta) \ , \tag{3.16}$$

$$\eta \equiv Br/t^{\beta} \ . \tag{3.17}$$

The constant A can be determined by enforcing $G(0) = 1$. The constant B can be chosen by transforming

$$2\pi\int_0^\infty G(\eta)\eta d\eta = \frac{B}{A}q \ , \tag{3.18}$$

into

$$\int_0^\infty G(\eta)\eta d\eta = 1 \ . \tag{3.19}$$

Because Eq. (3.15) is highly nonlinear and complex, and we can't solve it analytically, we are enforced to numerically integrate it. The original form of governing equation (Eq. (2.100)) for capillary spreading will be numerically solved and reported in the following subsections.

3.2 Numerical Method

The governing equations and boundary conditions we derived in previous chapters are discretized by using the finite difference method. We mainly utilize a second order central difference scheme for spatial discretization. The resulting non-linear equations are solved using a Newton-Raphson iteration procedure to handle non-linearity. An implicit time advancement scheme is employed to improve the stability of the program. Let's take Eq. (2.92) as our first example. The discretized form of Eq. (2.92) using an implicit scheme can be written as

$$\frac{(h_i)_{n+1}-(h_i)_n}{\Delta t} = F_{n+1}(h_i, h_i', h_i'', h_i''', h_i^{(iv)}) \tag{3.20}$$

$$= \frac{1}{6}\frac{1}{(r_i)_{n+1}}\frac{1}{dr_{n+1}}\Bigg[(r_{i+1})_{n+1}(h_{i+1})^3\frac{(p_{i+2})_{n+1}-(p_{i+2})_{n+1}}{2dr_{n+1}} - (r_{i-1})_{n+1}(h_{i-1})^3\frac{(p_i)_{n+1}-(p_{i-2})_{n+1}}{2dr_{n+1}}\Bigg] \tag{3.21}$$

Here, the variables marked with subscript i denote the variable at i-th grid point. The variables marked with subscript n and $n+1$, denote the variables at time step n and $n+1$, respectively. Because the radius of the droplet is changing with time, and we use the stretched grid to capture the moving contact line dynamics. $r_i = R\cdot i/(N-1)$ and $dr = R/(N-1)$ are functions of time and N is the total number of points. To implement the Newton-Raphson's method, we should define the residuals for governing equations and boundary conditions as follow:

$$Res_i \equiv (h_i)_{n+1} - (h_i)_n - \frac{\Delta t}{6}\frac{1}{(r_i)_{n+1}}\frac{1}{dr_{n+1}}\times \Bigg[(r_{i+1})_{n+1}(h_{i+1})^3\frac{(p_{i+2})_{n+1}-(p_{i+2})_{n+1}}{2dr_{n+1}} - (r_{i-1})_{n+1}(h_{i-1})^3\frac{(p_i)_{n+1}-(p_{i-2})_{n+1}}{2dr_{n+1}}\Bigg] \tag{3.22}$$

$$Rbc_1 \equiv \left(-\frac{11}{6}h_1 + 3h_2 - \frac{3}{2}h_3 + \frac{1}{3}h_4\right)\Big/ dr - 0.0 \tag{3.23}$$

$$Rbc_2 \equiv \left(-\frac{5}{2}h_1 + 9h_2 - 12h_3 + 7h_4 - \frac{3}{2}h_5\right)\Big/ dr^3 - 0.0 \tag{3.24}$$

$$Rbc_3 \equiv \frac{R_{n+1}-R_n}{dt} - Ca\Big[Cos(\theta_S) - Cos(\theta_D)\Big] \tag{3.25}$$

$$Rvc \equiv V_0 - 2\pi \sum_{i=1}^{n-1} \left(r_i h_i + 4 \frac{r_i + r_{i+1}}{2} \frac{h_i + h_{i+1}}{2} + r_{i+1} h_{i+1} \right) \frac{dr}{6} \tag{3.26}$$

Here, Rbc_1 and Rbc_2 present zero slope and axisymmetriy at the center of the droplet. Rbc_3 stands for moving contact-line description and can be replaced with other options discussed in chapter 2.6. The integration in volume constraint condition is performed numerically by the Simpson's rule. The height of profile at the edge of droplet is enforced to be zero :

$$h \Big|_{r=R} = 0 \tag{3.27}$$

The pressure term can be discretized as

$$p \Big|_{r=i \cdot dr} \approx p_i = \frac{\epsilon^3 L^2 \rho g}{\mu u_c} h_i - \frac{\sigma \epsilon^3}{\mu u_c} \left(\frac{1}{r_i} \frac{h_{i+1} - h_{i-1}}{2dr} + \frac{h_{i+1} - 2h_i + h_{i-1}}{dr^2} \right) \tag{3.28}$$

At boundary points, we should use forward or backward difference schemes to represent the derivatives at the boundary. Especially, at $r = 0$, the indeterminate condition 0/0 ("zero slope at the center of droplet"/"position of the first point") will occur. L'Hopital's rule is performed to evaluate the derivative as we approach $r = 0$.

$$\lim_{r \to 0} \frac{\partial h / \partial r}{r} = \frac{\partial}{\partial r} \left(\frac{\partial h}{\partial r} \right) \Big/ \left(\frac{\partial r}{\partial r} \right) = \frac{\partial^2 h}{\partial r^2} \Big|_{r=0} \tag{3.29}$$

Hence, discretized pressure at $r = 0$ is given by

$$p \Big|_{r=0} \approx p_0 = \frac{\epsilon^3 L^2 \rho g}{\mu u_c} h_0 - 2 \frac{\sigma \epsilon^3}{\mu u_c} \left(\frac{2h_0 - 5h_1 + 4h_2 - h_3}{dr^2} \right) \tag{3.30}$$

and the discretized pressure at $r = R$ is given by

$$\begin{aligned} p \Big|_{r=R} \approx p_0 = & \frac{\epsilon^3 L^2 \rho g}{\mu u_c} h_0 - \frac{\sigma \epsilon^3}{\mu u_c} \\ & \times \left(\frac{1}{r_N} \frac{\frac{3}{2} h_N - 2h_{N-1} + \frac{1}{2} h_{N-2}}{dr} + \frac{2h_N - 5h_{N-1} + 4h_{N-2} - h_{N-3}}{dr^2} \right) \end{aligned} \tag{3.31}$$

In the above discretized equations, the unknowns are "..., $(h_{i+1})_{n+1}$, $(h_i)_{n+1}$, $(h_{i+1})_{n+1}$, ...". We need to the take partial derivatives of the residuals above with respect to each unknown to form the Jacobian matrix. The detail arrangement will be provided below.

The resulting system of non-linear algebraic equations is mathematically expressed as :

$$\mathbf{J} \cdot (\mathbf{h}_{k+1} - \mathbf{h}_k) = -\mathbf{Res}(\mathbf{h}_k) \tag{3.32}$$

or

$$\mathbf{J} \cdot \Delta\mathbf{h}_k = -\mathbf{Res}(\mathbf{h}_k) \tag{3.33}$$

More specifically,

$$\begin{bmatrix} \frac{\partial Rbc_1}{\partial h_1} & \frac{\partial Rbc_1}{\partial h_2} & \frac{\partial Rbc_1}{\partial h_3} & \frac{\partial Rbc_1}{\partial h_4} & \cdots & \frac{\partial Rbc_1}{\partial R} \\ \frac{\partial Rbc_2}{\partial h_1} & \frac{\partial Rbc_2}{\partial h_2} & \frac{\partial Rbc_2}{\partial h_3} & \frac{\partial Rbc_2}{\partial h_4} & \cdots & \frac{\partial Rbc_2}{\partial R} \\ \frac{\partial Res_3}{\partial h_1} & \frac{\partial Res_3}{\partial h_2} & \frac{\partial Res_3}{\partial h_3} & \frac{\partial Res_3}{\partial h_4} & \cdots & \frac{\partial Res_3}{\partial R} \\ \frac{\partial Res_4}{\partial h_1} & \frac{\partial Res_4}{\partial h_2} & \frac{\partial Res_4}{\partial h_3} & \frac{\partial Res_4}{\partial h_4} & \cdots & \frac{\partial Res_4}{\partial R} \\ \vdots & \vdots & \vdots & \vdots & \ddots & \vdots \\ \frac{\partial Rvc}{\partial h_1} & \frac{\partial Rvc}{\partial h_2} & \frac{\partial Rvc}{\partial h_3} & \frac{\partial Rvc}{\partial h_4} & \cdots & \frac{\partial Rvc}{\partial R} \end{bmatrix} \begin{bmatrix} (h_1)_{k+1} - (h_1)_k \\ (h_2)_{k+1} - (h_2)_k \\ (h_3)_{k+1} - (h_3)_k \\ (h_4)_{k+1} - (h_4)_k \\ \vdots \\ R_{k+1} - R_k \end{bmatrix} = - \begin{bmatrix} (Rbc_1)_k \\ (Rbc_2)_k \\ (Res_3)_k \\ (Res_4)_k \\ \vdots \\ (Rvc)_k \end{bmatrix}$$

Note that, the subscripts stand for the number of iterations inside the Newton-Raphson's method in a given time step. Generally, the Jacobian matrix has the arrow-shape :

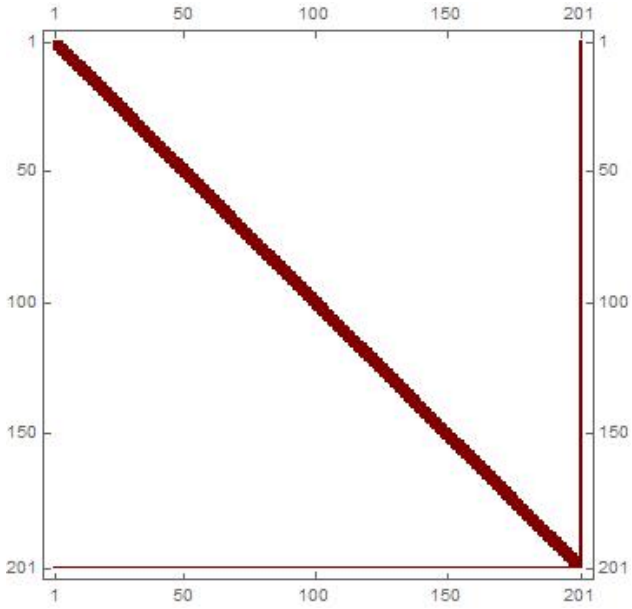

Figure 3.1. Plot of Jacobian matrix with 201 points.

For the case of spreading over a porous substrate, the discretized form of governing equations (Eq. (2.173) and Eq. (2.184)) can be expressed as

$$\frac{(h_i)_{n+1} - (h_i)_n}{\Delta t} = F_{n+1}(h_i, h_i', h_i'', h_i''', h_i^{(iv)}) \tag{3.34}$$

$$\frac{(h_{p_i})_{n+1} - (h_{p_i})_n}{\Delta t} = G_{n+1}(h_i, h_i', h_i'', h_{p_i}, h_{p_i}', h_{p_i}'') \tag{3.35}$$

The residuals for above two equations can be defined as

$$Resh_i \equiv \frac{(h_i)_{n+1} - (h_i)_n}{\Delta t} - F_{n+1}(h_i, h_i', h_i'', h_i''', h_i^{(iv)}) \tag{3.36}$$

$$Resh_{p_i} \equiv \frac{(h_{p_i})_{n+1} - (h_{p_i})_n}{\Delta t} - G_{n+1}(h_i, h_i', h_i'', h_{p_i}, h_{p_i}', h_{p_i}'') \tag{3.37}$$

Four discretized boundary conditions for Eq. (3.34) are given by

$$Rbc_1 \equiv \left(-\frac{11}{6}h_1 + 3h_2 - \frac{3}{2}h_3 + \frac{1}{3}h_4 \right) \Big/ dr - 0.0 \tag{3.38}$$

$$Rbc_2 \equiv \left(-\frac{5}{2}h_1 + 9h_2 - 12h_3 + 7h_4 - \frac{3}{2}h_5 \right) \Big/ dr^3 - 0.0 \tag{3.39}$$

$$Rbc_3 \equiv \left(\frac{3}{2}h_N - 2h_{N-1} + \frac{1}{2}h_{N-2} \right) - 0.0 \tag{3.40}$$

$$Rbc_4 \equiv h \underset{r=R}{} - 0.0 \tag{3.41}$$

Two discretized boundary conditions for Eq. (3.35) are given by

$$Rbc_5 \equiv \left(-\frac{11}{6}h_{p_1} + 3h_{p_2} - \frac{3}{2}h_{p_3} + \frac{1}{3}h_{p_4} \right) \Big/ dr - 0.0 \tag{3.42}$$

$$Rbc_6 \equiv h_p \underset{r=l}{} - 0.0 \tag{3.43}$$

Because the radius of droplet may not be the same as that of the wetting area inside the porous medium, the positions where zero height and zero depth are enforced can be different (Eq. (3.39) and Eq. (3.40)). The computations are performed for one-dimensional axisymmetric configurations within fixed rectangular domain. The figure to illustrate stretched grids or fixed domain is provided below.

To avoid encountering an issue due to the singularity of the governing equations for $h_p \to 0$, a layer of precursor film ($\approx 10^{-3} \sim 10^{-5}$) covers the area which has

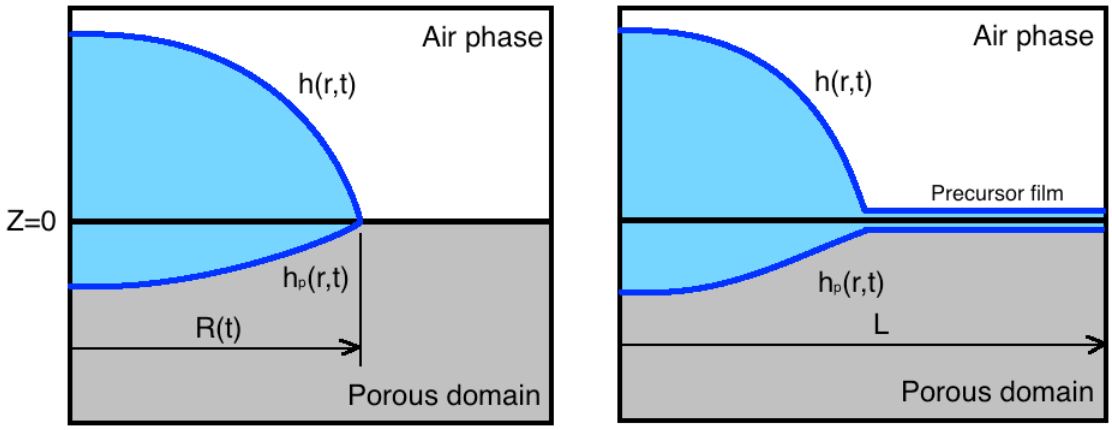

Figure 3.2. Schematic of problem with stretched grids (left) and fixed domain (right).

not been occupied by the droplet. Here, the thickness has already been scaled by the characteristic length ($\approx 10^{-3}$) and the dimensional value is around $10^{-6} \sim 10^{-8}$. Besides, the permeability number is set to be zero for positions not covered by the droplet to prevent the film being absorbed into the porous substrate.

The Jacobian matrix for system of non-linear algebraic equations is expressed as follows

$$\begin{bmatrix}
\frac{\partial Rbc_1}{\partial h_1} & \frac{\partial Rbc_1}{\partial h_2} & \frac{\partial Rbc_1}{\partial h_3} & \cdots & \frac{\partial Rbc_1}{\partial h_{p_1}} & \frac{\partial Rbc_1}{\partial h_{p_1}} & \frac{\partial Rbc_1}{\partial h_{p_3}} & \cdots & \frac{\partial Rbc_1}{\partial (h_p)_{N-1}} \\
\frac{\partial Rbc_2}{\partial h_1} & \frac{\partial Rbc_2}{\partial h_2} & \frac{\partial Rbc_2}{\partial h_3} & \cdots & \frac{\partial Rbc_2}{\partial h_{p_1}} & \frac{\partial Rbc_2}{\partial h_{p_2}} & \frac{\partial Rbc_2}{\partial h_{p_3}} & \cdots & \frac{\partial Rbc_2}{\partial (h_p)_{N-1}} \\
\frac{\partial Res_3}{\partial h_1} & \frac{\partial Res_3}{\partial h_2} & \frac{\partial Res_3}{\partial h_3} & \cdots & \frac{\partial Res_3}{\partial h_{p_1}} & \frac{\partial Res_3}{\partial h_{p_2}} & \frac{\partial Res_3}{\partial h_{p_3}} & \cdots & \frac{\partial Res_3}{\partial (h_p)_{N-1}} \\
\vdots & \vdots & \vdots & \ddots & \vdots & \vdots & \vdots & \ddots & \vdots \\
\frac{\partial Rbc_5}{\partial h_1} & \frac{\partial Rbc_5}{\partial h_2} & \frac{\partial Rbc_5}{\partial h_3} & \cdots & \frac{\partial Rbc_5}{\partial h_{p_1}} & \frac{\partial Rbc_5}{\partial h_{p_2}} & \frac{\partial Rbc_5}{\partial h_{p_3}} & \cdots & \frac{\partial Rbc_5}{\partial (h_p)_{N-1}} \\
\frac{\partial Resh_{p_2}}{\partial h_1} & \frac{\partial Resh_{p_2}}{\partial h_2} & \frac{\partial Resh_{p_2}}{\partial h_3} & \cdots & \frac{\partial Resh_{p_2}}{\partial h_{p_1}} & \frac{\partial Resh_{p_2}}{\partial h_{p_2}} & \frac{\partial Resh_{p_2}}{\partial h_{p_3}} & \cdots & \frac{\partial Resh_{p_2}}{\partial (h_p)_{N-1}} \\
\frac{\partial Resh_{p_3}}{\partial h_1} & \frac{\partial Resh_{p_3}}{\partial h_2} & \frac{\partial Resh_{p_3}}{\partial h_3} & \cdots & \frac{\partial Resh_{p_3}}{\partial h_{p_1}} & \frac{\partial Resh_{p_3}}{\partial h_{p_2}} & \frac{\partial Resh_{p_3}}{\partial h_{p_3}} & \cdots & \frac{\partial Resh_{p_3}}{\partial (h_p)_{N-1}} \\
\vdots & \vdots & \vdots & \ddots & \vdots & \vdots & \vdots & \ddots & \vdots \\
\frac{\partial Resh_{p_{N-1}}}{\partial h_1} & \frac{\partial Resh_{p_{N-1}}}{\partial h_2} & \frac{\partial Resh_{p_{N-1}}}{\partial h_3} & \cdots & \frac{\partial Resh_{p_{N-1}}}{\partial h_{p_1}} & \frac{\partial Resh_{p_{N-1}}}{\partial h_{p_2}} & \frac{\partial Resh_{p_{N-1}}}{\partial h_{p_3}} & \cdots & \frac{\partial Resh_{p_{N-1}}}{\partial (h_p)_{N-1}}
\end{bmatrix}$$

The vector for unknowns and residuals are arranged as follows

$$\mathbf{h} = \begin{bmatrix} (h_1)_k \\ (h_2)_k \\ (h_3)_k \\ \vdots \\ (h_{p_1})_k \\ (h_{p_2})_k \\ (h_{p_3})_k \\ \vdots \\ \left[(h_p)_{N-1}\right]_k \end{bmatrix} \quad , \mathbf{Res} = \begin{bmatrix} (Rbc_1)_k \\ (Rbc_2)_k \\ (Resh_3)_k \\ \vdots \\ (Resh_{p_3})_k \\ (Resh_{p_4})_k \\ (Resh_{p_5})_k \\ \vdots \\ \left[(Resh_p)_{N-1}\right]_k \end{bmatrix}$$

The resulting Jacobian matrix has the following form

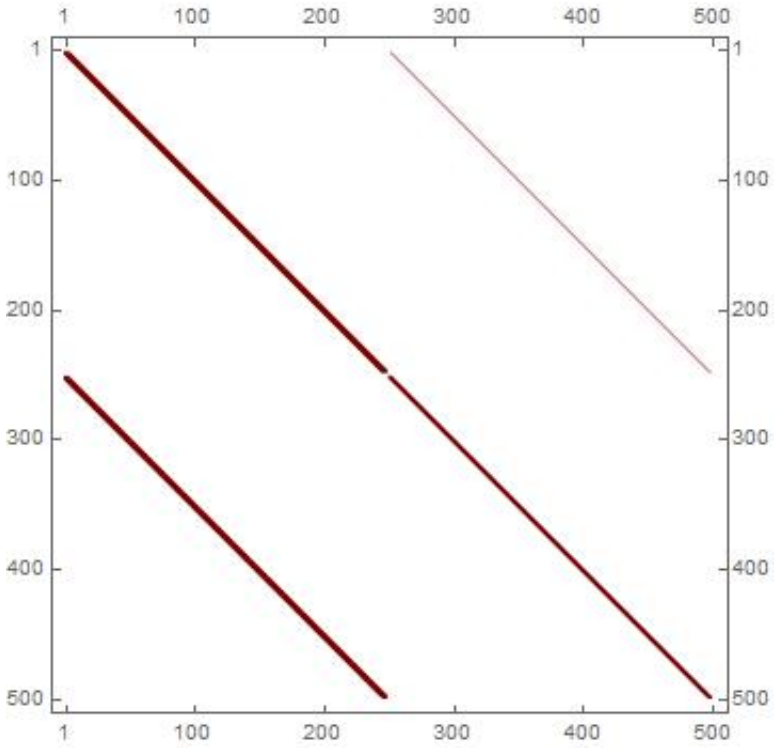

Figure 3.3. Plot of Jacobian matrix with 251 points.

251 grid points in the computational domain results in 500 unknown variables (for

both h and h_p except h_{N-1} and $(h_p)_{N-1}$). Therefore, the resulting dimension of matrix is 500×500. Along the main diagonal, the bandwidth of above matrix is 7 for entries corresponding to h and 5 for entries corresponding to h_p. Along the upper sub-diagonal, there is only one non-zero entry because terms for absorption don't contain derivatives with respect to h_p. Along the lower sub-diagonal, the bandwidth of this diagonal is 7 because it involves a fourth-order partial derivative of $Resh_p$ with respect to variable h.

The constraint for total volume including liquid in the droplet and inside porous substrate is not used in the simulation. However, it still can be used as a check for the accuracy of spatial and temporal discretization scheme. The lower order discretization schemes with coarse grid points could possibly decrease the total volume. Note that the decrease in total volume can not be avoided if we don't enforce total volume constraint in the calculation. In order to make total volume change as small as possible, it is required to choose a finer grid so that higher order terms, $\mathcal{O}(\Delta x^2)$, remain small. Generally, the number of grid points depends on the length of computational domain and is in the rage of 300 to 1000.

The discontinuity of permeability number near the edge of the droplet maybe one of the reasons causing a numerical issue and oscillation in the droplet profile. Therefore, to reduce the difference of permeability number for adjacent grid points near the moving-contact-line, the permeability number, Pm, is multiplied by a thickness-dependent prefactor (Alleborn & Raszillier [4]):

$$Pm(h) = \begin{cases} Pm \cdot \frac{1}{1+1/[C(h-h_g)]^2} & h > h_g \\ 0 & h \leq h_g \end{cases} \tag{3.44}$$

Here, C is a constant to control the effect of prefactor and h_g is the thickness of the precursor film.

For the case of power-law droplet spreading over a solid substrate, because the governing equations involves computation with a non-integer exponent (Eq. 2.256), we need to evaluate the absolute value of pressure gradient to make sure that the

viscosity is always positive. The discretized form of Eq. (2.256) is very similar to Eq. (3.45) :

$$\begin{aligned}\frac{(h_i)_{n+1}-(h_i)_n}{\Delta t} = \frac{n}{1+2n}\left(\frac{1}{m}\right)^{n-1}\frac{1}{(r_i)_{n+1}}\frac{1}{dr_{n+1}}\Bigg\{&(r_{i+1})_{n+1}(h_{i+1})^{1/n+2}\\ &\times\ \frac{(p_{i+2})_{n+1}-(p_{i+2})_{n+1}}{2dr_{n+1}}^{1/n-1}\left[\frac{(p_{i+2})_{n+1}-(p_{i+2})_{n+1}}{2dr_{n+1}}\right]\\ &-(r_{i-1})_{n+1}(h_{i-1})^{1/n+2}\ \frac{(p_i)_{n+1}-(p_{i-2})_{n+1}}{2dr_{n+1}}^{1/n-1}\left[\frac{(p_i)_{n+1}-(p_{i-2})_{n+1}}{2dr_{n+1}}\right]\Bigg\}\end{aligned} \tag{3.45}$$

After using the same geometry boundary conditions and contact-line description with different parameter setup for different liquids and forming a Jacobian matrix with the same arrangement as in Eq. (3.33), one can have the same shape of Jacobian matrix as that in Figure 3.1.

For the case of power-law droplet spreading over a porous substrate, the governing equations become even more complicated. The numerical setup requires all the procedures and functions mentioned in this chapter including the discretization, Jacobian matrix formulation. Besides, the contact-line dynamics for non-Newtonian liquids spreading over a porous substrate is poorly understood. Therefore, the way to circumvent this issue is to implement fixed grid points over the entire computational domain applying geometry boundary conditions at the center of droplet and right end of the precursor film : Eq. (3.38) to Eq. (3.43). Instead of using stretched grids to present moving-contact-line, we compute the unknowns within the entire domain (the right plot in Fig 3.2.) and define the distance to the points closet to the left end of precursor film as the current radius of droplet.

3.3 Numerical Results, Validation, and Discussion

The numerical results presented in this chapter are obtained by solving governing equations for four cases we introduced in chapter 2: those of Newtonian and power-law droplets spreading over a solid, smooth substrate and those of Newtonian and power-law droplets spreading over a homogeneous porous medium. Four models are presented in the cylindrical coordinate and the computations are performed in an one-dimensional axisymmetric configuration. For cases of spreading over a solid substrate, the computational domain is changing with time due to the implementation of stretched grid methods while for cases of spreading and absorption, the domain is fixed with a prescribed length of domain.

3.3.1 Newtonian Droplet Spreading over a Solid Substrate

In this subsection, the pressure p only includes the capillary effect in order to capture the Tanner's law which applies to cases when the capillary pressure dominates. The numerical results reported here are effectively independent of the sizes of time step and grid size. The test cases include the simulations based on experimental data and molecular kinematic theory for Runs 5 and 9 from Chen *et al.* Runs 5 and 9 represent different experimental setups. Here, we use experimental data for contact angle versus time as the contact-line boundary condition. Another way to provide the contact-line boundary conditions is using velocity-dependent contact angle derived from the molecular kinematic theory. Fig 3.4 presents the numerical results of apparent radius versus time for Run 5 and Run 9 based on experimental contact-line boundary condition and molecular kinematic theory. Fig 3.5 demonstrates the numerical results of center height of droplet versus time for Runs 5 and 9 based on experimental contact-line boundary condition and molecular kinematic theory. The choices for numbers of total grid points are 100, 200, and 500, respectively, presented by blue circles, orange triangles, and green squares. The difference for using different numbers of grid points is discernible but acceptable for each case ((a) and (b)

$Ca = 0.22$, $Bo = 0.0$; (c) and (d) $Ca = 0.1$, $Bo = 0.0$). The time step size of 0.1 is used. The results are reported in dimensional form.

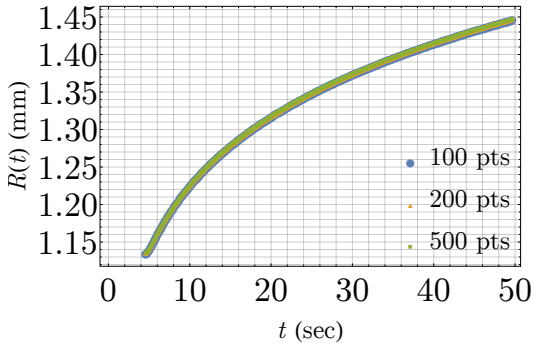

(a) Run 5: Using experimental data as contact-line boundary condition.

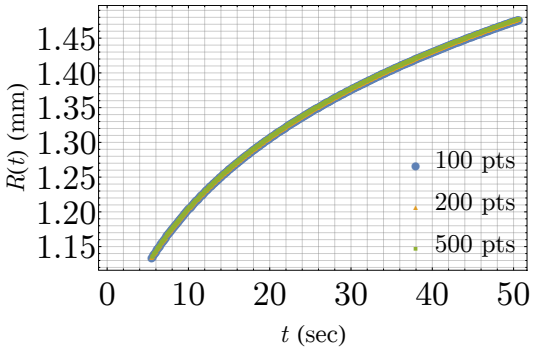

(b) Run 5: Contact-line boundary condition based on molecular kinematic theory.

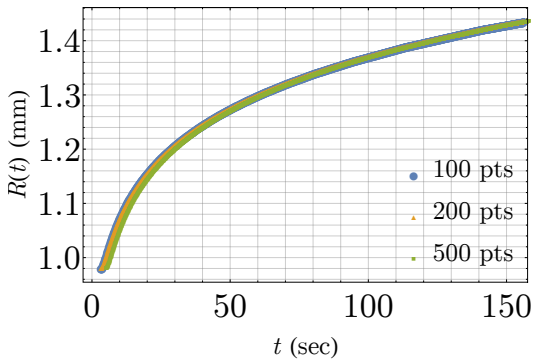

(c) Run 9: Using experimental data as contact-line boundary condition.

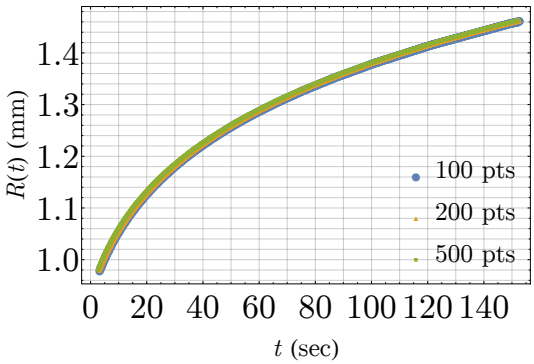

(d) Run 9: Contact-line boundary condition based on molecular kinematic theory.

Figure 3.4. Demonstration of grid independency test of numerical results for temporal evolution of radius, (a) and (b) $Ca = 0.22$, $Bo = 0.0$; (c) and (d) $Ca = 0.1$, $Bo = 0.0$.

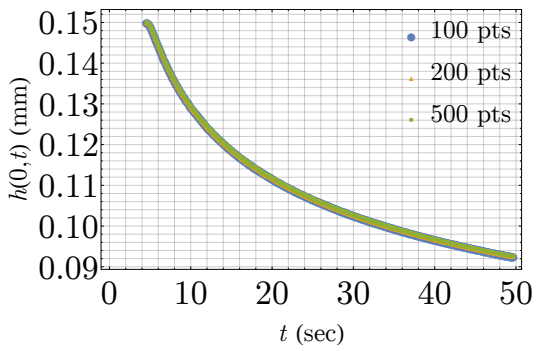

(a) Run 5: Using experimental data as contact-line boundary condition.

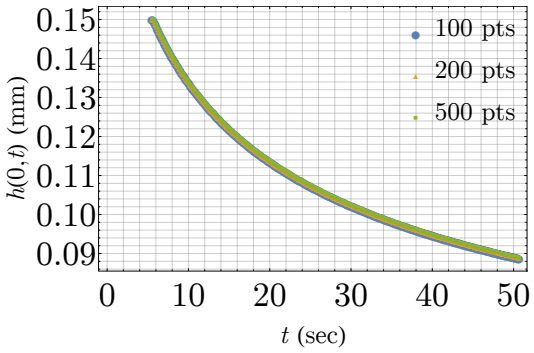

(b) Run 5: Contact-line boundary condition based on molecular kinematic theory.

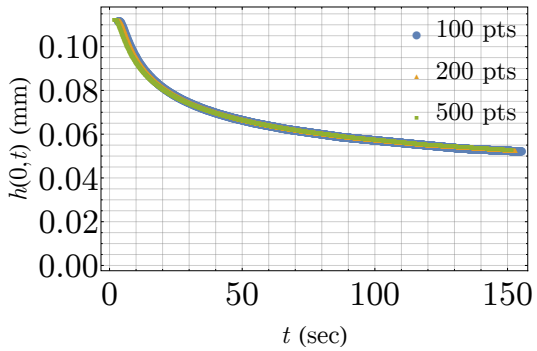

(c) Run 9: Using experimental data as contact-line boundary condition.

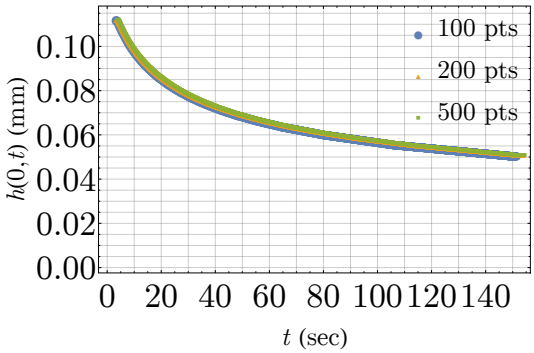

(d) Run 9: Contact-line boundary condition based on molecular kinematic theory.

Figure 3.5. Demonstration of grid independency test of numerical results for temporal evolution of center height, (a) and (b) $Ca = 0.22$, $Bo = 0.0$; (c) and (d) $Ca = 0.1$, $Bo = 0.0$.

The Bond number is set to be zero to focus on capturing the Tanner's law for capillary spreading, where the gravitational effects are neglected.

The tabular experimental results for Runs 5 and 9 are given as follow

Table 3.1. Data of Run 5 from Chen [15].

t (sec)	R (cm)	H (cm)	θ_D (deg)	$C \times 10^4$	$V \times 10^4$ (cm^3)
5.50	0.1135	0.0150	14.75	2.2	3.05
10.50	0.1230	0.0128	12.08	1.2	3.05
20.50	0.1325	0.0111	9.46	0.67	3.07
30.50	0.1380	0.0103	8.54	0.47	3.09
40.50	0.1425	0.0096	7.71	0,37	3.07
50.50	0.1455	0.0090	7.08	0,30	3.00

Table 3.2. Data of Run 9 from Chen [15]

t (sec)	R (cm)	H (cm)	θ_D (deg)	$C \times 10^4$	$V \times 10^4$ (cm^3)
3.25	0.0980	0.0112	12.17	3.1	1.70
13.25	0.1095	0.0087	8.34	0.88	1.64
18.25	0.1130	0.0081	7.50	0.66	1.63
33.25	0.1195	0.0073	6.03	0.39	1.64
73.25	0.1315	0.0059	4.60	0.19	1.60
93.25	0.1455	0.0054	3.91	0.16	1.59
148.25	0.1370	0.0045	3.16	0.10	1.47

In the table, C indicates the real time capillary number calculated by $C \equiv \mu u_c/\sigma$. In our simulation, the capillary number, Ca, is obtained by dividing the initial capillary number, C, reported in Tables 3.3 and 3.2 by the cubic ratio, ϵ. Here, ϵ is defined as the ratio of the initial center hight to the initial radius of the droplet. The unit for length is in millimeter while the unit for contact angle, θ_D, is in degree. The semi-numerical-experimental results well capture the exponent of Tanner's law, i.e.,

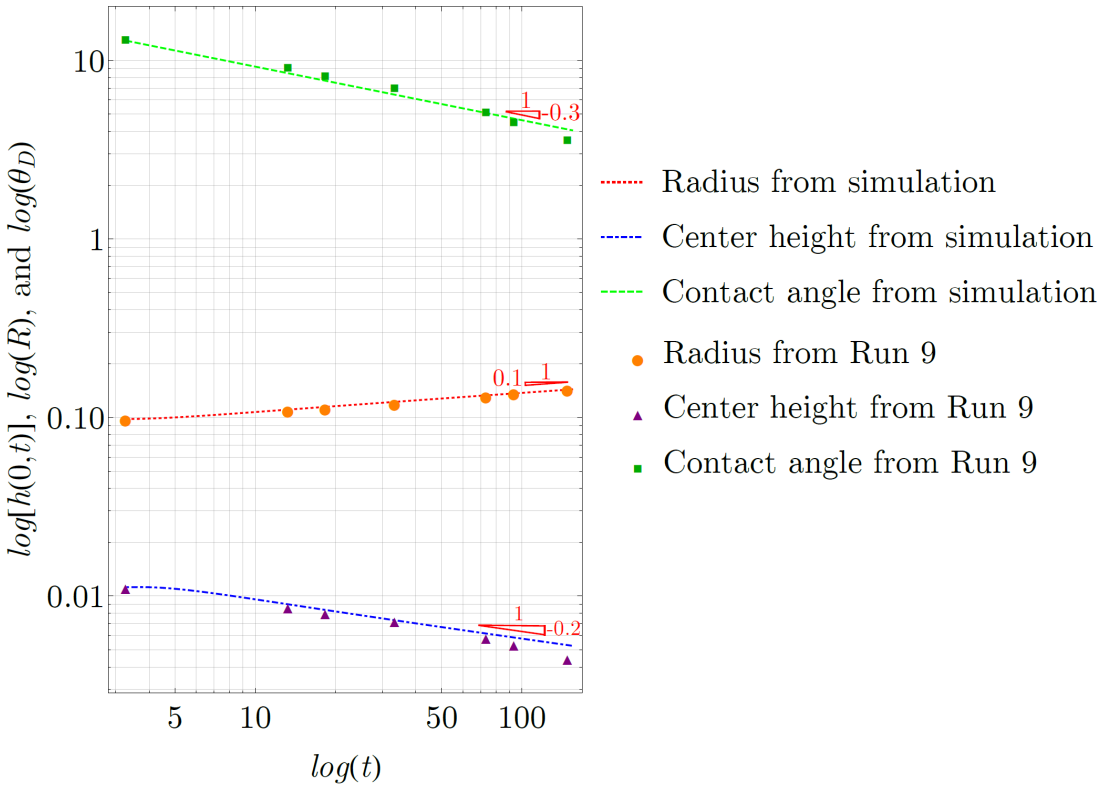

Figure 3.6. Comparison for semi-numerical-experimental results and Run 9 from Chen's paper.

0.1 for spreading, -0.2 for decrease in center height, and -0.3 for decrease in contact angle (Fig 3.6). The deviation in $h(0,t)$ and θ_D from experimental data becomes obvious at larger times. The possible reason for noticeable differences in Fig. 3.6 is that the evaporation effect becomes more effective than that in the initial stage due to increase in free surface area. Fig. 3.8 demonstrates the noticeable difference in volume between numerical results and experimental data. The evaporation rate is nonuniform across the droplet (Fig 3.7; Deegan *et al.* [36]): the liquid evaporating from edge is replenished by the liquid from the interior which could lower the center height more rapidly than that in simulation where the volume conservation condition is used as a global constraint to make sure that the total volume is not changing over time. The snapshots of a droplet spreading at different time steps are given in Fig. 3.9.

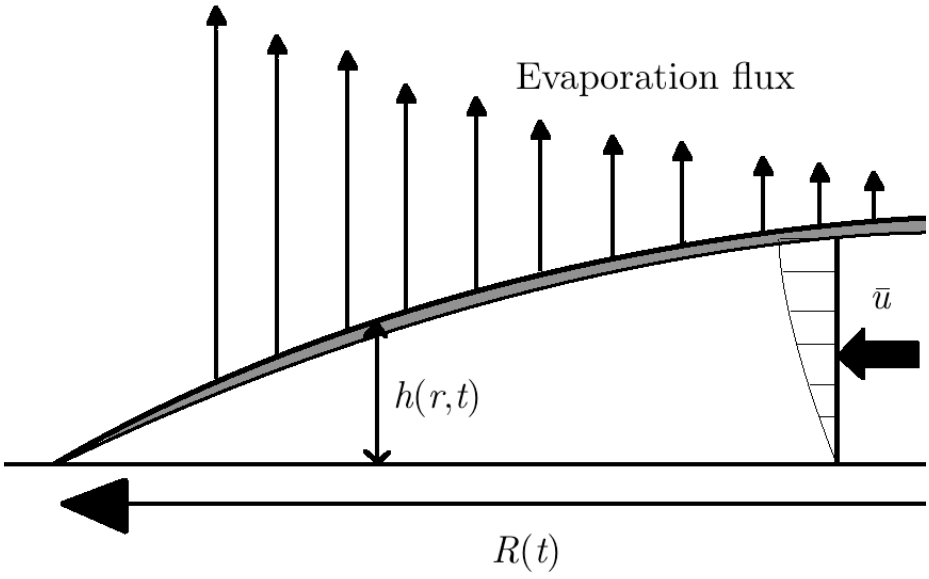

Figure 3.7. Schematic for the nonuniform evaporation rate.

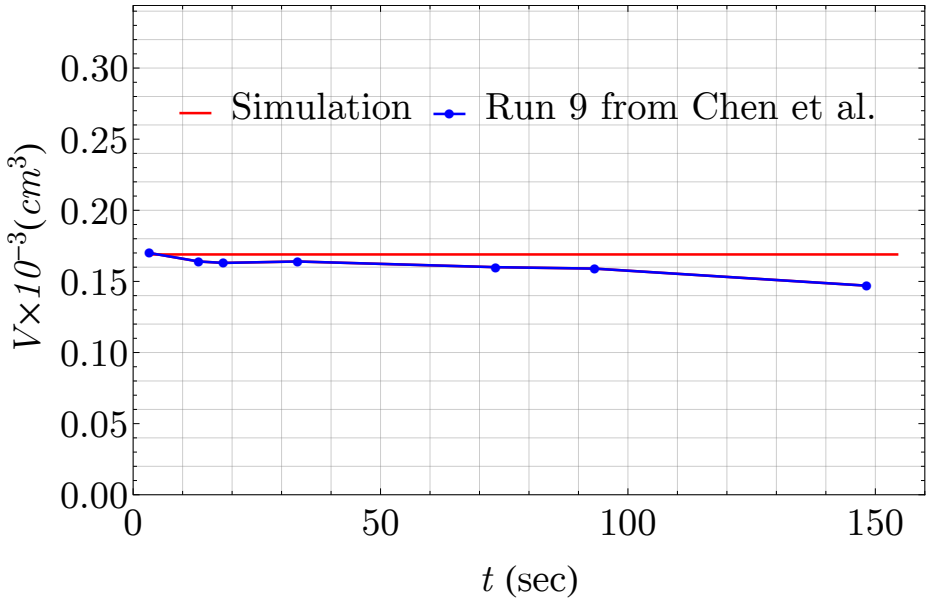

Figure 3.8. The comparison of volume history for numerical and experimental results. In simulation, the total volume is kept constant throughout the spreading process while volume decreases with time in experiments.

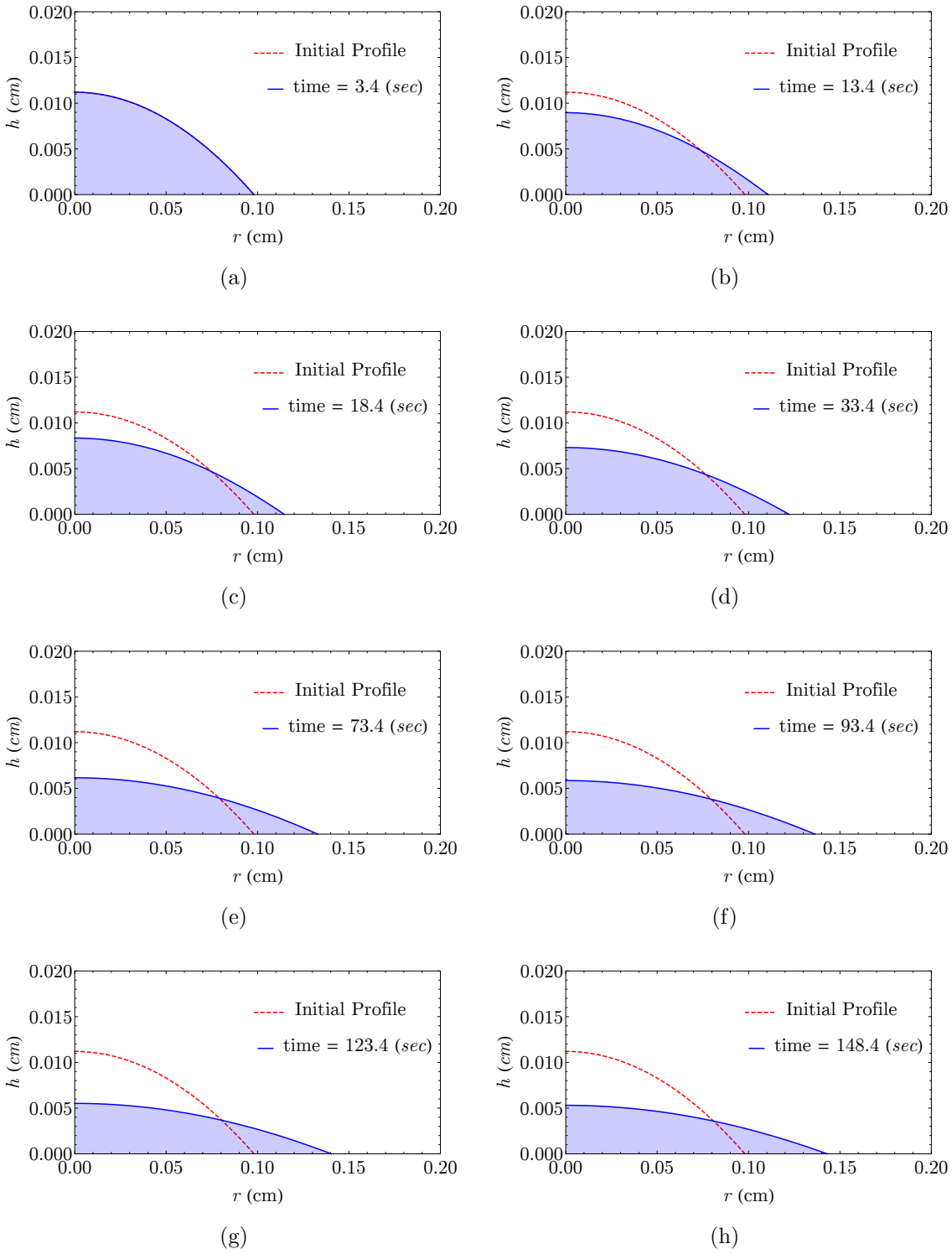

Figure 3.9. Droplet profile at different times.

The next set of numerical results for Run 9 uses contact-line boundary condition based on the molecular kinematic theory (Eq. 2.325).

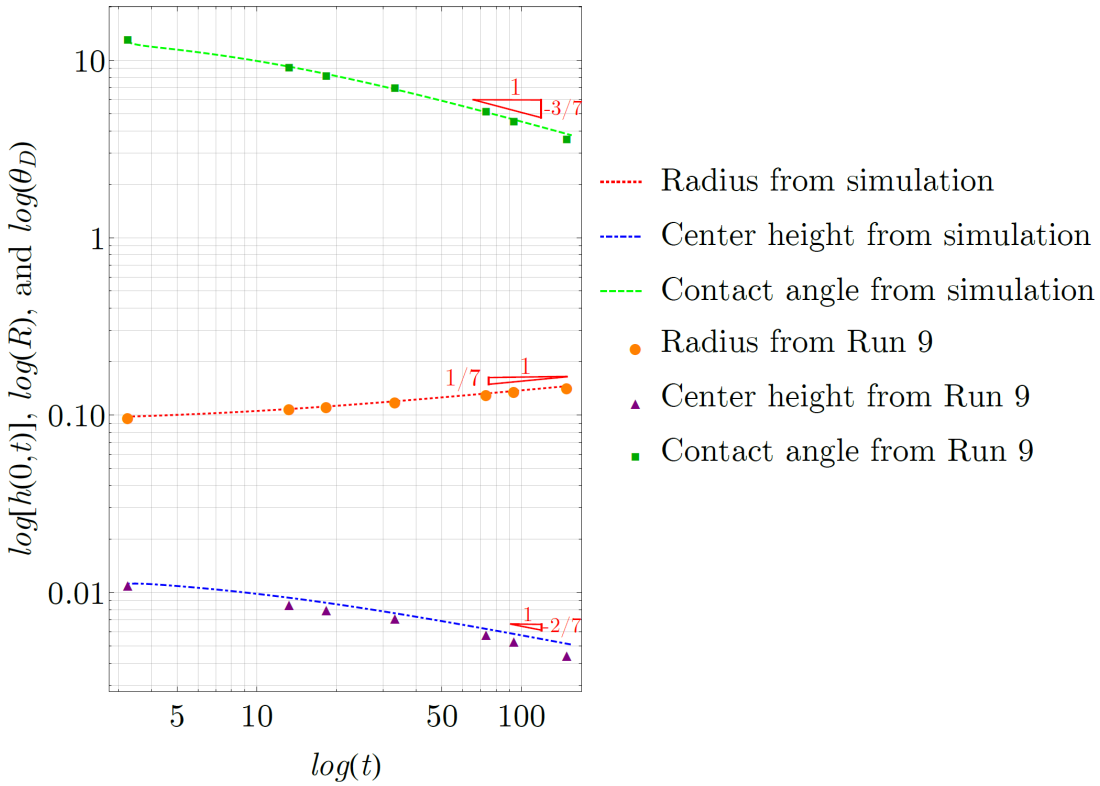

Figure 3.10. Comparison for numerical results and Run 9 from Chen [15].

It is obvious that the use experimental contact line boundary condition and molecular kinematic models can lead to different results. As shown in Fig. 3.10, the spreading exponent is around $1/7$ for R, $-2/7$ for $h(0,t)$, and $-3/7$ for θ_D. However, these results can still match the predictions from Blake [17] written as follow:

$$R \sim t^{1/7} \tag{3.46}$$

$$\theta_D \sim t^{-3/7} \tag{3.47}$$

The individual temporal evolution of variables (R and $h(0,t)$) are reported below to further demonstrate the difference between them. Although the results using molecular kinematic model matches experimental data quite well for initial stage in

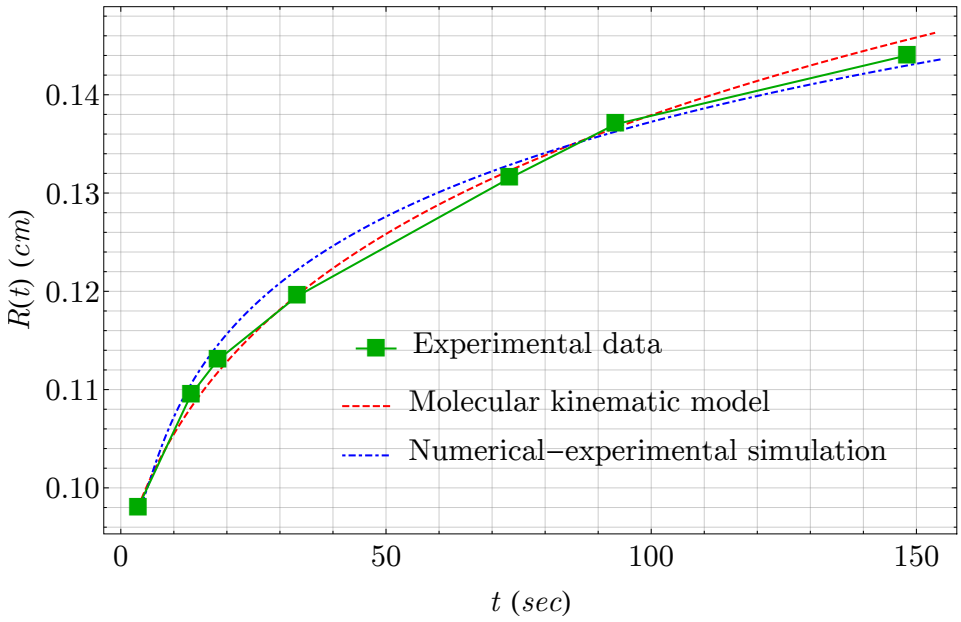

Figure 3.11. Comparison of R using experimental contact line boundary condition and molecular kinematic model.

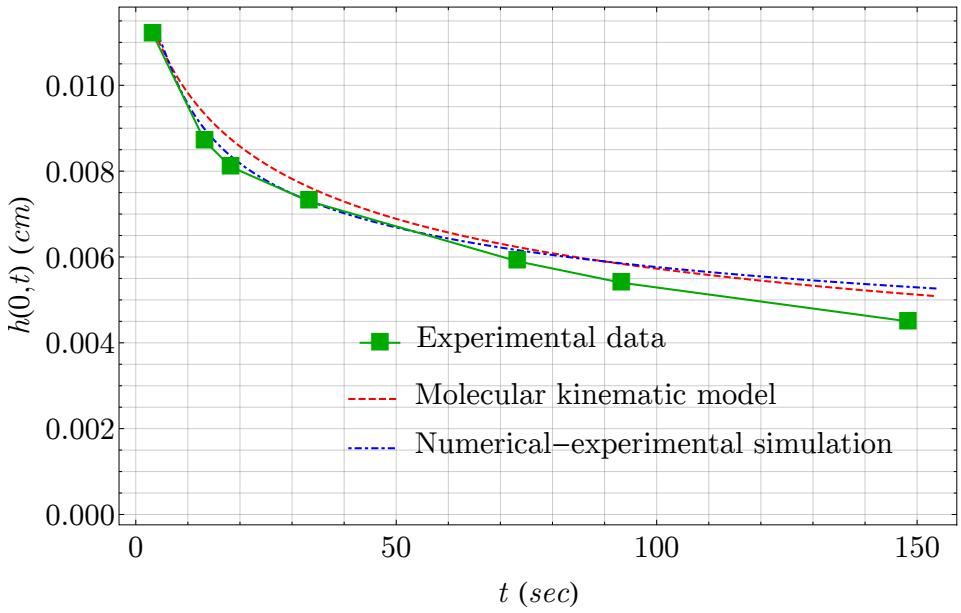

Figure 3.12. Comparison of $h(0,t)$ using experimental contact line boundary condition and molecular kinematic model.

Fig. 3.11, they predict a faster spreading than experiments, resulting in different spreading exponent: 0.1 in Tanner's law and 0.13 in simulation. In, Fig 3.12, there

is an obvious difference in $h(0,t)$ plot due to evaporation effect at larger times. The snapshots of droplet profile at various times are given below:

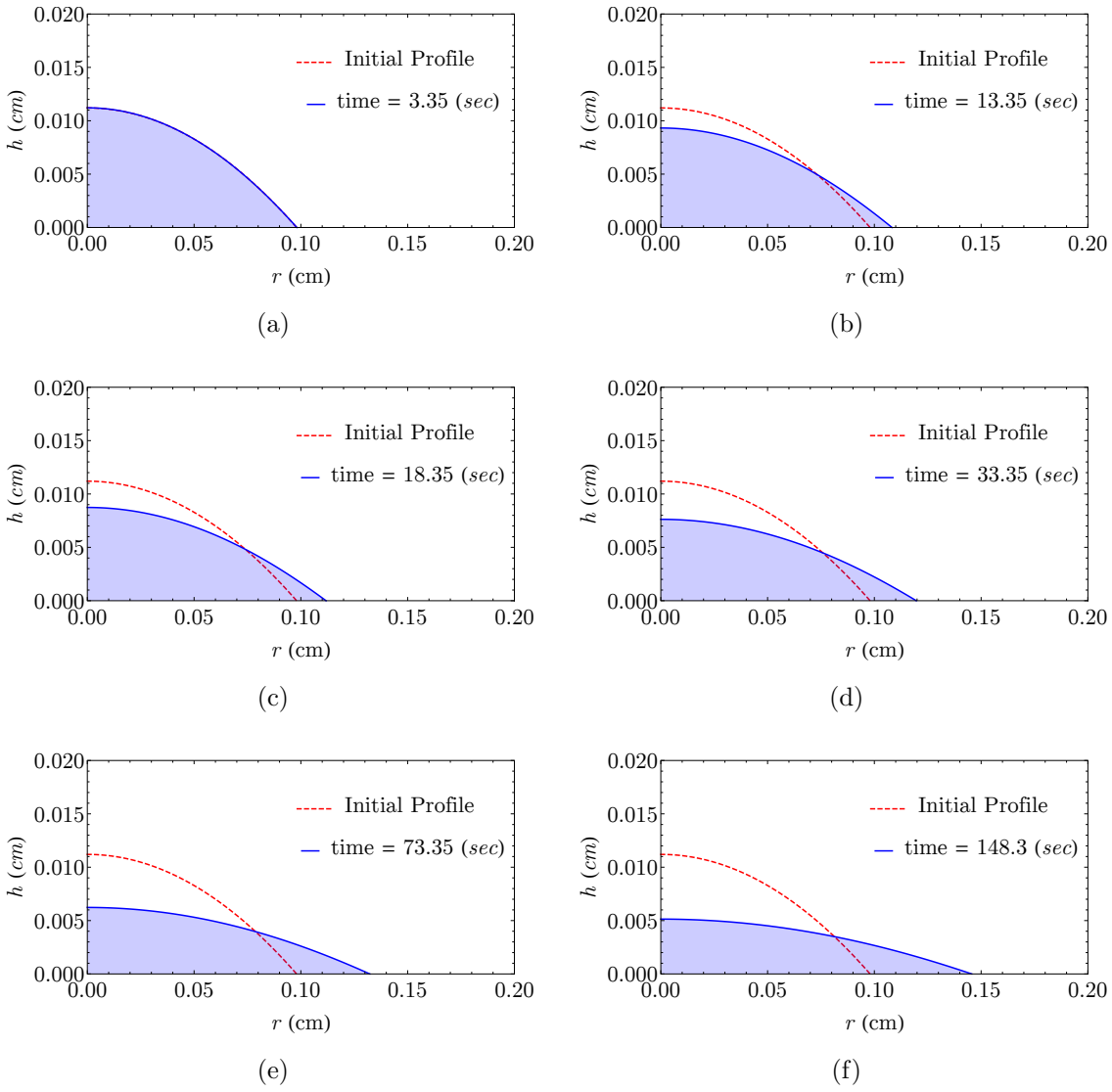

Figure 3.13. Droplet profile at different times.

The results and discussion for Run 5 are quite similar to those in Run 9. However, as shown in Table 3.3, the volume is kept constant during the experiment. Fig. 3.14 shows the temporal evolution of volume both for numerical results and experimental data reported from Run 5. One can observe that the maximum difference between two lines doesn't even exceed 2% with respect to original volume. Fig. 3.15 demonstrates the comparison of semi-numerical-experimental results with data from Table 3.3. As shown in Fig. 3.15, the numerical values for these three variables match experimental data reported in Run 5 very well. Besides, the Tanner's law which applies only to capillary spreading is captured in Fig. 3.15. Snapshots of droplet profile are provided in Fig 3.16.

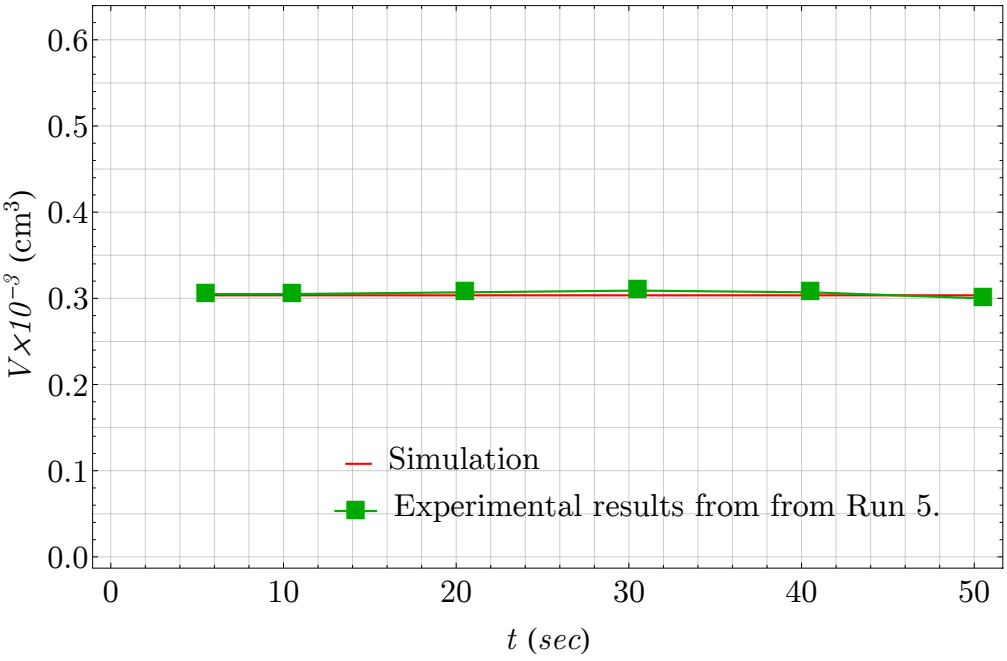

Figure 3.14. Plot of the temporal evolution of total volume against experimental data.

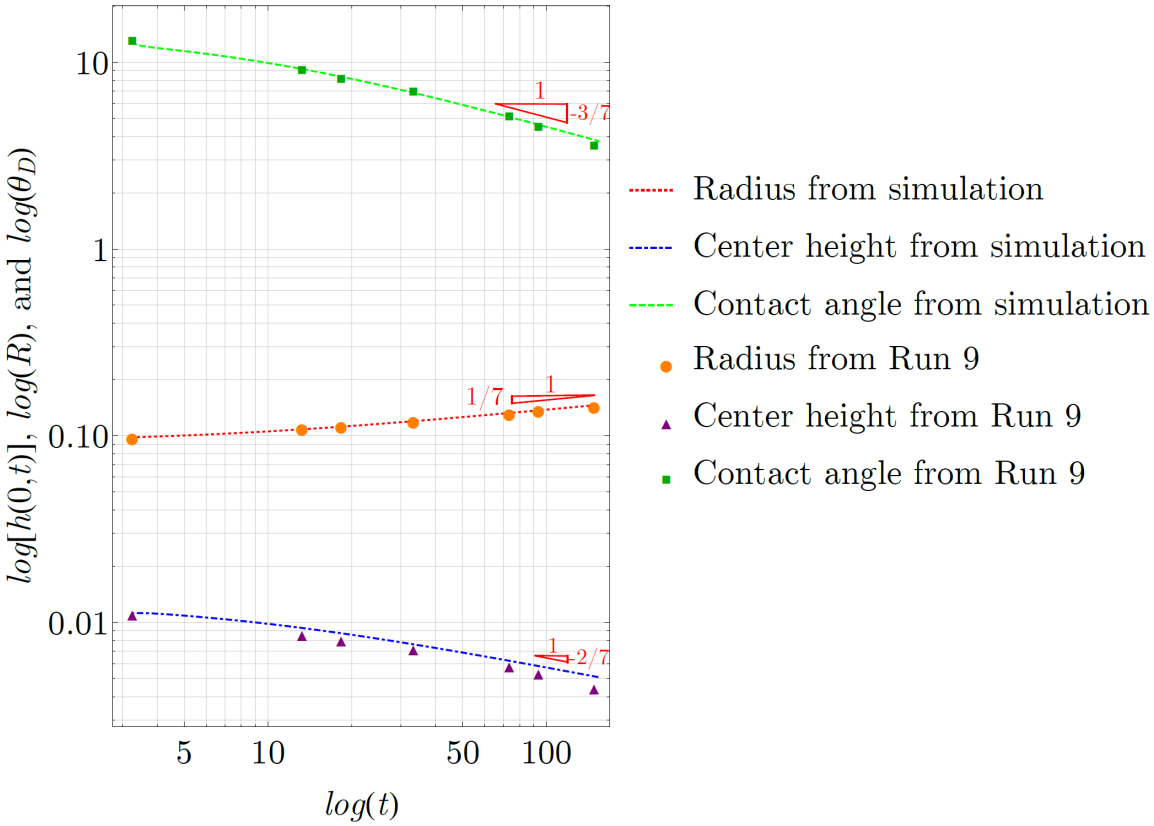

Figure 3.15. Plot of R, $h(0,t)$, and θ_D as functions of time t compared with experimental data.

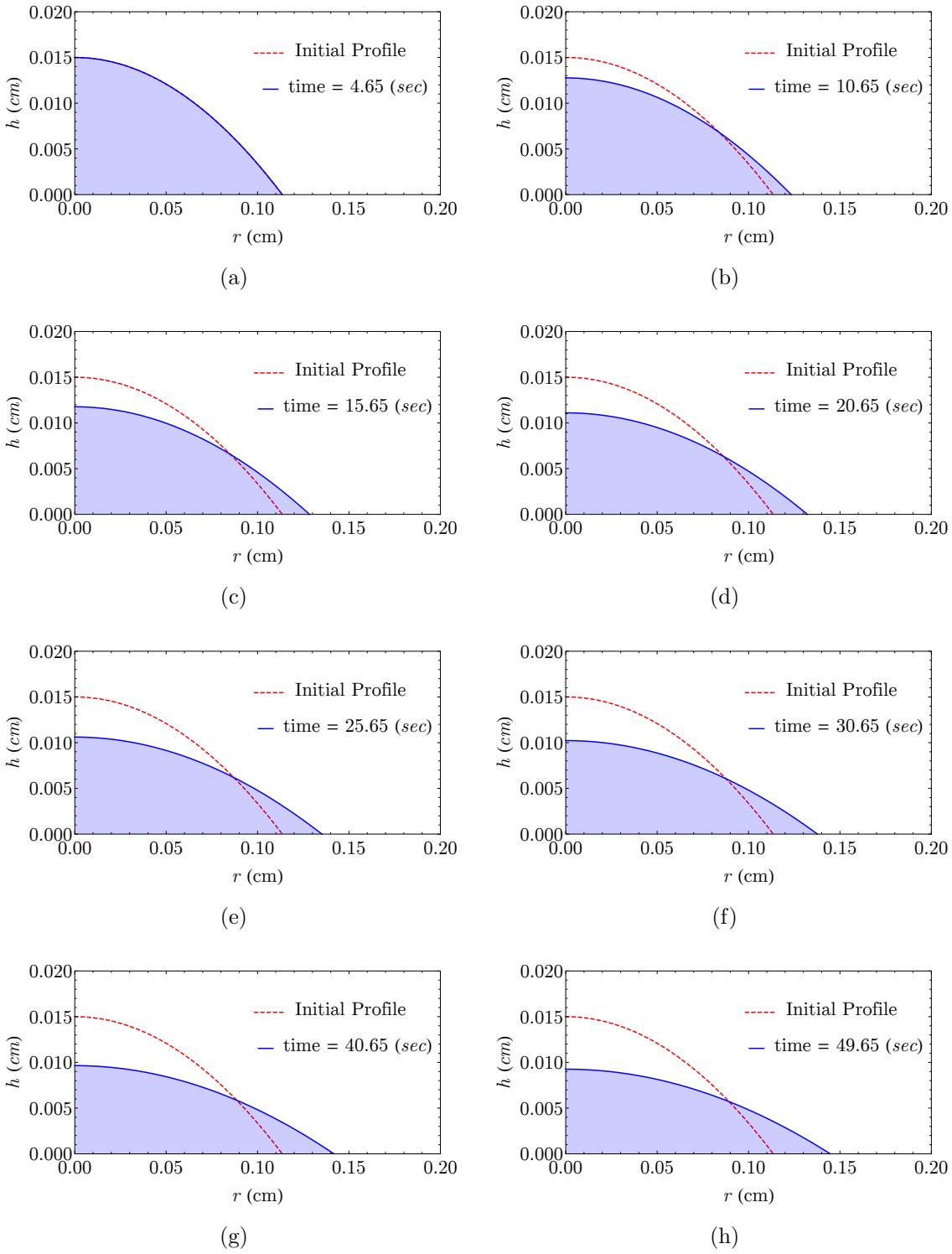

Figure 3.16. Droplet profile at different times.

3.3.2 Power-Law Droplet Spreading over a Solid Substrate

Eq. (2.256) is solved subjected to the following boundary conditions: Eq. (2.318), Eq. (2.319), Eq. (2.320), and Eq. (2.321). Here, the length scales of droplet is small enough for us to only involve capillary effects in the pressure. Typically, the horizontal length scale is smaller than the capillary length scale $\sqrt{\sigma/\rho g} \approx 2.7$mm. The system of equations with zero slope boundary condition at the rim of droplet ($\frac{\partial h}{\partial r}_{r=R}$) has been analytically solved in Starov *et al.* [1]. The spreading exponent α is given by

$$\alpha = \frac{n}{7+3n} \tag{3.48}$$

The plot of spreading exponent is shown below to demonstrate how rheological exponent affects the behavior of spreading. In the present study, the contact-line boundary

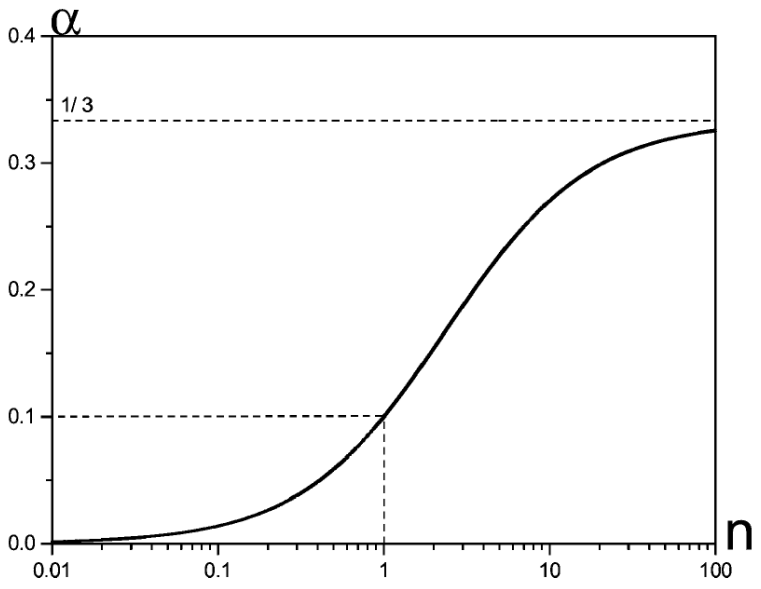

Figure 3.17. Plot of spreading exponent versus power-law exponent.

condition implemented in the simulation is based on the molecular kinematic theory (Eq. (2.325)) instead of using zero slope condition at the edge of droplet. The plots

of values of R as a function of time and logarithm of radius have been shown here to illustrate the spreading exponent.

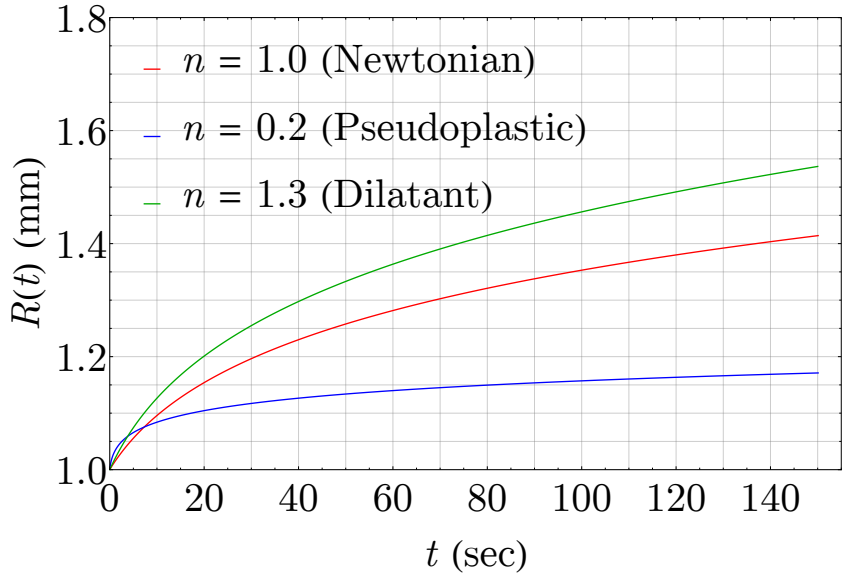

Figure 3.18. Plot of radius as a function of time.

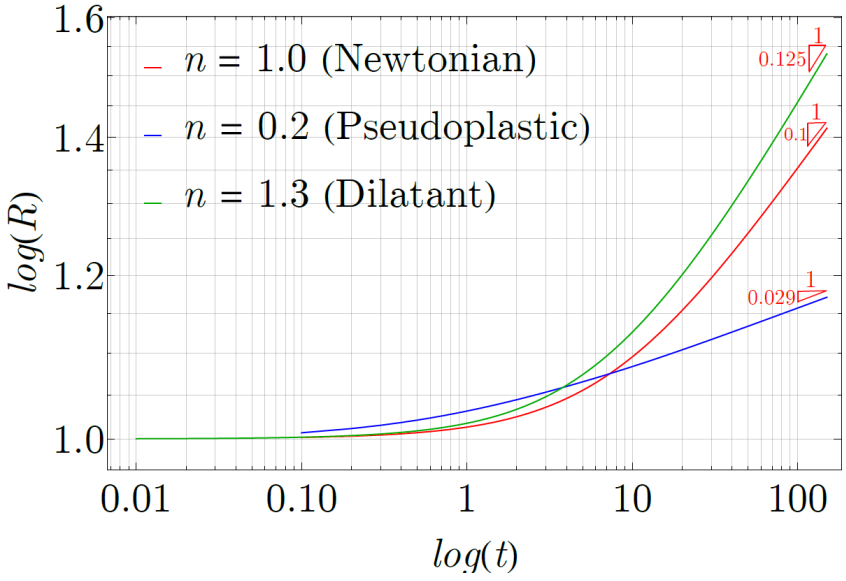

Figure 3.19. Logarithm of radius as a function of time.

The snapshots of droplet profile for spreading of shear-thinning and shear-thickening droplets are reported below.

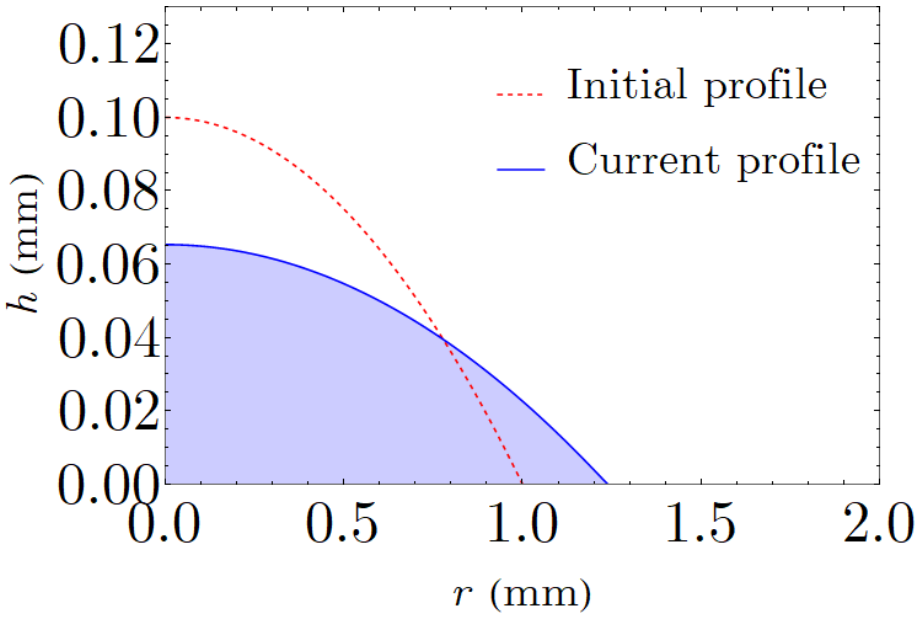

Figure 3.20. Profile of shear-thickening droplet ($n = 1.3$).

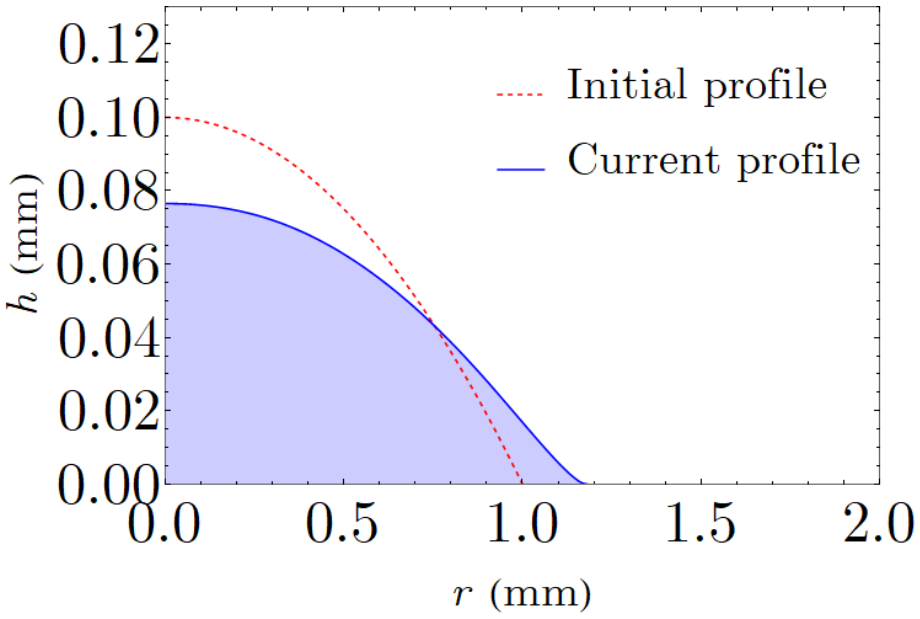

Figure 3.21. Profile of shear-thinning droplet ($n = 0.2$).

Comparisons against Eq. (3.48) for different power-law exponents from 0.1 to 2.0 are reported in the table and Fig. 3.22.

Table 3.3. Table of comparison for the spreading exponents obtained from simulations against the ones obtained using Eq. (3.48) for different power-law exponents.

Power-law exponents	Spreading exponents from Starov *et al.* [1]	Spreading exponents from simulations
$n = 0.1$	0.0137	0.0123
$n = 0.2$	0.0263	0.0292
$n = 0.3$	0.0380	0.0401
$n = 0.4$	0.0488	0.0484
$n = 0.5$	0.0588	0.0556
$n = 0.6$	0.0682	0.0642
$n = 0.7$	0.0769	0.0780
$n = 0.8$	0.0851	0.0851
$n = 0.9$	0.0928	0.0911
$n = 1.0$	0.1	0.1
$n = 1.1$	0.1068	0.1142
$n = 1.2$	0.1132	0.1134
$n = 1.3$	0.1193	0.1192
$n = 1.4$	0.1250	0.1254
$n = 1.5$	0.1304	0.1311
$n = 1.6$	0.1356	0.1352
$n = 1.7$	0.1405	0.1401
$n = 1.8$	0.1452	0.1442
$n = 1.9$	0.1496	0.1484

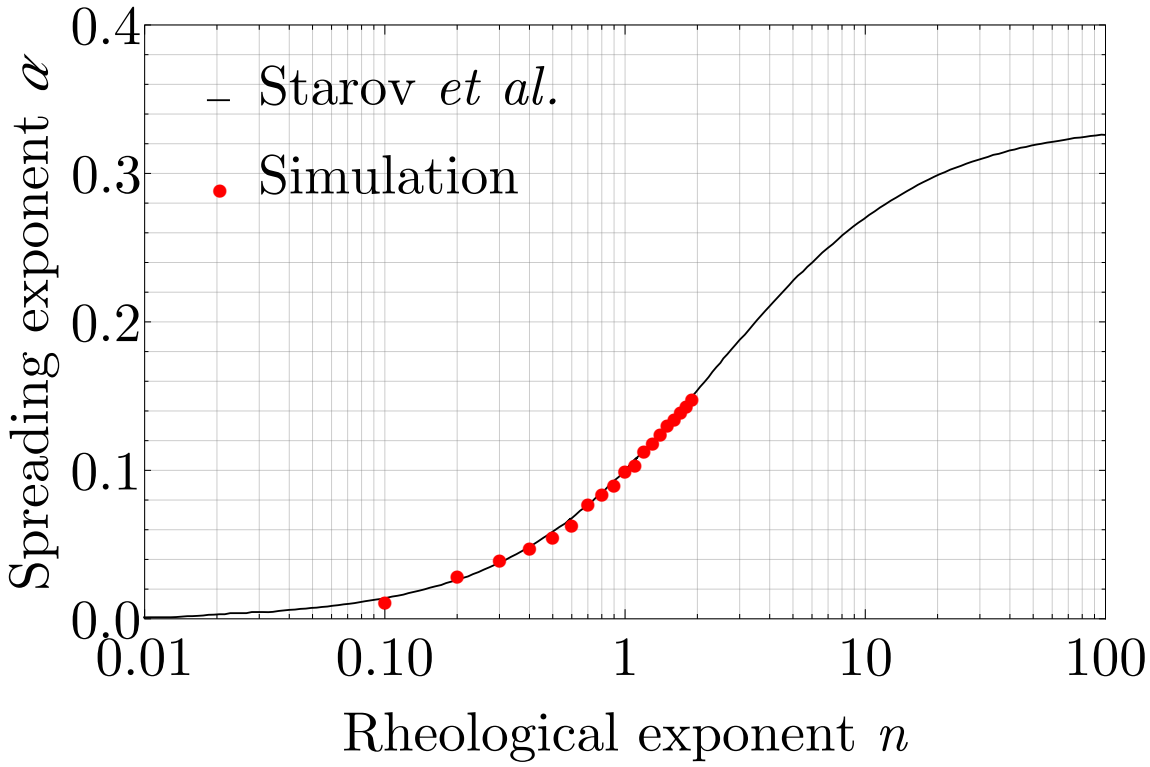

Figure 3.22. Plot of radius as functions of time.

As Shown in Fig 3.18 and Fig 3.19, increase in the the power-law exponent results in a larger spreading exponent which means that a shear-thickening droplet spreads faster than Newtonian and shear-thinning droplets. Because shear rate increases upon approaching the contact-line, the liquid closer to the rim moves faster than interior liquid causing more advancement of contact line and decrease in the apparent contact angle. Therefore, a shear-thinning droplet has a larger spreading rate than a shear-thickening droplet at the initial stage. Besides, the feature of reverse-curve tail for shear-thinning droplet (Fig 3.20) results from the increase in the shear rate near the contact line. The force that drives the moving-contact line in a given direction is equal to the out-of-balance surface-tension force arising from the deviation of current contact angle from the static angle. In other words, the spreading velocity varies with the difference of current contact angle from the static contact angle: the smaller difference between current state and static state, the smaller the driving force for

spreading and the slower contact-line moves. Therefore, the shear-thinning droplet has the lower spreading rate than Newtonian and shear-thickening droplets after a long time.

The following results are for a Xanthane droplet spreading over a solid substrate. The surface tension for the air/Xanthane solution is $72 \pm 2\text{mNm}^{-1}$ at 20°C independent of various concentrations used in the experiments from Rafaï, Bonn, & Boudaoud [2] and in our simulation. The shear-thinning behavior is described by a shear rate dependent viscosity as $\mu = \mu_0 \dot{\gamma}^{n-1}$, where μ_0 is the zero shear rate viscosity and n is the power-law factor reflecting the shear-thinning property of liquids. The plot of viscosity versus shear rate describing shear-thinning behavior of xanthane solutions is provided in Rafaï *et al.* [2]. The simulations for polymer concentration of 125, 1000, 2500, and 5000 p.p.m are carried out and reported below.

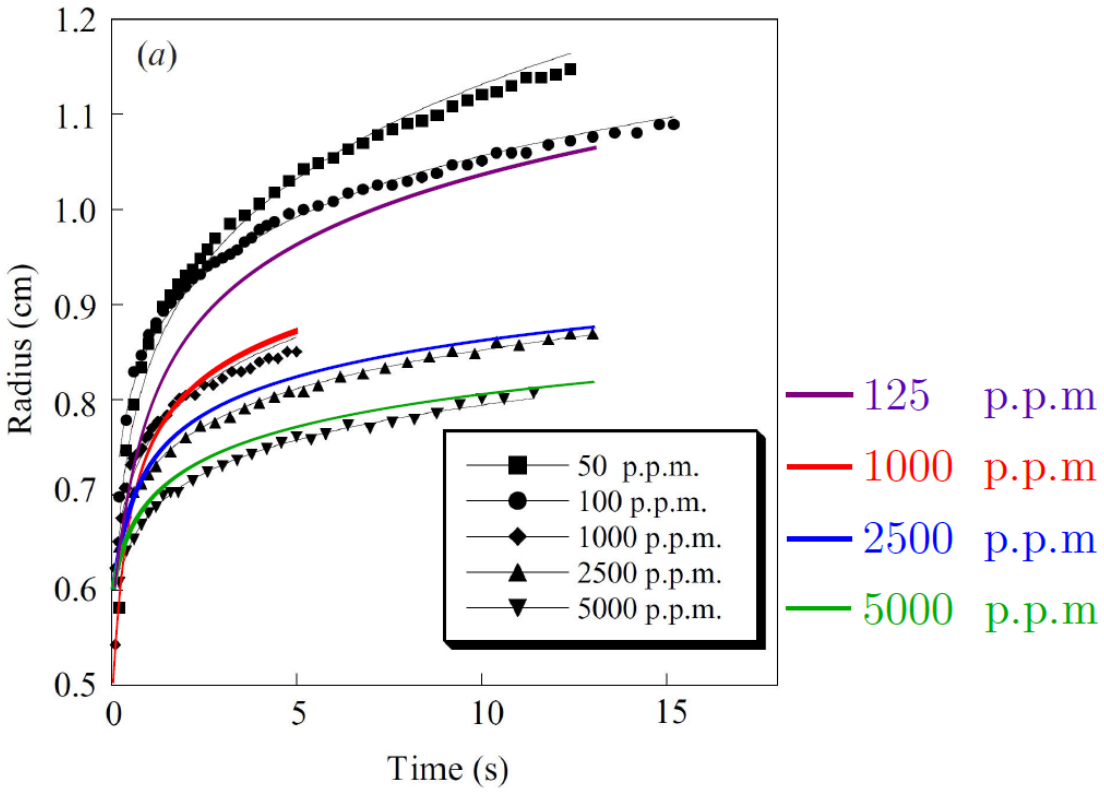

Figure 3.23. Radius of xanthane droplets versus time from measurements and simulations.

The zero-shear-rate viscosities μ_0 for polymer concentrations of 125, 1000, 2500, and 5000 p.p.m. are 21.115, 34.191, 4666.593, and 21602.000 mPa, respectively. The power-law exponent are 0.7173, 0.3918, 0.3025, and 0.1777, respectively. Though we can not match the experimental data exactly, we still capture the trend of spreading for each case. The evaporation effect and the contact-line boundary condition may lead to the some deviation from experimental results. However, the evaporation effect can be ruled out due to high averaged molecular weight of xanthane solution for relatively short time experiments. The contact-line condition (Eq. (2.325)) could be replaced with a more advanced and complicated boundary condition including energy dissipation not only due to the wetting-line friction but also due to viscous losses in the thin wedge adjacent to the moving-contact line. Besides, the energy dissipation due to viscous losses can be generalized based on the shear rate dependent viscosity. This portion of total energy dissipation can possibly bring the numerical results closer to the measured data.

3.3.3 Newtonian Droplet Spreading over a Porous Substrate

For the case of the spreading over an impermeable medium, i.e., $\phi = 0$ and $Pm = 0$, the evolution of the contact radius $R(t)$ and the center height $h(0,t)$ shows the Tanner law behavior in Figs. 3.25 and 3.26 and approaches its equilibrium shape for $t \gg 1$.

$$R \sim t^{1/10}, \text{ and } h(0,t) \sim t^{-2/10} \ . \tag{3.49}$$

When the spreading is coupled with the absorption effect (Figs. 3.27 and 3.28), the evolution of the center height, $h(0,t)$, and contact radius, $R(t)$, follows the Tanner's law behavior during the initial phase of spreading and absorption, since the liquid withdrawn from the droplet during this comparatively short period is small (about 1 % of the total absorption time). At around $t = 1.99$, the advancement of contact radius is greatly delayed after the radius reaches its maximum value. Then the absorption effect starts to become dominant due to the increase in the contact radius, $R(t)$. The central height of the droplet starts to drastically decrease. Hence, the contact line recedes until the droplet has been completely absorbed. The entire absorption process is considered complete when the center height approaches the thickness of thin film. The competition between the spreading and the absorption is measured at $r = 0$ and plotted in Fig. 3.32. Figs. 3.27 and 3.28 show the evolution of the center height, $h(0,t)$, and contact radius, $R(t)$, of the droplet on a porous substrate ($Pm = 5 \times 10^{-6}$ and $\phi = 0.25$). The snapshot of profiles of the free surface and the wetting front is plotted in Fig. 3.29. The flat wetting profile inside the porous medium near the center of the droplet results from the uniform absorption rate near the center. We can observe that the terms governing the evolution equation of the wetting front (Eq. (2.184)) are the suction number and the pressure at the free surface of the droplet. If we neglect the gravitational effect for a small droplet, the pressure at the free surface is related to the droplet shape by the Young-Laplace equation.

$$p(r,t) = Pa + 2H\sigma \ , \tag{3.50}$$

where Pa is the atmosphere pressure, σ is the surface tension of the fluid and H is the mean curvature. For thin film, H is given by

$$H \approx \frac{1}{2r}\frac{1}{r}\frac{\partial}{\partial r}\left(r\frac{\partial h}{\partial r}\right) . \tag{3.51}$$

Under the effect of thin film approximation, the curvature, H, near the center of the droplet, $r = 0$, stays constant during the entire process of spreading and absorption. The suction number, only affected by the characteristic lengths and the capillary pressure jump inside the porous medium, can be considered a constant throughout the computational domain. Therefore, the uniform propagation of wetting profile near the center of the droplet results in a flat penetration front. The similar profile near the center of the droplet can be found in Alleborn & Raszillier [4]; Zadražil, Stepanek & Matar [26]. Another feature is that when the contact radius recedes, the wetting front ahead of the contact point barely propagates. The absorption velocity is zero for the points located at the right-hand-side of the contact point because there is no mass withdrawn from above, i.e., $r > 0.87$ in Fig. 3.29. Another possible cause of propagation is the radial velocity, u_p, inside the porous medium as shown in Fig. 3.33. However, the scale of this radial velocity (Eq. (2.171)) is much smaller than that of the vertical velocity (Eq. (2.170)) inside the porous medium as shown in Eq. (3.52):

$$\frac{u_p}{w_p} \approx \frac{1/L^2}{1/H^2} = \epsilon^2 . \tag{3.52}$$

Therefore, the combination of the above effects leads to a nearly zero propagation of the wetting front.

The evolutions of the contact radius and the central height for different permeability numbers are plotted in Figs. 3.30 and 3.31. We observe that a larger permeability number enhances the absorption effect and decreases the maximum contact radius. Thus, the droplet spreading follows the Tanner's law for a shorter time as permeability number increases. The total time for the droplet to be completely absorbed into the porous substrate gets shorter as well. For cases with stronger absorption effects, the contact radius of the droplet can even decrease in the beginning without showing

the spreading behavior as shown in Fig 3.29. The absorption effect dominates the governing equations during the entire simulation causing a monotonic decrease in the radius and the central height as time goes by.

Finally, in Fig 3.25, we compare the evolution of contact radius against the experimental results reported in Denesuk *et al.* [3] using the new model (Eq. (2.173) and Eq. (2.184)) we proposed in chapter 2.

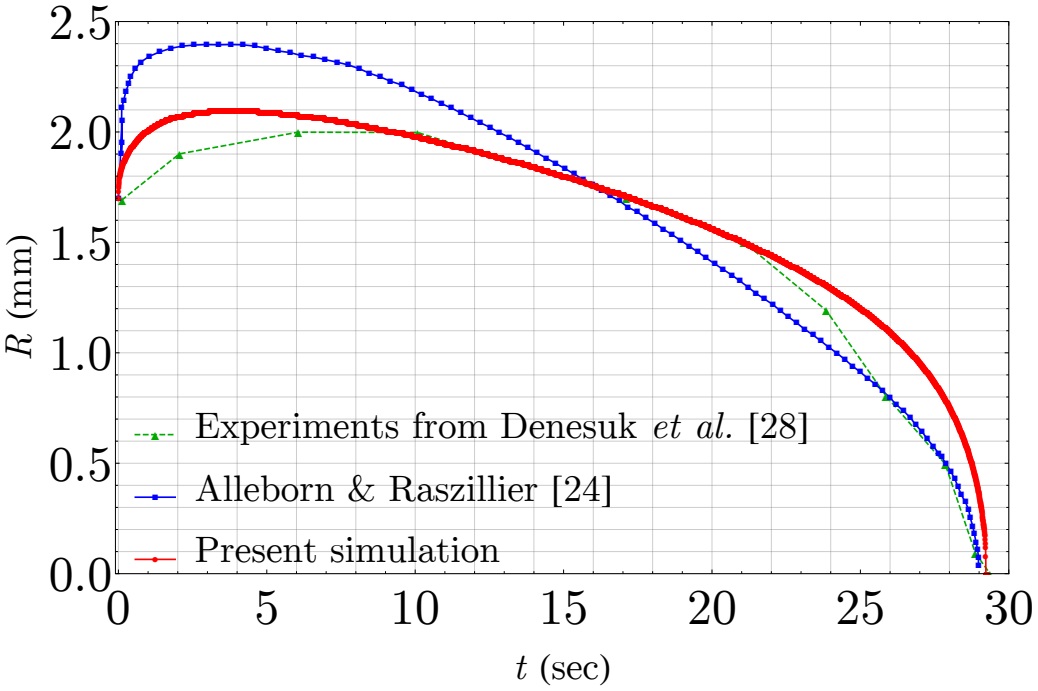

Figure 3.24. The contact radius, $R_c(t)$, of a droplet versus t. The green line indicates the experimental values of Denesuk *et al.* [3] for a PDMS droplet on a porous soda-lime-silicate substrate. The blue line indicates the numerical results from Alleborn & Raszillier [4]. The red line is the current numerical study. ($Pm = 2.076 \times 10^{-6}$, $Su = 680$, and $\phi = 0.64$)

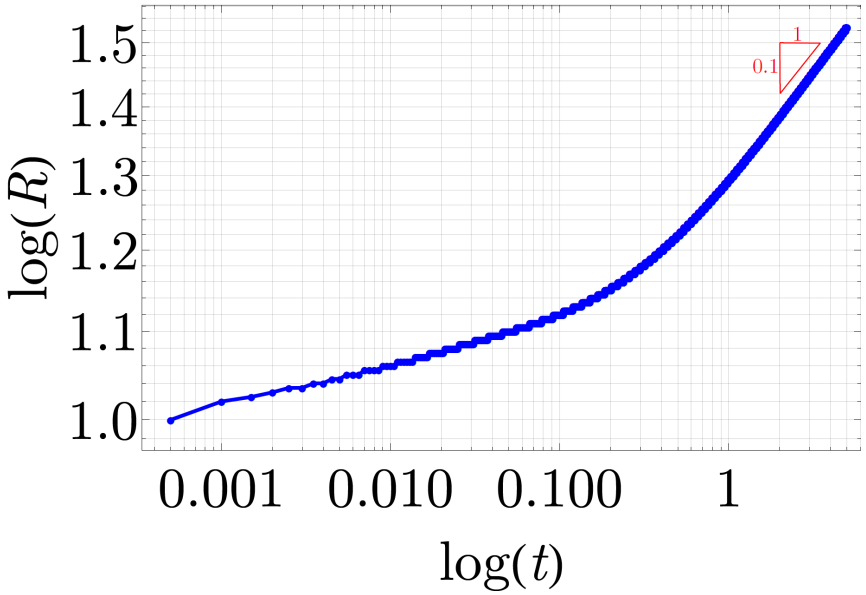

Figure 3.25. Plot of the radius as a function of time. ($Pm = 0$ and $\phi = 0.25$)

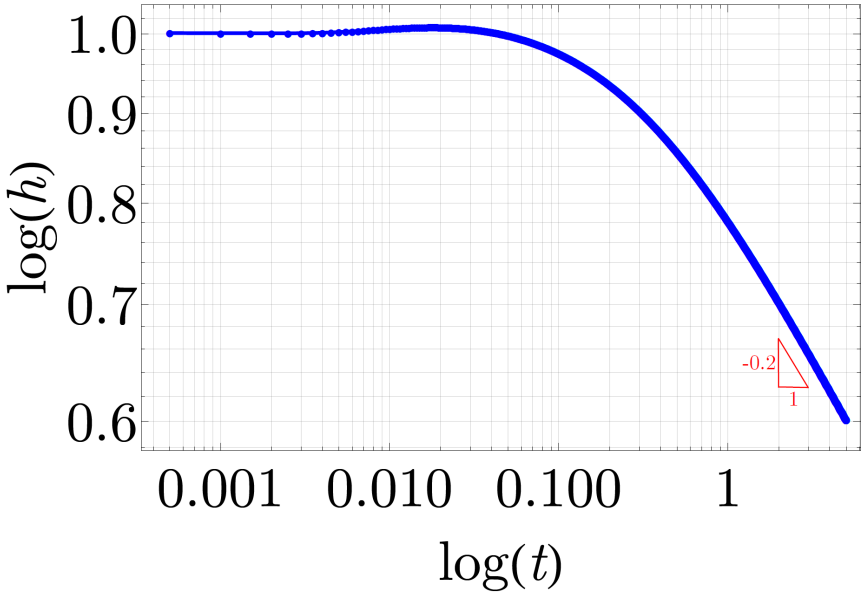

Figure 3.26. Plot of the center height as a function of time. ($Pm = 0$ and $\phi = 0.25$)

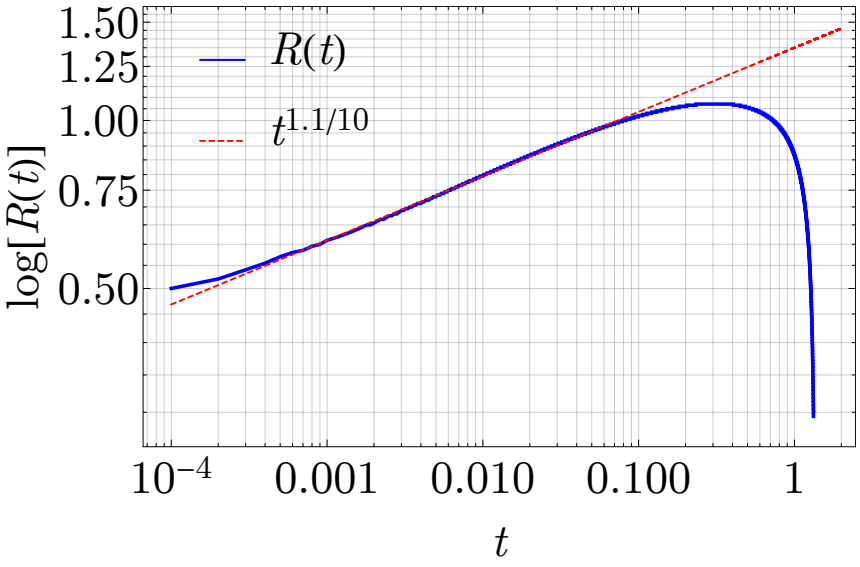

Figure 3.27. Spreading and absorption of a droplet: contact radius $R(t)$ as a function of time. ($Pm = 5 \times 10^{-6}$, $Su = 10^5$, and $\phi = 0.25$)

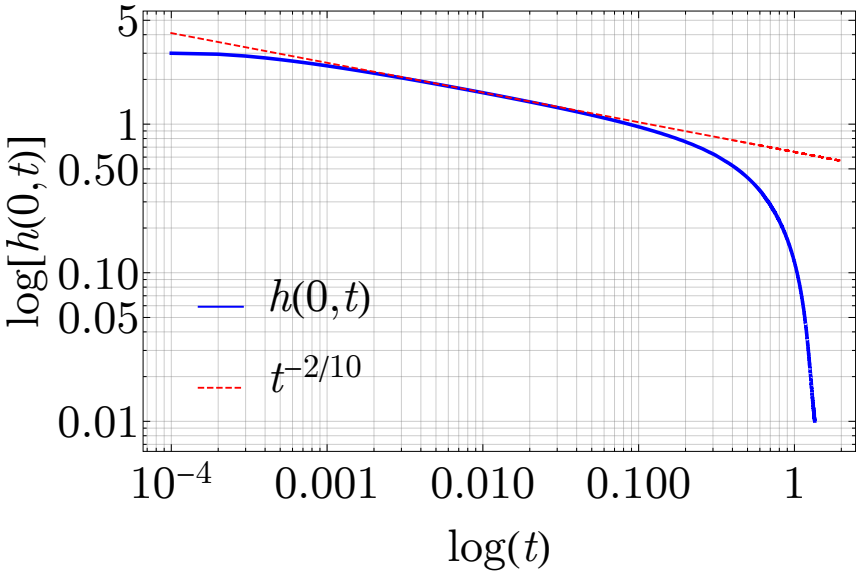

Figure 3.28. Spreading and absorption of a droplet: center droplet height $h(0,t)$ as a function of time. ($Pm = 5 \times 10^{-6}$, $Su = 10^5$, and $\phi = 0.25$)

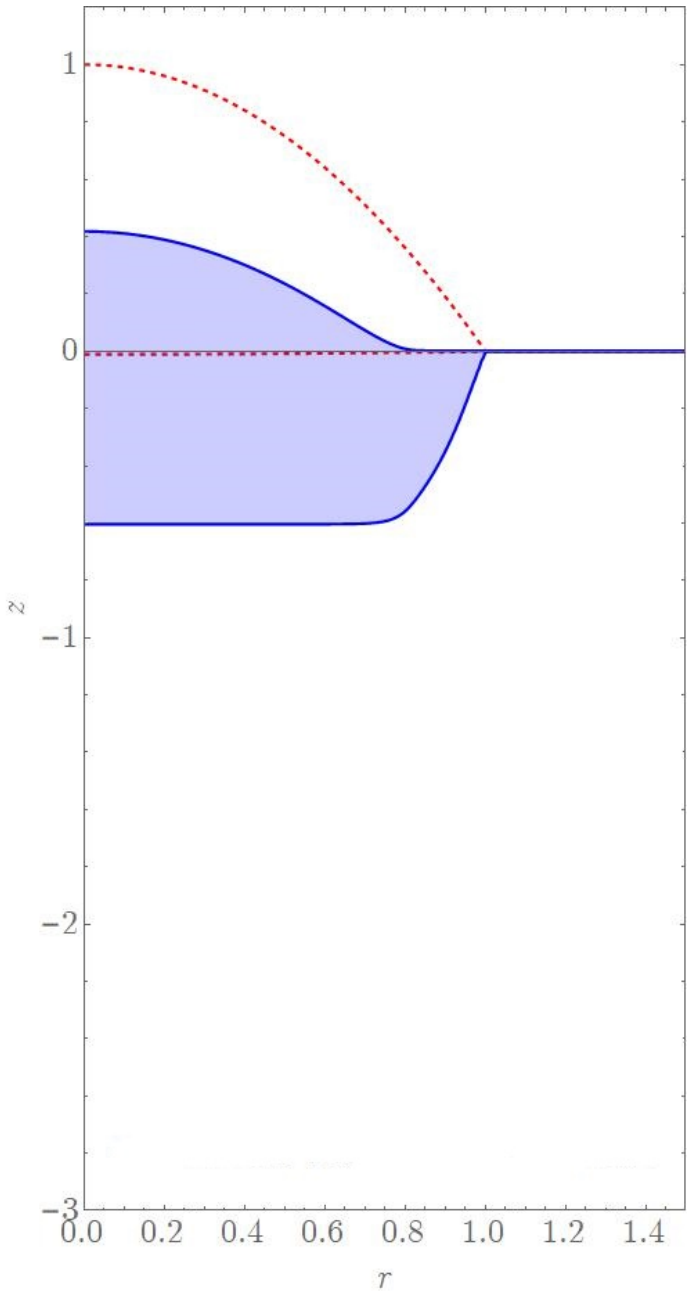

Figure 3.29. Dimensionless profiles of the free surface and the wetting front. The red-dashed line indicates the profiles at $t = 0$. The blue-solid line indicates the profiles at $t = 0.23$.

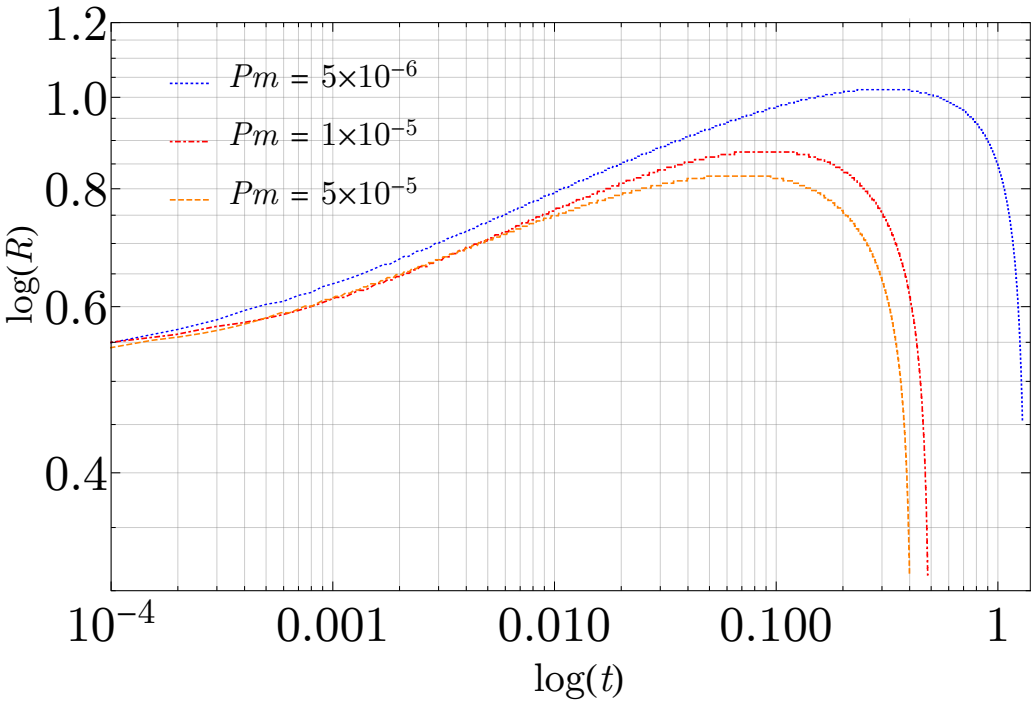

Figure 3.30. The contact radius, $R(t)$, versus t for $Su = 10^5$ and $\phi = 0.25$.

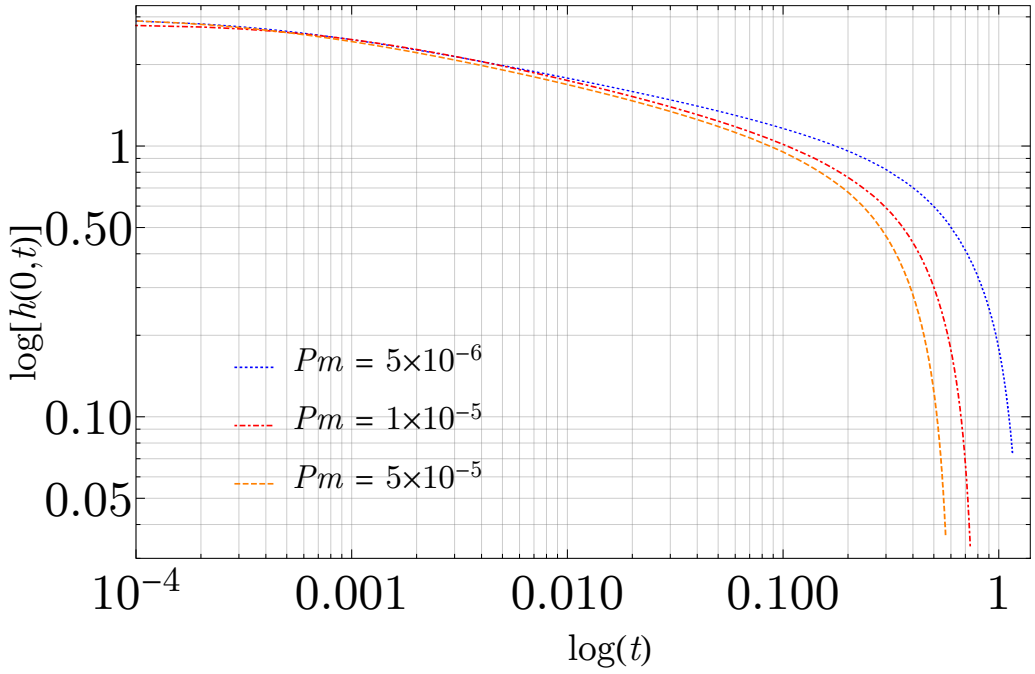

Figure 3.31. The central height, $h(0,t)$, versus t for $Su = 10^5$ and $\phi = 0.25$.

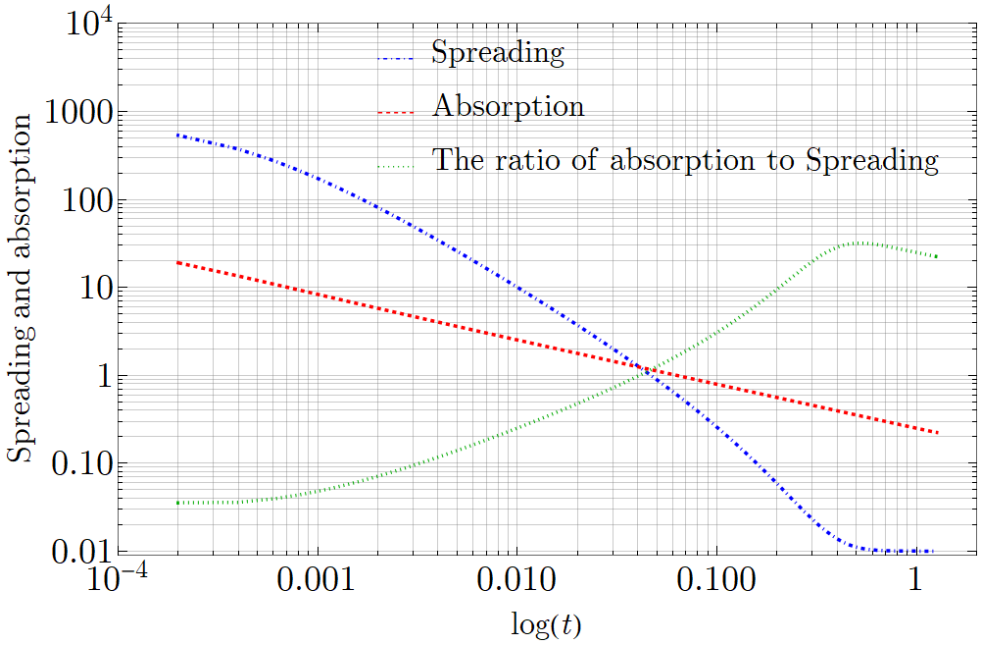

Figure 3.32. The spreading and absorption terms in Eq. (2.173) as functions of time. The spreading and absorption terms indicate the second and the third terms in Eq. (2.173), respectively.

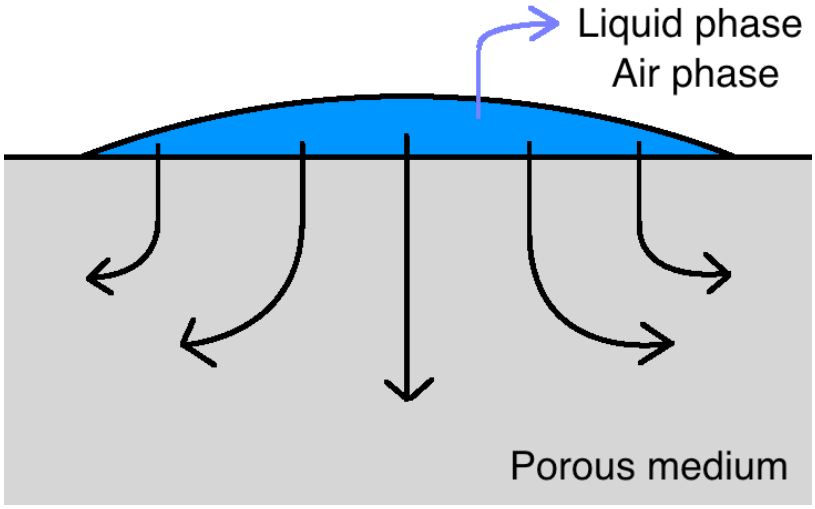

Figure 3.33. The schematic of flow inside the porous medium.

4. RECOMMENDATIONS FOR FUTURE WORK

4.1 Better Physical Representation of Contact Line

The physics at the contact line is complicated. The boundary condition based on the molecular kinematic theory only accounts for the part of rate of the energy dissipation due to wetting-line friction. According to the review by Blake [17], the rate of energy dissipation per unit length of the wetting line is the product of the flux U and the out-of-balance surface tension force $\sigma\big(\cos\theta_S - \cos\theta_D\big)$. The total energy is assumed to be composed of the energy losses due to viscous bending of the liquid-gas interface near the moving contact line, i.e., the viscous dissipation, plus the losses due to wetting-line friction. The above statement can be written in the following equation

$$\sigma\big(\cos\theta_S - \cos\theta_D\big)U = \frac{6\mu U}{\theta_D}\ln\left(\frac{L}{L_m}\right)U + \zeta U^2 \ , \tag{4.1}$$

i.e.

$$U = \frac{\sigma\big(\cos\theta_S - \cos\theta_D\big)}{\zeta + \frac{6\mu}{\theta_D}\ln\big(\frac{L}{L_m}\big)} \ . \tag{4.2}$$

Here, the length scale L is the characteristic size of the droplet and L_m is the appropriate chosen microscopic length scale. ζ is the coefficient of the wetting-line friction.

4.2 Higher Order Model for Flow inside the Substrate: The Brinkman Equation

In chapter 2., we assume the flow inside the porous substrate is governed by the Darcy's law for the Newtonian liquids and the modified Darcy's law for the power-law fluids. In Darcy's law, the flow inside the porous medium is only affected by the pressure gradient as shown in Eq. (4.3).

$$\mathbf{u} = -\frac{\kappa}{\mu}\nabla p \ . \tag{4.3}$$

In a low Reynolds number regime, we can still neglect the inertial effect. Nevertheless, neglecting the viscous effect may result in large deviation from the actual phenomenon. Therefore, we need an equation that can better describe the flow inside the porous media. The Brinkman equation (Brinkman [37]), neglecting the inertial effects and considering the viscous and pressure terms, is given by

$$\frac{\mu}{\kappa}\mathbf{u} = -\nabla p + \Delta \mathbf{u} \ . \tag{4.4}$$

Here, $\mathbf{u} = (u, v, w)$ is the averaged velocity, μ is the dynamic viscosity, and κ is the permeability of the porous media. The relevant analysis of the Brinkman equation can be found in Durlofsky & Brady [38].

REFERENCES

REFERENCES

[1] V. M. Starov, A. N. Tyatyushkin, M. G. Velarde, and S. A. Zhdanov. Spreading of non-newtonian liquids over solid substrates. *Journal of Colloid and Interface Science*, 257(2):284–290, 2003.

[2] S. Rafaï, D. Bonn, and A. Boudaoud. Spreading of non-newtonian fluids on hydrophilic surfaces. *Journal of Fluid Mechanics*, 513:77–85, 2004.

[3] M. Denesuk, G.L. Smith, B.J.J. Zelinski, N.J. Kreidl, and D.R. Uhlmann. Capillary penetration of liquid droplets into porous materials. *Journal of Colloid and Interface Science*, 158(1):114–120, 1993.

[4] N. Alleborn and H. Raszillier. Spreading and sorption of droplets on layered porous substrates. *Journal of Colloid and Interface Science*, 280(2):449–464, 2004.

[5] C. Huh and L. E. Scriven. Hydrodynamic model of steady movement of a solid/liquid/fluid contact line. *Journal of Colloid and Interface Science*, 35(1):85–101, 1971.

[6] E. B. Dussan V. and S. H. Davis. On the motion of a fluid-fluid interface along a solid surface. *Journal of Fluid Mechanics*, 65(1):71–95, 1974.

[7] P. G. de Gennes. Wetting: statics and dynamics. *Rev. Mod. Phys.*, 57(0):827–863, Jul 1985.

[8] C. Huh and S. G. Mason. The steady movement of a liquid meniscus in a capillary tube. *Journal of Fluid Mechanics*, 81(3):401–419, 1977.

[9] L. M. Hocking. A moving fluid interface. part 2. the removal of the force singularity by a slip flow. *Journal of Fluid Mechanics*, 79(2):209–229, 1977.

[10] S. H. Davis. Contact-line problems in fluid mechanics. *Journal of Applied Mechanics, Transactions ASME*, 50(4):977–982, 1983.

[11] P. J. Haley and M. J. Miksis. The effect of the contact line on droplet spreading. *Journal of Fluid Mechanics*, 223:57–81, 1991.

[12] R. L Hoffman. A study of the advancing interface. i. interface shape in liquidgas systems. *Journal of Colloid and Interface Science*, 50(2):228–241, 1975.

[13] R. E. Johnson, R. H. Dettre, and D. A. Brandreth. Dynamic contact angles and contact angle hysteresis. *Journal of Colloid and Interface Science*, 62(2):205–212, 1977.

[14] E. B. Dussan V. The moving contact line: the slip boundary condition. *Journal of Fluid Mechanics*, 77(4):665–684, 1976.

[15] J. D. Chen. Experiments on a spreading drop and its contact angle on a solid. *Journal of Colloid and Interface Science*, 122(1):60–72, 1988.

[16] L. H. Tanner. The spreading of silicone oil drops on horizontal surfaces. *Journal of Physics D: Applied Physics*, 12(9):1473, 1979.

[17] T. D. Blake. The physics of moving wetting lines. *Journal of Colloid and Interface Science*, 299(1):1–13, 2006.

[18] H. P. Greenspan. On the motion of a small viscous droplet that wets a surface. *Journal of Fluid Mechanics*, 84(1):125–143, 1978.

[19] J. Lopez, C. A. Miller, and E. Ruckenstein. Spreading kinetics of liquid drops on solids. *Journal of Colloid and Interface Science*, 56(3):460–468, 1976.

[20] D. Izbassarov and M. Muradoglu. Effects of viscoelasticity on drop impact and spreading on a solid surface. *Phys. Rev. Fluids*, 1:023302, Jun 2016.

[21] M. F. Tome, N. Mangiavacchi, J. A. Cuminato, A. Castelo, and S. McKee. A finite difference technique for simulating unsteady viscoelastic free surface flows. *Journal of Non-Newtonian Fluid Mechanics*, 106(2):61 – 106, 2002.

[22] J. R. King. Two generalisations of the thin film equation. *Mathematical and Computer Modelling*, 34(7):737–756, 2001.

[23] N. C. Reis, R. F. Griffiths, and J. M. Santos. Numerical simulation of the impact of liquid droplets on porous surfaces. *Journal of Computational Physics*, 198(2):747–770, 2004.

[24] B. D. Nichols, C. W. Hirt, and R. S. Hotchkiss. Sola-vof: A solution algorithm for transient fluid flow with multiple free boundaries. 39, 08 1980.

[25] L. L. Zheng and H. Zhang. An adaptive level set method for moving-boundary problems: Application to droplet spreading and solidification. *Numerical Heat Transfer, Part B: Fundamentals*, 37(4):437–454, 2000.

[26] A. Zadražil, F. Stepanek, and O. K. Matar. Droplet spreading, imbibition and solidification on porous media. *Journal of Fluid Mechanics*, 562:1–33, 2006.

[27] L. Espín and S. Kumar. Droplet spreading and absorption on rough, permeable substrates. *Journal of Fluid Mechanics*, 784:465–486, 2015.

[28] R. C. Daniel and J. C. Berg. Spreading on and penetration into thin, permeable print media: Application to ink-jet printing. *Advances in Colloid and Interface Science*, 123–126:439–469, 2006. Special Issue in Honor of Dr. K. L. Mittal.

[29] S. H. Davis and L. M. Hocking. Spreading and imbibition of viscous liquid on a porous base. *Physics of Fluids*, 11(1):48–57, 1999.

[30] S. H. Davis and L. M. Hocking. Spreading and imbibition of viscous liquid on a porous base. ii. *Physics of Fluids*, 12(7):1646–1655, 2000.

[31] G. S. Beavers and D. D. Joseph. Boundary conditions at a naturally permeable wall. *Journal of Fluid Mechanics*, 30(1):197–207, 1967.

[32] H. E. Huppert and J. E. Simpson. The slumping of gravity currents. *Journal of Fluid Mechanics*, 99(4):785–799, 1980.

[33] L. G. Leal. *Advanced Transport Phenomena: Fluid Mechanics and Convective Transport Processes*. Cambridge Series in Chemical Engineering. Cambridge University Press, 2007.

[34] P. B. Warren. Late stage kinetics for various wicking and spreading problems. 69:041601, 05 2004.

[35] A. M. Cazabat and M. A. Cohen Stuart. Dynamics of wetting: effects of surface roughness. *The Journal of Physical Chemistry*, 90(22):5845–5849, 1986.

[36] R. D. Deegan, O. Bakajin, T. F. Dupont, G. Huber, Sidney R. N., and T. A. Witten. Capillary flow as the cause of ring stains from dried liquid drops. *Nature*, 389:827–829, 1997.

[37] H. C. Brinkman. A calculation of the viscous force exerted by a flowing fluid on a dense swarm of particles. *Flow, Turbulence and Combustion*, 1(1):27, Dec 1949.

[38] L. Durlofsky and J. F. Brady. Analysis of the brinkman equation as a model for flow in porous media. *The Physics of Fluids*, 30(11):3329–3341, 1987.